

For Reference

NOT TO BE TAKEN FROM THIS ROOM

University of Alberta

Department of Chemical and Petroleum Engineering

THE LOW TEMPERATURE CARBONISATION OF COAL IN A

FLUIDISED BED

by

C. G. Sinclair

April 1956

For Reference

NOT TO BE TAKEN FROM THIS ROOM

Ex LIBRIS
UNIVERSITATIS
ALBERTAENSIS





Digitized by the Internet Archive
in 2018 with funding from
University of Alberta Libraries

<https://archive.org/details/lowtemperatureca00sinc>

UNIVERSITY OF ALBERTA

SCHOOL OF GRADUATE STUDIES

The undersigned hereby certify that they have
read and recommend to the School of Graduate
Studies for acceptance, a thesis entitled:-

The Low Temperature Carbonisation of Coal in a
Fluidised Bed.

submitted by Charles Gordon Sinclair B.Sc. Tech.
in partial fulfilment of the requirements for the
degree of Master of Science.

PROFESSOR.

PROFESSOR.

PROFESSOR.

Date. *16 Apr 1956*

THESIS
1956
#124

THE UNIVERSITY OF ALBERTA

The Low Temperature Carbonisation

of Coal in a Fluidised Bed.

A DISSERTATION

SUBMITTED TO THE SCHOOL OF GRADUATE STUDIES
IN PARTIAL FULFILMENT OF THE REQUIREMENTS FOR THE DEGREE
OF MASTER OF SCIENCE

FACULTY OF ENGINEERING

DEPARTMENT OF CHEMICAL AND PETROLEUM ENGINEERING

BY

CHARLES GORDON SINCLAIR

EDMONTON, ALBERTA.

ACKNOWLEDGEMENTS

The author is indebted to Dr. D.B. Robinson for his inspiration, guidance and unstinting assistance, and to the staff of the department for their help and suggestions.

H. Louey who assisted in the work described in Part 1 of this thesis, R. Stogryn who helped with the commissioning of the carboniser and N. Nakonechny who assisted with the construction of the equipment have contributed to the success of the work.

Acknowledgement is due to the Research Council of Alberta for their suggestions, in the preparation of some of the drawings and for the analysis work. The carboniser was financed by the Research Council.

The author is also indebted to the Consolidated Mining and Smelting Co. of Canada Ltd. for the award of their fellowship covering the first part of this thesis, and to the National Research Council of Canada whose financial assistance made possible the second part.

Table of Contents.

Page No.

List of Tables

List of Figures

List of Plates

Abstract	1.
General Introduction	2.
Part 1. Fluidisation of coal particles.	4.
A. Introduction.	4.
B. Solid liquid fluidisation.	5.
C. Solid gas fluidisation.	8.
D. Scope of fluidisation work.	34.
E. Experimental fluidising equipment.	34.
1. Equipment	34.
2. Calibration of the orifice plates	38.
3. Calibration of the pressure drop across the empty fluidisation tube.	42.
4. Preparation of coal samples.	44.
5. Experimental procedure.	46.
F. Results and their comparison with work of previous investigators.	48.
G. Conclusions	64a.
Table of nomenclature for Part 1.	65.
Part 2. Carbonisation of coal in a fluidised bed.	67.
A. The low temperature carbonisation of coal.	67.

Table of Contents. (cont.)

Part 2. (cont.)

B.	Properties of Alberta coals.	68.
C.	Equipment design.	71.
D.	Experimental results.	89.
E.	Conclusions.	100.
F.	Future work.	100.
	Bibliography.	102.
Appendix A.	Experimental fluidisation results.	104.
Appendix B.	Equipment design.	110.
Appendix C.	Equipment commissioning.	125.

List of Tables

Table		Page No.
1	Value of $\epsilon^{1.65}(1 - \epsilon)$ for various values of ϵ .	26.
2	Evaluation of ϵ at the quiescent state of a fluidised bed.	27.
3	Evaluation of orifice coefficients.	41.
4	Prepared coal samples.	45.
5	Tyler screen analyses of wide fraction coal samples.	46.
6	Critical and other properties of narrow size coal particles.	58.
7	Void fractions in coal.	63.
8	Typical properties of Alberta subbituminous B coals.	71.
9	Screen analyses of coal feed and semi-coke.	94.
10	Proximate analyses of coal feed and semi-coke.	95.
11	Gross calorific value of coal feed and semi-coke.	95.
12	Analysis of liquid product, run 5.	96.
13	Orsat analyses of gaseous products.	96.
14	Operating variables, runs 5 and 6.	97-98.

List of Figures

Figures		Page No.
1	Generalised pressure drop vs. velocity curve for narrow size fractions.	16.
2	Generalised pressure drop vs. velocity curve for wide size fractions.	16.
3	Fluidisation apparatus.	35.
4	Details of fluidisation tube.	37.
5	Pressure drop vs. air flow rate for empty fluidisation tube and screen.	43.
6	All results. Pressure drop vs. air flow rate as air flow rate is being reduced.	49.
7	Pressure drop vs. air flow rate coal sample 1A.	50.
8	Pressure drop vs. air flow rate coal sample 8A.	51.
9	Pressure drop vs. air flow rate coal sample 1B.	52.
10	Pressure drop vs. air flow rate coal sample 3A	53.
11	Critical gas velocity of coal particles vs. particle diameter.	59.
12	Comparison of present work with that of other investigators.	61.
13	Void fraction in coal.	64.
14	Coal map of Alberta.	69.
15	Fluidised coal burner.	74 and 119.
16	Complete flow sheet.	76.
17	Details of carboniser, heater and accessories.	83.

List of Figures (cont.)

Figures		Page No.
18	Simplified flow sheet fluidised coal carbonisation.	84.
19	Temperature conditions during run 5.	91.
20	Temperature conditions during run 6.	93.
21	Detailed drawing of carboniser and heater.	123.
22	Calibration of screw feeders.	128.
23	Calibration of purge gas orifice plates.	129.
24	Pressure drop vs. gas flow rate for coal in the carboniser and sand in the heater.	132.

List of Plates

Plate		Page No.
1	General view of the equipment.	77
11	General view of the panel board.	78
111	Rear of panel board.	79
1V	Heater and heater feed hopper.	80
V	Coal feed hopper.	81
VI	Semi-coke receivers.	82

ABSTRACT.

The critical gas velocities of coal particles in a $5\frac{1}{2}$ in. diameter fluidised bed have been determined using dry air at atmospheric conditions. Nine samples ranging in size from 0.0099 to 0.224 in. diameter and one wide size range sample (less than $1/16$ th. in.) were used. The results are compared with those predicted using the methods of three other workers. The void fraction in the fixed and fluidised state have also been determined for the nine samples.

The design and commissioning of a plant for the low temperature carbonisation of 60 lb./hr. of pulverised coal in a fluidised bed is described. Some operating data are included.

THE LOW TEMPERATURE CARBONISATION OF COAL IN A
FLUIDISED BED.

GENERAL INTRODUCTION

The Research Council of Alberta is engaged in a long term project dealing with the low temperature carbonisation of coal. The history of the low temperature carbonisation of coal has been beset with difficulties due mainly to the low heat transfer rates at the low temperature gradients involved and the adverse swelling characteristics of ^{coking} coals at these temperatures. It is not surprising then that the technique of the fluidised bed of particles has been adapted to this problem, involving as it does high heat transfer coefficients from wall to bed, improved solids handling methods and almost complete absence of temperature gradients within the bed. As a part of this work, the Chemical Engineering Department of the University has constructed a small pilot plant using the technique. It was decided after making a preliminary search of the literature that information on the dynamic properties of beds of coal particles should be obtained in the laboratory. The results, apart from their immediate practical value would also be of some use in checking the various proposed formulae for determining the design

constants of a fluidised bed.

The two objectives of this thesis were to determine, by batch fluidisation of coal particles at room temperature, the design constants for a fluidised coal carboniser and to design, construct and operate it. The first objective is covered in part 1 and the second in part 2 and appendices B and C.

PART 1 FLUIDISATION OF COAL PARTICLES

A. INTRODUCTION

Fluidisation is that operation involving the suspension of a bed of solid particles in the counter gravity flow of a fluid. There will be more or less relative motion between the particles according to the properties of the fluid, particles, and retaining vessel. The phenomenon is not of particularly recent origin. G. Martin in his treatise on Chemical Engineering, London, 1928, devotes a chapter to the behaviour of fluidised solids and gives some design data; and a full size vertical Portland cement kiln operating on this principle was built in the 1920's but was not a commercial success. Fluidisation has been long known in the ore dressing industry where it is called the 'teeter' condition, when water is used as the fluidising agent. However, the recent upsurge of interest dates from World War 2, and its use in the American petroleum industry where it provided a most elegant method for handling the large quantities of catalyst used in cracking petroleum stocks. It is now well established as a unit operation but the state of knowledge of the subject still leaves much to be desired. Fluidisation falls

naturally into two divisions viz. solid/liquid and solid/gas systems; they will now be treated separately.

B. Solid/liquid Fluidisation.

When a bed of solid in a retaining vessel supported on some kind of porous screen is subjected to a gradually increasing upward flow of liquid, it is observed that after the flow is increased to a point such that the pressure drop is equal to the effective mass of the bed after buoyancy is taken into account, then, the bed will expand to present a greater cross-section for liquid flow to keep the pressure drop constant. At the lower flow rates there is a tendency for the liquid to channel, that is for a large proportion of liquid to flow through one section of the bed, but as the flow is increased beyond the point where the bed expansion takes place, this tendency decreases and there will eventually be a point at which the liquid flow is distributed regularly across the bed. The phenomenon occurring after bed expansion is termed fluidisation. The bed particles are separated from each other by the liquid and are agitated and the upper boundary of the bed is quite sharp and horizontal. As the flow is increased the bed will continue to expand uniformly

until the terminal velocity of the particles is reached when the bed will disperse in the liquid.

Hancock has described this phenomenon (7) and correlated (8) the data of Hirst (11) for the sand/water system by a combination of the equation for the free fall of a sphere i.e. $Bl = f(Rep)$ with the function of the bed voidage ϵ^6 . In this paper (8) Hancock recognises the phenomenon of gas/solid fluidisation but did not publish formal equations until 1949 (6).

Wilhelm and Kwauk have published work (26) on the fluidisation of uniform spherical particles (up to 0.02 inches diameter) with water, and correlated their data by means of plots of the Blake number multiplied by the Reynolds number squared against the Reynolds number, with the bed voidage as parameter. They made no attempt to determine a function of bed voidage which would bring all their points on one curve. They concluded only that the function will be complicated.

Morse (22) replotted the ^{above} data including the voidage function $\epsilon^3/(1 - \epsilon)$ in an attempt to obtain a single line plot but with disappointing results.

Lewis, Gilliland and Bauer (19) included all their data for air and water fluidisation of glass spheres on a single line by using the voidage raised to the 4.65 power as a multiplier of the Blake number, but the range of Reynolds number and voidage involved is

too small for this treatment to be proved conclusive.

Young (27) resolved the problem into two parts. One is determining $f(\epsilon)$ in the relation $Bl.f(\epsilon) = F(Rec)$, where Rec is Reynolds number as modified by Carman (4). This equation is the equivalent of the Blake-Carman correlation for fixed beds. The other involves determining $f'(\epsilon)$ and $f''(\epsilon)$ in $Bl.f'(\epsilon) = F(Rep.f''(\epsilon))$ where the function F is given by the curve of Bl against Re for free falling particles. This is an extension of the method proposed by Hancock, previously discussed. This was done using the data of Wilhelm and Kwauk as well as their own. The correlations are reasonably good but can only be expected to apply for near spherical particles.

Jottrand (14) presents data for the fluidisation of crushed sand with water in the region $Rep < 0.5$. His data cannot be correlated on a straight line using the voidage function $\epsilon^3/(1-\epsilon)^2$ as proposed by Leva and associates (15), (16) for air fluidised beds, however, they find that $\epsilon^{5.6}$ is the best function, cf. Lewis, Gilliland, and Bauer, and Hancock above.

The related problems of flow through fixed beds, hindered settling and free fall of particles, and pneumatic transport of solids have been extensively covered in the literature.

C. Solid gas Fluidisation.

When we come to the question of the fluidisation of solid particles with a gas the state of knowledge of the phenomenon is more complicated. In the first instance most work has been done on small sized particles so that the flow is wholly laminar; and those correlations and data which deal with the transitional and turbulent flow regions are contradictory and often represent unjustifiable extrapolations. What is actually observed when a bed of particles is fluidised in a transparent tube is described in most papers dealing with this question (1) (9) (10) (13) (15) (19) (26), and may be summarised thus. At low flow rates of gas through the packed bed, no movement is observed and the pressure drop across the bed varies as a power of the superficial gas velocity, the value of the exponent ranging from 1 to 2 depending on the state of flow. When the pressure drop becomes equal to the hydrostatic head of the bed the particles will rearrange to present an increased area for flow with the possibility of a decrease in the pressure drop. These rearrangements may occur several times or not at all, and more or less violently depending upon the initial packing and uniformity of the bed. This process will come to an end when the particles are in their loosest stable packing. A further increase

in the flow will now cause the particles to separate, and if the bed is completely uniform with respect to particle size, mass and shape, this will occur throughout the whole of the bed. If on the other hand the bed is not homogeneous, the separation of particles may first occur in certain regions. Thus in the case of a range of particle sizes the boundary between the fixed and separated phases will move from the top downwards as the gas velocity is increased until the whole of the bed is in this condition. This condition of expansion where the particles, though separate, do not appreciably change their relative positions is the same as in the fluidisation with a liquid and is known as "particulate" fluidisation after Wilhelm and Kwaak (26). There is however, a limit to the amount of gas which can be passed through the bed while it still preserves its homogenous nature. After this point the gas passes through the bed in the form of bubbles through which the particles drop. The continuous solid/gas phase still appears to have about the same density as before the bubbling, but it is now violently agitated and has been compared to a boiling liquid. Depending upon the properties of the solid and the geometry of the retaining vessel, bubbles may occupy the whole cross-section of the bed, when this happens sections

of the bed are repeatedly projected violently upwards, disintegrate and fall back. This is known as slugging and is comparable to the phenomenon known by the same name in gas lifts. With increasing gas flow the discontinuous low density phase grows at the expense of the continuous phase until the limit of zero continuous or high density phase is reached and the fluidised bed no longer exists.

Before the design of a fluidised bed can be undertaken, the following problems amongst others must be solved.

1. Prediction of pressure drop across any given bed at any given flow rate of a specific gas.
2. Rigorous definition of reproducible critical points in the fluidisation process.
3. Determination of critical gas velocities for a given bed and gas, and determination of bed density or fractional voids at the given critical gas velocities.
4. Prediction of the bed density or fractional voids for any given bed at any given flow rate of a specific gas.

The work done under each of these headings will now be discussed in detail.

1. Prediction of pressure drop across any given bed at any given flow rate of a specific gas.

If a fluidised bed is considered as a fluid then

the pressure drop through it would be expected to conform to the laws of hydraulics and be equal to M/A , where M equals the effective mass of bed (mass of solid corrected for buoyancy), and A equals the cross-sectional area of bed. This relationship was proposed and confirmed by Parent, Yagol and Steiner (23) . Defining:-

ΔP = Pressure drop across the bed.

L = Height of bed at any time.

ϵ = Fraction void space in the bed.

ρ_s = Density of solid.

ρ_f = Density of fluid (mean value).

then the following relationship can be set up:-

$$\Delta P = M/A = LA(1 - \epsilon)(\rho_s - \rho_f)/A$$

i.e.

$$\Delta P/L = (1 - \epsilon)(\rho_s - \rho_f) \dots \dots \dots (1).$$

This equation proposed by Wilhelm and Kwauk (26) and Leva et al. (15) has been confirmed by them and most other investigators at the point of fluidisation. It would appear obvious that energy is required over and above that required to support the bed, and that in general

$$\Delta P/L > (1 - \epsilon)(\rho_s - \rho_f)$$

and that the magnitude of this difference would depend

upon frictional drag at the walls of the retaining vessel, acceleration of particles, entrance effects and the like. Lewis et al. (19) have plotted (ΔP experimental + ΔP calculated), for beds of 0.0061 inch glass spheres fluidised with air. Deviations up to 20% greater than the theoretical value of 1 were obtained, the extent of the deviation increasing with increase of the bed height to diameter ratio and Reynolds no. They relate this with the increase in the tendency for slugging with consequent energy losses at the walls of the container. However, these conclusions are based on data from $2\frac{1}{2}$ and $4\frac{1}{2}$ I.D. tubes where wall effects would be expected to be extensive. Toomey and Johnstone (25) have proposed a mechanism to account for the excess pressure drop over that just required to initiate fluidisation by taking account of the work done by the discontinuous phase in rotating particles at the boundary between the phases, (assumed proportional to $D_p^{\frac{1}{2}}$) and wall effects (assumed constant). They then relate the gas velocity and pressure drop through the continuous phase (assumed equal to the critical conditions, minimum fluidisation), the excess of the gas velocity and pressure drop over these values (assumed due to the discontinuous phase), and the nominal particle diameter raised to the one half power. The proposed relationship apparently checks their own data and that of Lewis, Gilliland

and Bauer (19) mentioned above.

2. Rigorous definition of reproducible critical points in the fluidisation process.

It is obviously most important to be able to predict the gas velocity necessary to fluidise a given solid particle system and to predict the limits of satisfactory fluidisation. From the description of the fluidisation process there would appear to be three definable critical points; first, the gas velocity for the onset of single phase fluidisation, secondly, for two phase fluidisation and thirdly, for the disappearance of the fluidised bed. The first named is called the "critical" gas velocity and has received with one exception all the attention of workers in this field. Many workers (5), (6), (12), (22), (25), and (26), have only been concerned with the problem of relating the gas velocity to the bed properties and fractional voids, also called bed voidage. Leva et al. (15), proposed setting the pressure drop term in the equation for flow through a packed bed equal to the weight of the bed, and then, substituting the bed voidage obtained from a correlation of the maximum fixed bed voidage, they obtained the critical gas velocity.

Baerg, Klassen and Gishler in their studies of heat transfer (2) noted a sharp discontinuity in the plot of heat transfer coefficient to the walls of the retaining vessel versus the superficial gas velocity, when taken over both fixed and fluidised conditions. They assume that this point corresponds to the critical gas velocity though it would seem more likely to correspond to the point of incipient two phase fluidisation and the consequent increase in bed turbulence.

Agarwal and Storrow (1) defined the critical gas velocity by visual observation of a bed fluidised in a transparent tube, as being for even fluidisation the point at which the bed becomes static as the gas velocity is reduced, or for uneven fluidisation (mixed particle sizes) the point at which all the bed is fluidised (i.e. in motion) as the velocity is increased. For a given bed the latter definition will give a higher value than the former. They find that their observed critical gas velocities do not check with the values calculated by the method of Leva et al. described above.

Lewis, Gilliland and Bauer (19) define a quiescent quicksand-like state of the fluidised bed which would seem to correspond with the critical gas velocity, and show how to find the corresponding velocity. Their method involves the simultaneous solution of two curves relating system properties and bed voidage with Reynolds

no. for fixed and fluidised beds respectively. This would appear to give the velocity at which the fixed bed changes to the fluidised condition but as will be shown later the method gives erroneous results for the bed voidage in the quiescent state and ^{it's use} so [^]would not be advisable without further study.

The pressure drop versus velocity plot forms the basis of two definitions of critical gas velocity. If this plot is made it is found that during the fixed bed condition the pressure drop increases regularly (linearly in viscous flow) with increase in gas velocity. At the approach of fluidisation the curve falls off and during fluidisation the pressure is substantially constant; now, if the velocity is reduced slowly the curve will be retraced along the same path in the fluidised region, but will fall off at a higher velocity, so that in the fixed bed region for any given velocity, the pressure drop will be lower when the velocity is being reduced than when it is being increased. Such a curve appears in Fig. 1. The lower curve is obviously obtained at maximum voidage in the bed and if there is any jarring of the equipment or if the velocity is reduced suddenly the points will be above the line. The slope of the increasing line depends upon the initial packing of the bed and consequently if the horizontal

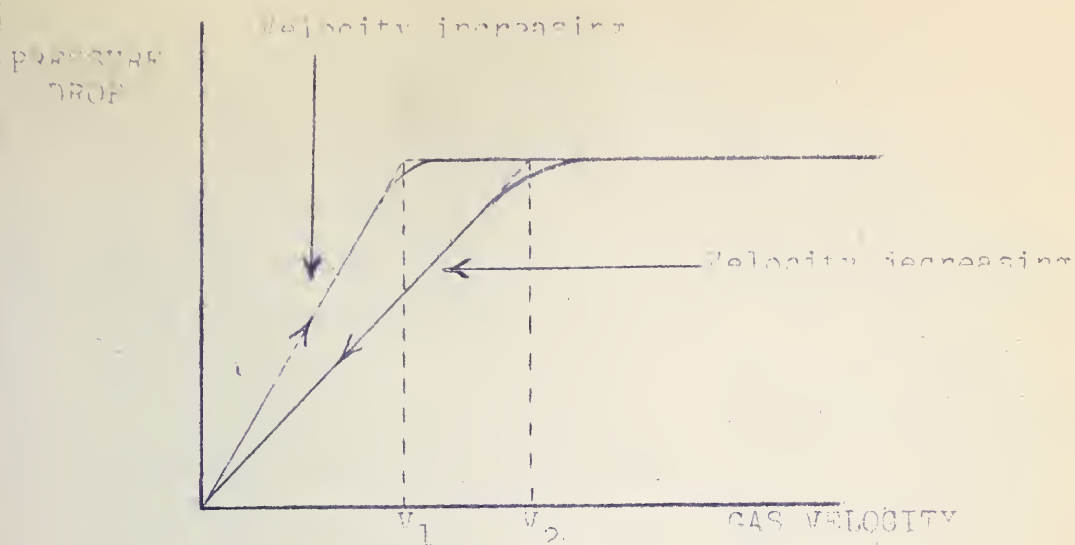


FIGURE 1 Generalised Pressure Drop vs. Velocity Curve for Narrow Size Fractions.

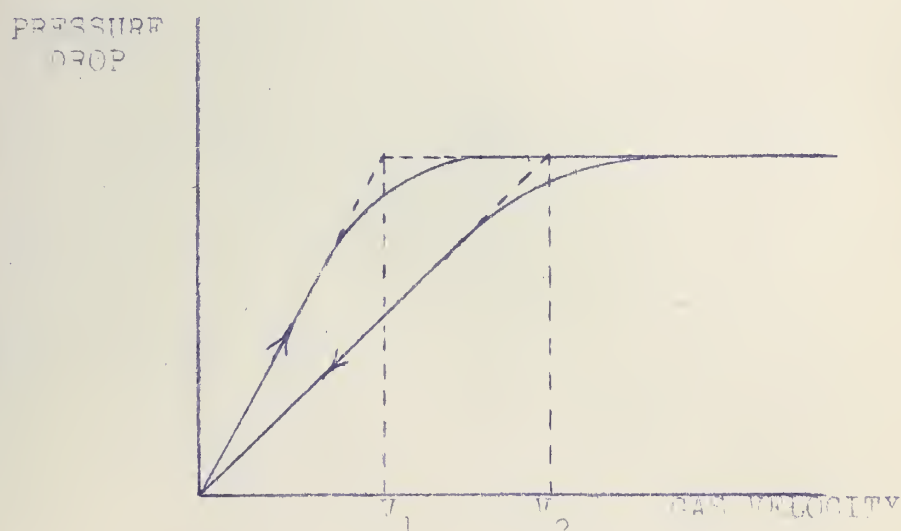


FIGURE 2 Generalised Pressure Drop vs. Velocity Curve for Wide Size Fractions.

and increasing line are extended to intersect at V_1 the value of V_1 will depend on the initial packing of the bed. Jolley and Stanton (13) use this point to define the critical gas velocity provided the bed is mechanically shaken, but it would not be reproducible unless the exact design of the shaker were specified. However, the point V_2 of intersection of the decreasing and horizontal curves is reproducible since the bed is always settled in a constant manner and at maximum voidage, and represents a velocity above which the bed will always be fluidised. This definition independently proposed by Van Heerden et al. (10) and Miller and Logwinuk (21) is superior to the others in the matter of reproducibility and in that it is directly obtained from experimental data. It is the one adopted in the present work. There are difficulties however, when dealing with wide size range mixtures since the pressure drop/velocity curve obtained has the shape shown in Fig. 2, and there is some doubt as to the point of intersection of the lines in the range V_1 to V_2 . It was noticed that on the velocity increasing readings there was still some segregation of larger particles at velocities greater than V_2 though after thorough fluidisation there was no segregation until the velocity dropped below V_2 . Accordingly V_2 has been taken as

the critical gas velocity.

The point at which the type of fluidisation changes from single phase to two phase (from particulate to aggregative in Wilhelm and Kwauk's nomenclature) has only been considered by Ergun and Orning (5), who found that two phase fluidisation began for spherical particles when the void fraction exceeded about 0.46 which corresponds to cubical packing, the loosest stable arrangement. It should be noted that Van Heerden (9) and Lewis et al. (19) quote a void fraction of 0.406 and 0.409 respectively for the onset of fluidisation (single phase). Toomey and Johnstone's treatment (25) of increased pressure drop at velocities greater than minimum fluidising velocity (critical gas velocity) presupposes the coincidence of the onset of single and two phase fluidisation.

The upper limit of fluidisation occurs at gas velocities such that the bed is destroyed. It seems reasonable and was stated by Wilhelm and Kwauk in their pioneer paper (26), that for beds of narrow size range this upper limit is the free fall velocity of the particles and their data confirm this. Lewis, Gilliland and Bauer (19) found that their plots of fraction voids against gas velocity extrapolate to the free fall velocities of the given bed at fraction voids equal unity for the larger sized particles but that for very small sizes

the velocities for 100 percent voids are several times the free fall velocities. In the discussion on the paper of Wilhelm and Kwauk (26), data are presented on the fluidisation of very small commercial catalysts which show that fluidisation proceeds smoothly at velocities greater than that corresponding to the free fall velocity of the weighted average particle size. This phenomenon is also mentioned by Matheson et al. (20). The subject is usually treated as a very minor problem in the literature and nothing very definite is said about it. The position would appear briefly to be that, for narrow size range beds the terminal velocity of the particles is the upper limit for a stable fluidised bed except in the case of very fine particles in the range -300 mesh, when smooth fluidisation can take place at velocities higher than the terminal. This may be due to the formation of aggregates containing a number of particles which behave as one. For beds containing a range of particle sizes the weighted mean diameter alone is not significant in determining these limits. If the gas velocity is lower than the critical gas velocity of the large size they will be segregated as a fixed bed layer (9); if higher than the terminal velocity of the smaller sizes they will be entrained at a definite rate, which depends

on their concentration in the bed and the bed properties. Some data on entrainment rates is given in the literature (13), (18). For beds into which material is continually fed and from which it is continually removed it is possible to obtain a stable bed under conditions which would not support batch fluidisation. Lewis, Gilliland and Bauer (19) have done experimental work using a 10 ft. 1.25 in. I.D. tube feeding solid at the base and removing it at the top, almost corresponding to vertical pneumatic transport, but the more normal industrial case (feeding to and from a well defined bed) has not been investigated.

3. Determination of critical gas velocities for a given bed and gas, and determination of bed density or fraction voids at the critical point.

In earlier studies effort was concentrated on determining the nature of the relationship connecting velocity and void fraction in the fluidised bed. The two theoretical approaches to the fluidisation process are from consideration of fixed beds and of free falling particles. The equations connecting pressure drop and gas velocity in fixed beds are modified to apply to fluidised beds by substituting the identity

$$\Delta P/L = (1 - \epsilon)(\rho_s - \rho_f) \text{ developed previously. (Eqn. 1).}$$

Any of the equations developed for fixed beds may be used. It is generally found though that the function of the bed voids so obtained does not successfully correlate the data and further correction coefficients have to be determined. By a further correlation of the bed voids at the critical gas velocity ϵ_{mf} against the particle diameter it is possible to solve for the critical gas velocity. This was the procedure adopted by Leva et al. (15). The derivation of the general equation though not stated correctly in the paper proceeds as follows:-

For fixed beds Leva has shown (15) that pressure drop data may be correlated by the general expression:-

$$\Delta P/L = \frac{k}{g} \left(\frac{D_p G}{\mu} \right)^n \frac{\mu^2}{\rho_f} \frac{1^{3-n}}{D_p^3} \frac{(1 - \epsilon)^{3-n}}{\epsilon^3} \dots\dots\dots(2).$$

where $1 \leq n \leq 2$ and $n = \phi(Re)$

Multiply both sides by Re^{2-n} , where $Re = G D_p / \mu$

and setting $f = k/2 \cdot Re^{2-n}$

we have

$$\Delta P = \frac{2f g^2 L}{D_p g \rho_f} \frac{1^{3-n}}{\epsilon^3} \frac{(1 - \epsilon)^{3-n}}{\epsilon^3} \dots\dots\dots(3).$$

Plots of f versus Re and n versus Re are given in

the paper.

Treating the fluidised bed as a fixed bed we can substitute the analogy

$$\Delta P/L = (1 - \epsilon)(\rho_s - \rho_f)$$

developed previously (Eqn. 1)

giving:

$$G^2 = \frac{\sigma D_p \rho_f (\rho_s - \rho_f)}{2f \lambda^{3-n}} \frac{\epsilon^3}{(1 - \epsilon)^{2-n}} \dots \dots \dots (4).$$

and setting $\epsilon = \epsilon_{mf}$, the fraction voids at the critical gas velocity, we can find

$$G = G_{mf} = V_{mf} \rho_f, \text{ the critical gas velocity.}$$

Plots of ϵ_{mf} versus D_p are given by Leva et al. for sand (16) and for anthracite coal (17).

Van heerden, Nobel and Van Krevelen (10) studied fluidisation only in the laminar region where $Re_p < 5$. For fixed beds the pressure drop expressed in force units can be evaluated by an equation of the type

$$\Delta p/L = f(Re_p) g(\epsilon) \lambda^{2\rho_f} V^2/\eta_p \dots \dots \dots (5).$$

usually $g(\epsilon) = (1 - \epsilon)^2/\epsilon^3$

For $Re_p < 5$ Lewis, Gilliland and Bauer (19) have found that,

$$f(Re_p) = 77/Re_p$$

and for fluidisation one can set

$$\Delta p/L = g \rho_{bm}$$

Where ρ_{bm} = density of the bed at the critical point
so that:-

$$Re_0 = \rho_f \rho_{bm} g D_p^{3/15} \mu^2 g(\epsilon_{mf}) \lambda \dots \dots \dots (6).$$

This equation connects the critical gas velocity V_{mf} in

$Re_0 = V_{mf} \rho_f D_p / \mu$ with the fraction voids at
the critical, ϵ_{mf} .

They find, however, that λ as determined using
this equation varied with D_p for substances with micro-
porosity such as coke. However, it is known that
spheres have a very definite ϵ of 0.406 at the critical
point both from their data, and that of Lewis, Gilliland
and Bauer (19), so that the function $g(\epsilon)$ may be
combined with λ to give a new shape factor which will
determine the shape of particles by comparison of their
fluidising properties with those of spheres. This leads to

$$Re_0 = 0.00123 g \rho_{bm} \rho_f D_p^{3/8} \mu^2 \dots \dots \dots (7).$$

Values of B evaluated using this equation show much
less spread than the corresponding λ values. Though
this equation holds for particles of uniform size they
found that for mixtures of wide size range the B is

still not constant with the arithmetic mean diameter of the particles, but, if the equivalent diameter of the particles is redefined as the diameter of those spheres with the same number per unit volume of the bed as the particles, both measured at maximum porosity, then, the discrepancy is eliminated.

Ergun and Orning (5) have also developed equations for fluidising gas velocity and presumably they could be used to predict the critical gas velocity by substituting the value of the bed voids at the critical point.

Agarwal and Storrow (1) tackling the problem from the other end so to speak, found that the fluidising gas velocity is proportional to the terminal velocity of the particles calculated from a mean diameter (equal to six over the particle surface area) and proportional to the bed voidage raised to the sixth power. They have plots of the critical bed voidage against particle diameter for the materials they worked with, thus the critical gas velocity can be determined. They found that their experimental results did not check with values calculated from Leva's correlation.

Miller and Logwinuk (21) tackled the problem of the critical gas velocity determination using the technique of dimensional analysis which resulted in the following equation involving particle and gas properties

raised to various powers.

$$G_{mf} = 0.00125 D_p^2 (\rho_s - \rho_f)^{0.9} \rho_f^{1.1} g / \mu \dots \dots \dots (8).$$

ft. lb.hr. units. D_p = geometric mean diameter.

It does not include bed voidage and is obviously absolutely limited to the system they have studied.

Lewis, Gilliland and Bauer (19) in the course of their study of fluidisation obtained two plots of friction factor for the fixed bed, and for the fluidised bed, plotted against particle Reynolds number. These two plots are:-

$$f_F \epsilon^{4.65} = 4gD_p(\rho_s - \rho_f) \epsilon^{4.65} / 3V^2 \rho_f \text{ vs. } Re_p$$

for the fluidised bed,

$$\text{and } f_B \epsilon^3 / (1 - \epsilon)^2 = \frac{g D_p (\Delta P/L)}{2V^2 \rho_f} \frac{\epsilon^3}{(1 - \epsilon)^2} \text{ vs. } Re_p$$

for the fixed bed.

They say then that these two plots can be solved for the fraction voids ϵ and the gas velocity V at what is called the quiescent quicksand-like state which corresponds to the critical point.

Developing this idea we note that at the critical point

$$\Delta P/L = (\rho_s - \rho_f)(1 - \epsilon)$$

and calling the ratio

$$\frac{f_F \epsilon^{4.65}}{f_B \frac{\epsilon^3}{(1 - \epsilon)^2}} = R$$

by cancelling out terms we find that,

$$R = 8 \epsilon^{1.65} (1 - \epsilon) / 3 \dots\dots\dots (9).$$

We have solved the two plots for the fraction voids at the quiescent quicksand-like state if we select from the graphs the two values to give R at the same Reynolds no. Johnson (12) made the mistake of stating that this ratio would equal unity at any Reynolds number so that $\epsilon^{1.65} (1 - \epsilon) = 0.375$. He plotted values of $\epsilon^{1.65} (1 - \epsilon)$ against ϵ and showed that the function has a maximum of 0.173 at $\epsilon = 0.62$. His table is reproduced below (Table 1).

TABLE 1. Value of $\epsilon^{1.65} (1 - \epsilon)$ for various values of ϵ

ϵ	0.3	0.4	0.5	0.6	0.7	0.8	0.9
$\epsilon^{1.65} (1 - \epsilon)$	0.097	0.132	0.155	0.172	0.167	0.140	0.081

Actually, the ratio has to be obtained from the experimental data on each graph at the same Reynolds no. The results of this correct treatment are presented in

Table 2. Values of the friction factors were read from the plots of Lewis, Gilliland and Bauer at fixed Reynolds number and the corresponding void fractions evaluated. It would appear then that the gas velocity and fraction voids at the quicksand-like state cannot be evaluated in this manner.

TABLE 2. Evaluation of ϵ at the quiescent state of a fluidised bed.

Re_p	$f_F \epsilon^{4.65}$	$f_B \frac{\epsilon^3}{(1-\epsilon)^2}$	R	ϵ
1	26	77	0.338	0.38
2	16	38.5	0.415	0.504
3	11	25.7	0.427	0.524
4	9	19.3	0.466	Imaginary
5	7.5	15.4	0.487	Imaginary
6	6	13.0	0.461	0.62
7	5	11.0	0.455	0.594
8	4.4	9.6	0.459	0.60
9	4.2	8.6	0.488	Imaginary
10	4.0	7.7	0.520	Imaginary

Finally Baerg, Klassen and Gishler (2) propose the empirical equation

$$Gmf = 1,300(D_p \rho_b)^{1.23} \dots\dots\dots(10).$$

where:- G_{mf} = critical gas velocity lbs./hr. ft.²

4. Prediction of the bed density or fractional voids for any given bed at any given flow rate of a specific gas.

The subject matter of this section has already been touched upon in previous discussion, and there will be some repetition. The number and variety of treatments of the problem are quite considerable. None has found wide acceptance, and there is still a great mass of detail to be cleared up. Dividing the problem into sections we have

a. Arbitrary experimental plots used to relate gas velocity and fraction voids.

Wilhelm and Kwauk (26)

Lewis, Gilliland and Bauer (19)

Morse (22)

b. Reasoning from flow through fixed beds.

Leva et al. (16), (17)

Ergun and Orning (5)

Van Heerden, Nobel, and Van Krevelen (10)

c. Reasoning from free fall of a particle.

Hancock (6)

Johnson (12)

These sections will now be treated separately.

a. Wilhelm and Kwauk (26) presented their data in the form of plots of the dimensionless groups $K_{\Delta p}$ and $K_{\Delta p}$ against the modified Reynolds number Rep . It should be noted that

$$2K_{\Delta p} = (1 - \epsilon)K_{\Delta p}$$

after fluidisation by virtue of the relation

$$\Delta p/L = (1 - \epsilon)(\rho_s - \rho_f)$$

developed earlier (Eqn. 1),
and also

$$K_{\Delta p} = Bl. Rep^2$$

They obtained a curve for each particle type of the same general shape viz. an initial high slope curve describing the fixed bed up to fluidisation and a horizontal line after fluidisation when Δp is substantially constant, terminated by the point corresponding to the free fall of the particle through the fluid.

Lewis, Gilliland and Bauer (19) related gas velocity and fraction voids by a plot of:-

$$4g D_p (\rho_s - \rho_f) \epsilon^{4.65} / 3V^2 \rho_f \text{ vs. } D_p V \rho_f / \mu$$

on log-log co-ordinates,
or by the relationship

$$\epsilon - \epsilon_{mf} = 0.065 (V - V_{mf}) / D_p^{0.5} \dots \dots \dots (11).$$

Where ϵ_{mf} and V_{mf} correspond to the quiescent quicksand-like state. These two quantities are obtained as indicated in the previous section which also showed that this method is erroneous. Of course the first plot is quite valid within the limits of the system they studied, viz. glass spheres 0.0016-0.0224 in. diameter.

Morse (22) has replotted the data of Leva et al. (15) and Wilhelm and Kwauk (26) as the dimensionless groups,

$$\Delta P/L \quad \frac{g \quad D_p \quad \phi_s \quad \epsilon^3}{V^2 \rho_f (1 - \epsilon)} \quad \text{vs.} \quad Re_c$$

Where ϕ_s = shape factor of particle < 1 .

This approach was suggested by the Carman correlation for flow through fixed beds and the independent variable is Reynolds number as modified by Carman (4).

b. Leva et al. (15)(16) plotted for fixed beds the friction factor f against Re_p where,

$$f = \Delta P/L \cdot \frac{D_p \quad g \quad \rho_f \quad \epsilon^3}{2G^2(1 - \epsilon)^2}$$

They found that $f = 100/Re_p$ in the laminar flow region. Combining these two relationships and substituting

$$\Delta P/L = (\rho_s - \rho_f)(1 - \epsilon)$$

and introducing a shape factor λ , since they were dealing with non-spherical particles gave:-

$$G = 0.005 D_p^2 \epsilon^3 (\rho_s - \rho_f) \rho_f g / \lambda^2 (1 - \epsilon) \mu \dots \dots \dots (12)$$

where $\lambda = A_p / A_{sph}$

A_p = surface area of the particle,

A_{sph} = surface area of sphere with the same volume as the particle.

This equation connects G and ϵ after fluidisation.

However, they found that this equation holds only for the critical point, $G = G_{mf}$ and $\epsilon = \epsilon_{mf}$. They propose the following equation to evaluate G as a function of ϵ .

$$G = (G_{mf}/le)(G_{cle}/G_{mf})^{|m|} \dots \dots \dots (13)$$

where G = actual fluidising mass velocity.

G_c = G calculated from equation (12).

le = expansion ratio $(1 - \epsilon_{mf})(1 - \epsilon)$.

m = exponent obtained from a plot of m vs. D_p .

Ergun and Orning (5) have developed an equation for pressure drop through a fixed bed in the differential form,

$$dP/dL = aV + bV^2$$

where the constants a and b have definite theoretical significance. Both involve functions of ϵ, μ and the specific surface of the particles as well as statistical constants arising from the random nature of the packed beds. By fixed bed experiments the statistical constants and specific surface can be evaluated. Integration and substitution of $\Delta P/L = (\rho_s - \rho_f)(1 - \epsilon)$ yields

an equation connecting V and ϵ namely

$$\beta S_v f_f V^2/8 + 2 \alpha S_v^2 \mu (1 - \epsilon) V - \epsilon^3 (\rho_s - \rho_f) g = 0 \dots (14).$$

where α and β are the statistical constants and S_v = specific surface of the particles. βS_v and αS_v^2 are determined from fixed bed experimental data and include all the effects of particle size and shape.

The equation Van Heerden et al. (10) proposed for the critical gas velocity was:-

$$Re_o = 0.00123 \rho_f \rho_{bm} g D_p^3 / B \mu^2 \dots \dots \dots (7).$$

They propose in the same paper to modify it for velocities greater than the critical by introducing a packing fraction

$$\psi(m)$$

where,

$$m = \rho_b / \rho_{bm}$$

and,

ρ_b = density of bed at any velocity $V > V_{mf}$

and with limited data they tentatively proposed that

$$\psi(m) = (1/m)^{6.8} \text{ so that,}$$

$$Re = V D_p \rho_f / \mu = 0.00123 \rho_f \rho_{bm} g D_p^3 (\rho_{bm} / \rho_b)^{6.8} / B \mu^2 \dots (15).$$

C. Hancock (6) quotes the following equation for fluidisation:-

$$4g D_p^2 \epsilon^6 (\rho_s - \rho_f) / 3\mu V = \text{Re } \psi$$

which is a modification of the equation for determining the free fall of a sphere. It can be more easily understood as

$$V = V_{ts} \epsilon^6 \dots\dots\dots(16).$$

Johnson (12) considering the free fall of a single particle through a bed of particle density

$$\rho_b = (1 - \epsilon)\rho_s + \epsilon\rho_f \text{ and viscosity } \mu_b = f(\epsilon)\mu$$

(as developed for colloidal suspensions by Einstein and others), the equations developed for hindered settling, and equations for flow through a packed bed, developed an equation for the fluidising velocity in the laminar region of the general type

$$V = g D_p^2 (\rho_s - \rho_f) \phi^2 f(\epsilon) / 18\mu \dots\dots\dots(17).$$

where ϕ = a shape factor,

and $f(\epsilon)$ = a function of the fraction voids; and a much more complicated one derived using free fall equations in the transitional regional. The above equation is used for

$$\text{Re} = D_p V \rho_b / \mu_b < 2$$

i.e.

$$\text{Re} = D_p V [\epsilon\rho_f + (1 - \epsilon)\rho_s] 0.0123 \epsilon^2 / (1 - \epsilon)\mu$$

D. Scope of Fluidisation Work.

Since any commercial coal carbonisation plant will handle large quantities of material for which size reduction costs will be a major expense, it was decided that an investigation of particles ranging in size from 200 to -3 mesh would give data of use in striking an economic balance. Air was selected as the fluidising gas for convenience; however, the effects of density and viscosity have been reasonably well accounted for. The tests were conducted at room temperature.

E. Experimental Fluidising Equipment.

1. Equipment.

Equipment for fluidisation investigations is generally of a very standard pattern and has been described by many investigators (1), (13), (17), (19).

Essentially all that is needed is a constant metered supply of gas to a tube with a permeable support at the base on which the fluidised bed rests. The equipment used in these experiments is sketched in Fig. 3.

Laboratory air passed through the pressure regulating valve A to a water separator B. The air at 40 psig.

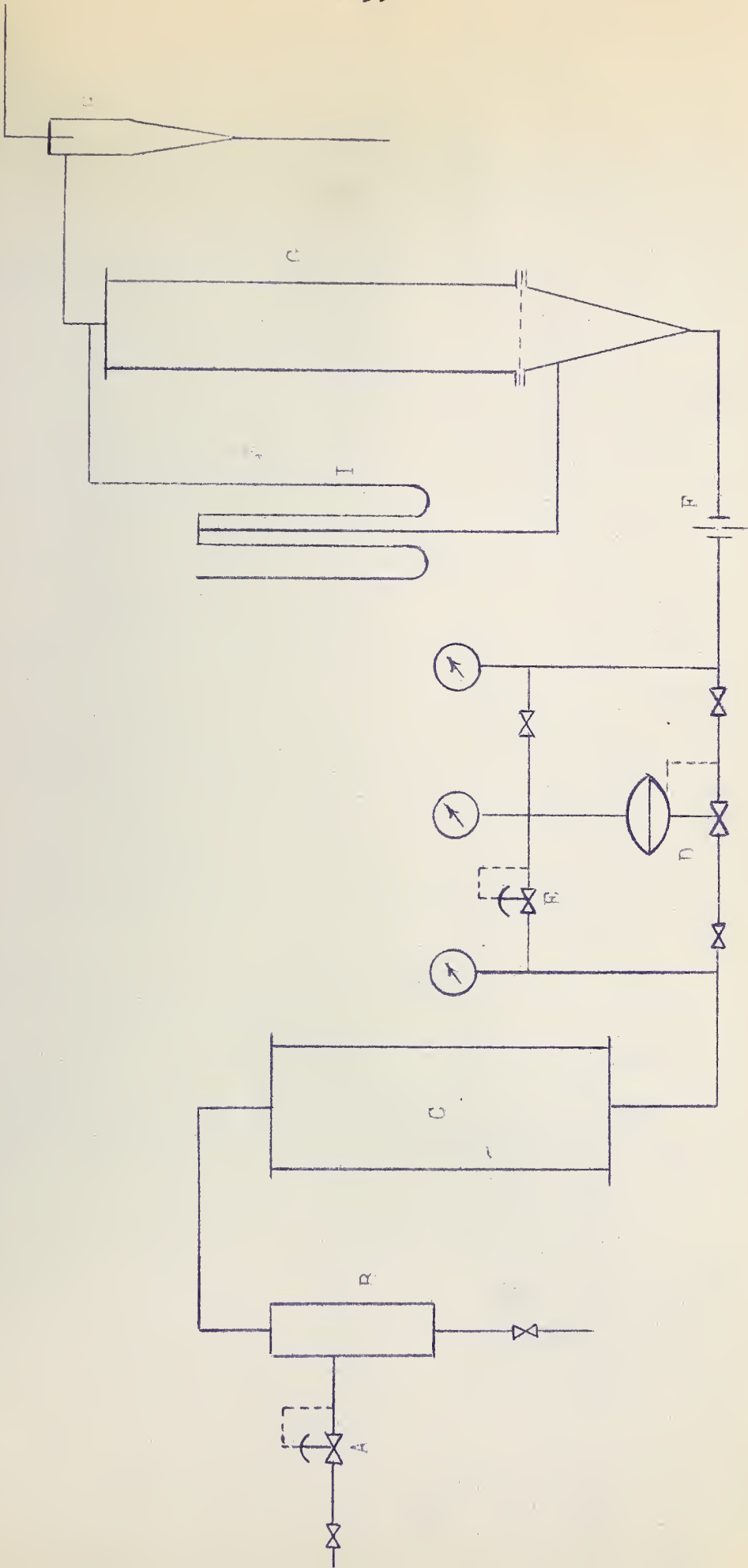
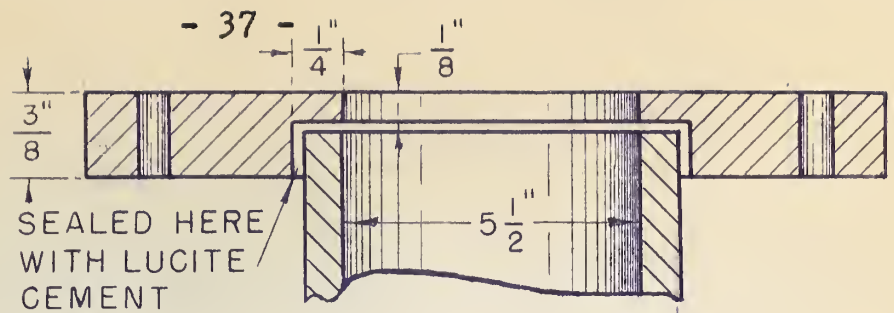


FIGURE 3
FLUIDISATION APPARATUS

then went through a bed of silica gel contained in an 8 in. diameter steel vessel where it was dried. From here it either passed through a Hammel-Dahl high flow pressure regulator D, the outlet pressure being equal to that on the delivery side of the Moore Nullmatic regulator E, or directly through E for low flows, to the orifice plate F. The pressure drop across the orifice plate and the downstream pressure were measured by suitable manometers not shown. The temperature of the air was measured by taking a bleed from before the orifice plate and passing it over a thermometer bulb. The air from the orifice metering assembly was delivered to the fluidisation tube G, which consisted of a cone, a porous bronze supporting screen, and a $5\frac{1}{2}$ I.D. tube (transparent Lucite). This is shown in detail in Fig. 4. The static pressure in the cone and the pressure drop from the cone to the outlet of the fluidisation tube were measured with two manometers. The air then passed through cyclone H, to remove entrained material, and to the atmosphere. It is interesting to note that Grohse (28), has found by X ray studies of bed density that porous metal plates give better fluidisation than either wire mesh screens or drilled plates.

The drier C was charged with 40 lb. of -6 to +16 mesh silica gel, which lasted for the whole series of experiments. Initially the dew point of the air was



DETAIL SECTION, LUCITE FLANGE

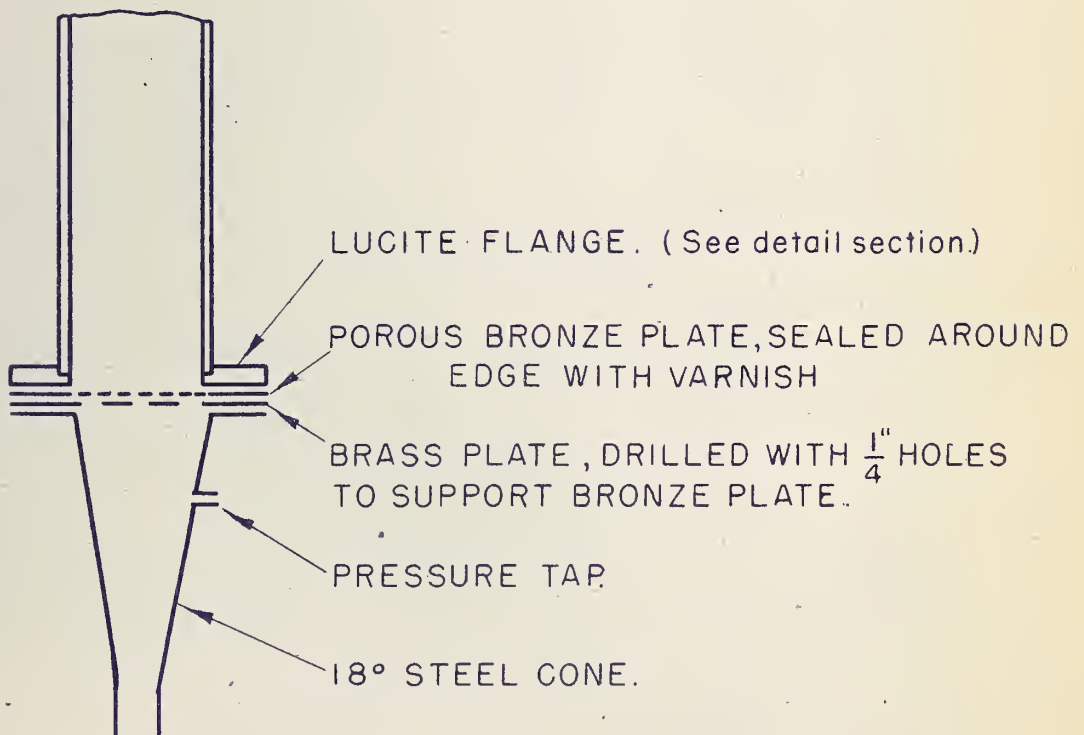
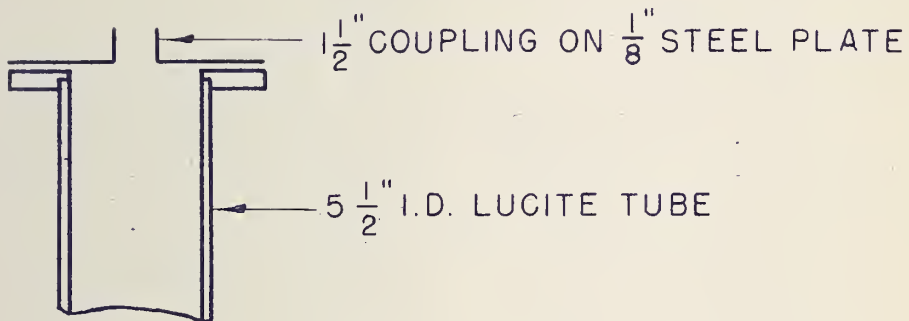


FIGURE 4. DETAILS OF FLUIDISATION TUBE.

-50°F, after the series of runs it was 0°F.

2. Calibration of the orifice plates.

Since the range of air flow rates required to fluidise the coal particles ranging from -3 Tyler mesh down would be from zero to about one scf./sec. it was decided to mount the orifice plates in a $1\frac{1}{2}$ in. standard pipe union with its faces ground flat. The orifice was preceded by 17 in. of $1\frac{1}{2}$ in. pipe and followed by 12 in. of $1\frac{1}{2}$ in. pipe. All the orifice plates were constructed of $1/8$ in. brass plate and held between two thick rubber gaskets in the union. In all cases the downstream side of the orifice was beveled at 45° so that the actual thickness of the orifice was always less than the smaller of one twentieth of an inch or one eighth of the orifice diameter. The pressure taps were $1/8$ in. brass fittings screwed at right angles into the union fitting, $1\frac{1}{2}$ in. upstream and 1 in. downstream of the orifice plate.

In order to cover the range of flow rates required using a five foot water manometer, orifice plates were constructed with diameters of 1.0, 0.5, 0.3, and 0.1875 in.

All orifice plates except the 1.0 in. one were calibrated using dry gas meters, two rated at 10 cuft./min. and one rated at 5 cuft./min. were used. First air was passed through them in series and they were

found to check against each other within 1 %.

The particular form of the orifice equation used was taken from Brown (3) namely:-

$$Q = 719 C A_0 (T_S/P_S)(\Delta H P_2/MZT_1)^{\frac{1}{2}} \dots \dots \dots (18).$$

where:-

Q = cuft./sec. flowing at T_S °R and P_S psfa.

$$C = C_0/(1 - \beta^4)^{\frac{1}{2}}$$

β = orifice diameter/pipe diameter.

A_0 = area of the orifice ft.²

C_0 = orifice coefficient.

ΔH = manometer differential pressure, in. of water.

P_2 = downstream pressure psfa.

M = molecular weight of the gas.

Z = compressibility factor.

T_S = base temperature °R.

T_1 = upstream temperature °R.

P_S = base pressure psfa.

The base pressure was taken as 14.7 psia equals 2116.8 psfa, and the base temperature as 520°R. Since the air was to all intents and purposes dry, its molecular weight is 28.97 and at these low temperatures and pressures the compressibility factor can be taken as unity. Substituting these values, the equation reduces to:-

$$Q = 32.8 C A_0 (\Delta H P_2/T_1)^{\frac{1}{2}} \dots \dots \dots (19).$$

or

$$C = Q/32.8 A_0 (\Delta H P_2/T_1)^{\frac{1}{2}} \dots \dots \dots (20).$$

Equation (20) was used to calibrate the orifice plates. Since the combined capacity of the three dry gas meters was only 25 cuft./min. they could not be used calibrate the 1.0 in. diameter orifice. In this instance, the orifice coefficient was presumed equal to that of the 0.5 in. orifice. Using the superscript ' for the 1.0 in. orifice and " for the 0.5 in. orifice we have: =

$$C_o' = C_o''$$

or

$$C'(1 - \beta'^4)^{\frac{1}{2}} = C''(1 - \beta''^4)^{\frac{1}{2}}$$

i.e.

$$C' = C'' \left(\frac{1 - \beta''^4}{1 - \beta'^4} \right)^{\frac{1}{2}} \dots \dots \dots (21).$$

That this assumption was valid was justified when on plotting the head loss across the empty fluidisation tube against the air flow rate as measured by the orifice plates, no break in the curve was evident on changing from the 0.5 in. to the 1.0 in. diameter orifice plates.

The procedure for calibrating the orifices was to connect one or more of the dry gas meters in place of the fluidisation tube, record the atmospheric pressure and temperature and then for a set flow of air to measure

the differential pressure across the orifice plate in in. of water, the upstream temperature in °C, the downstream static pressure in millimetres of mercury, and the time in seconds for the flow of 5 cuft. of air through each meter. This was repeated for different flow rates and C as given by Eqn. 20 calculated. Since these values of C will indicate the errors of measurement they are tabulated in Table 3 below:-

TABLE 3. Evaluation of orifice coefficients.

Orifice	1.0 in.	0.5 in.	0.3in.	0.1875 in.
		0.619	0.637	0.600
		0.612	0.590	0.598
		0.617	0.630	0.6115
		0.609	0.636	0.615
		0.612	0.627	0.615
		0.625	0.631	0.615
		0.625	0.634	0.621
		0.629	0.638	0.619
		0.618	0.646	0.628
		0.623	0.632	-
		0.614	0.630	-
		0.625	0.636	-
		0.616	-	-
		0.619	-	-
Average C (arithmetic)	0.668	0.619	0.634	0.614
Discard		None	Low reading	None
Standard deviation		0.0057	0.0047	0.009

Greater accuracy would not have been of any advantage, since the accuracy of the dry gas meters is only 1%. The average values of C as obtained were substituted in equation (19) to give the flow equation for use with each orifice.

3. Calibration of the pressure drop across the empty fluidisation tube.

In determining the critical gas velocity for a fluidised bed it is necessary to plot the pressure drop across the bed itself against the gas flow through the bed. On the equipment the manometer was connected from unstream of the supporting screen to the outlet of the fluidisation tube. It was therefore necessary to determine the pressure drop across the screen and empty tube as a function of the air flow rates. These data were obtained by running tests on the empty equipment using the 0.5 and 1.0 in. diameter orifice plates to cover the range of flow. The data are presented in Fig. 5 as a plot of centimetres of water manometer differential, against air rate in scf./sec. The circles represent points taken using the 0.5 in. orifice plate and triangles using the 1.0 in. orifice. As can be seen, they form a continuous curve justifying the adoption of the same orifice coefficients for the two plates as mentioned earlier. The data scatter considerably at

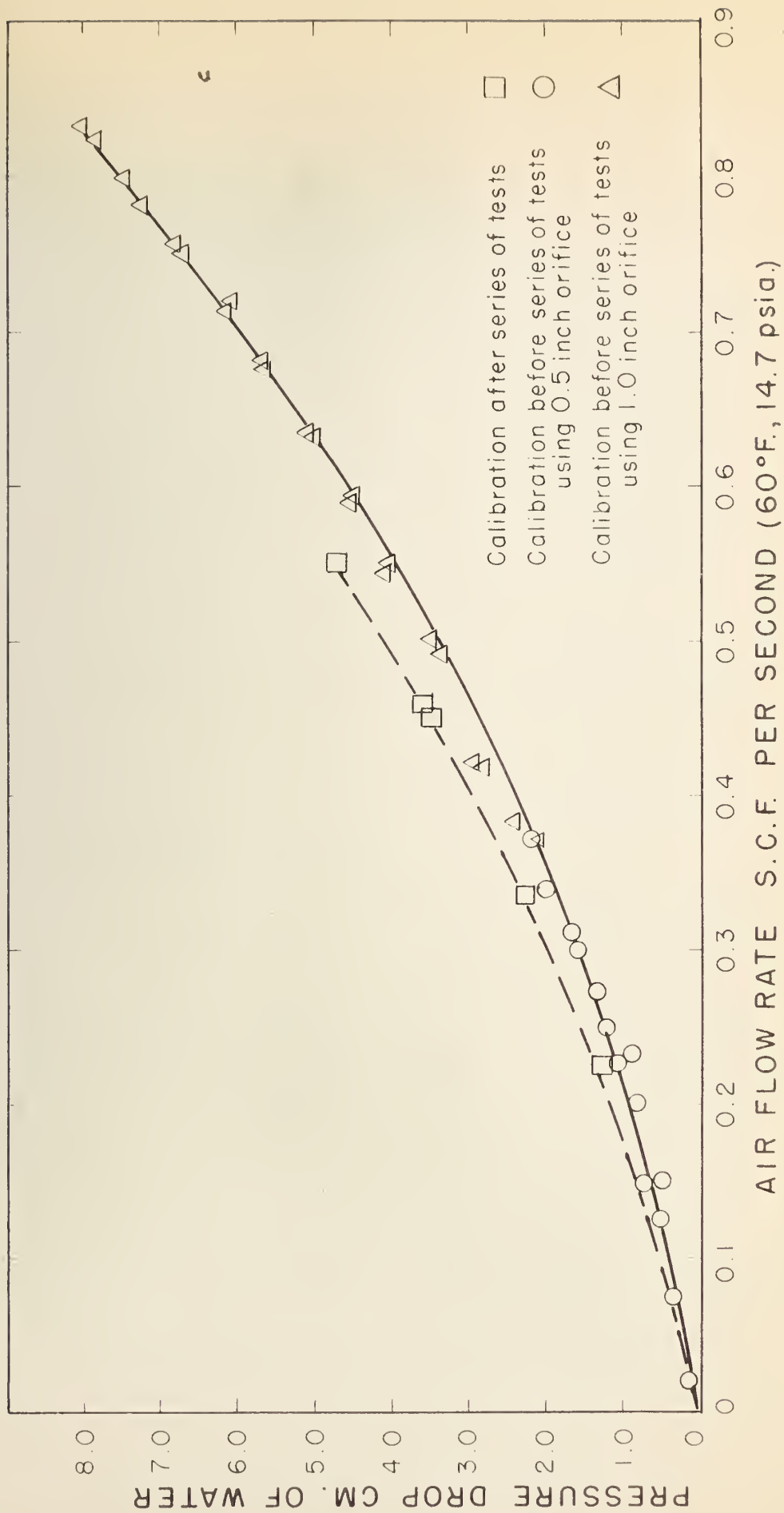


FIGURE 5. PRESSURE DROP VS. AIRFLOW RATE FOR EMPTY FLUIDISATION TUBE AND SCREEN.

the lower flow rates. This is due to the difficulty of reading the manometers at low values. The full line represents the data taken before the series of fluidisation tests. The pressure drop shows a continuous increase during the tests which could only be due to gradual clogging of the screen. However, this is not a serious error as the pressure drop versus gas velocity curves for the fluidised bed were used only to determine the critical gas velocity which is the point of sudden change in slope, and an error in this calibration curve though it will affect the accuracy of the pressure drop will not affect the position on the gas velocity axis of the break point.

4. Preparation of coal samples.

A sample of non-coking coal from East Coulee, Alberta with a moisture content of 16% was crushed in a hammer mill to yield approx. 99% less than Tyler 4 mesh. This mixture was roughly sized into 8 fractions on a reciprocating double screen. These roughly sized particles were further separated into narrower size ranges with a series of standard Tyler screens. The fractions and weights of coal eventually obtained are tabulated in Table 4 following:-

TABLE 4. Prepared coal Samples.

Screen limits.	Weight in lbs.	Sample No.
+3	-	-
-3 +4	-	13A
-4 +8	60.5	1A
-8 +10	39.5	2A
-10 +14	36.0	3A
-14 +20	25.0	4A
-20 +28	20.0	5A
-28 +35	15.5	6A
-35 +48	12.5	7A
-48 +65	7.5	8A
-65 +100	7.5	9A
-100 +150	3.5	10A
-150 +200	1.0	11A
-200	9.0	12A

Later a cut between the 3 and 4 screens was taken from the + 4 fraction. These fractions were stored in 10 gallon cans for subsequent use.

Three samples of crushed coal from West Canadian Collieries Ltd., Blairmore, were prepared using a hammer mill with a $\frac{1}{4}$ in., $\frac{1}{8}$ th. in., and $\frac{1}{16}$ th. in. screens labelled 3B, 2B, and 1B, respectively. The Tyler screen analysis of these three samples is given in Table 5 following:-

TABLE 5. Tyler screen analyses of wide fraction coal samples.

Tyler Screen	Sample 3B -1/4 in. %	Sample 2B -1/8 in. %	Sample 1B -1/16 in. %
+8	6.7	0.4	-
-8 +10	13.8	4.4	-
-10 +14	16.4	15.6	0.4
-14 +20	14.8	17.3	11.1
-20 +28	12.0	16.1	18.8
-28 +35	9.3	13.2	17.4
-35 +48	8.1	10.6	14.4
-48 +65	5.3	6.6	9.5
-65 +100	4.3	5.0	7.5
-100 +150	3.0	3.8	6.4
-150 +200	2.0	2.0	3.8
-200	4.3	5.0	10.7

5. Experimental Procedure

The procedure was relatively simple. After checking the equipment, a weighed amount of the coal sample was charged to the fluidisation tube, and the correct orifice plate to cover the range of air rates anticipated put in position. The equipment was closed up. The coal

sample was then gently fluidised to even out the surface. By manipulation of the control valves the air rate was increased in steps, allowing sufficient time for equilibrium at each step. A set of readings consisted of:-

1. Temperature upstream of the orifice, °C.
2. Pressure differential across the orifice plate, in. of water.
3. Static pressure downstream of the orifice plate, in. of mercury.
4. Pressure differential across the coal bed, tube, and supporting screen, centimetres of water.
5. Static pressure upstream of the fluidisation tube, centimetres of water.
6. The height of the bed, read from a scale attached to the tube, in.
7. Notes on the appearance of the bed.

The above readings were taken after each step change of air flow with the exception of the temperature which was taken every alternate reading. In addition to these, for every complete run, the weight, grade, and condition of the coal, the size of orifice, the barometric pressure in millimetres of mercury, date, and time were recorded. For a complete run on any sample the air rate was increased in steps up to and beyond fluidisation, then reduced stepwise to zero and in some increased again. A typical set of readings would be 5 up to fluidisation, 6 after

fluidisation as the air rate was increased for the first time, 9 as the air rate was decreased to zero and then a further 7 points as the air rate was increased again.

After fluidisation the bed height readings were less accurate and when the bed began to slug an approximate average was all that could be read. Similarly after fluidisation the manometer levels would oscillate slightly and an average reading was determined by eye from the maximum and minimum values.

F. Results and their comparison with the work of previous investigators.

The basic data of this study are the pressure drop versus air rate plots for the various samples, from which the critical gas velocities are determined. All the results of air flow rate against pressure drop when the gas velocity is being reduced are plotted in Fig. 6 and all the data are tabulated in Appendix A. Fig. 7 to 10 show in more detail all the results on specific samples plotted on arithmetic paper. The general form of the curves as described earlier can be seen. In addition the influence of the initial bed packing can be clearly seen in Fig. 10 where the dashed line is the

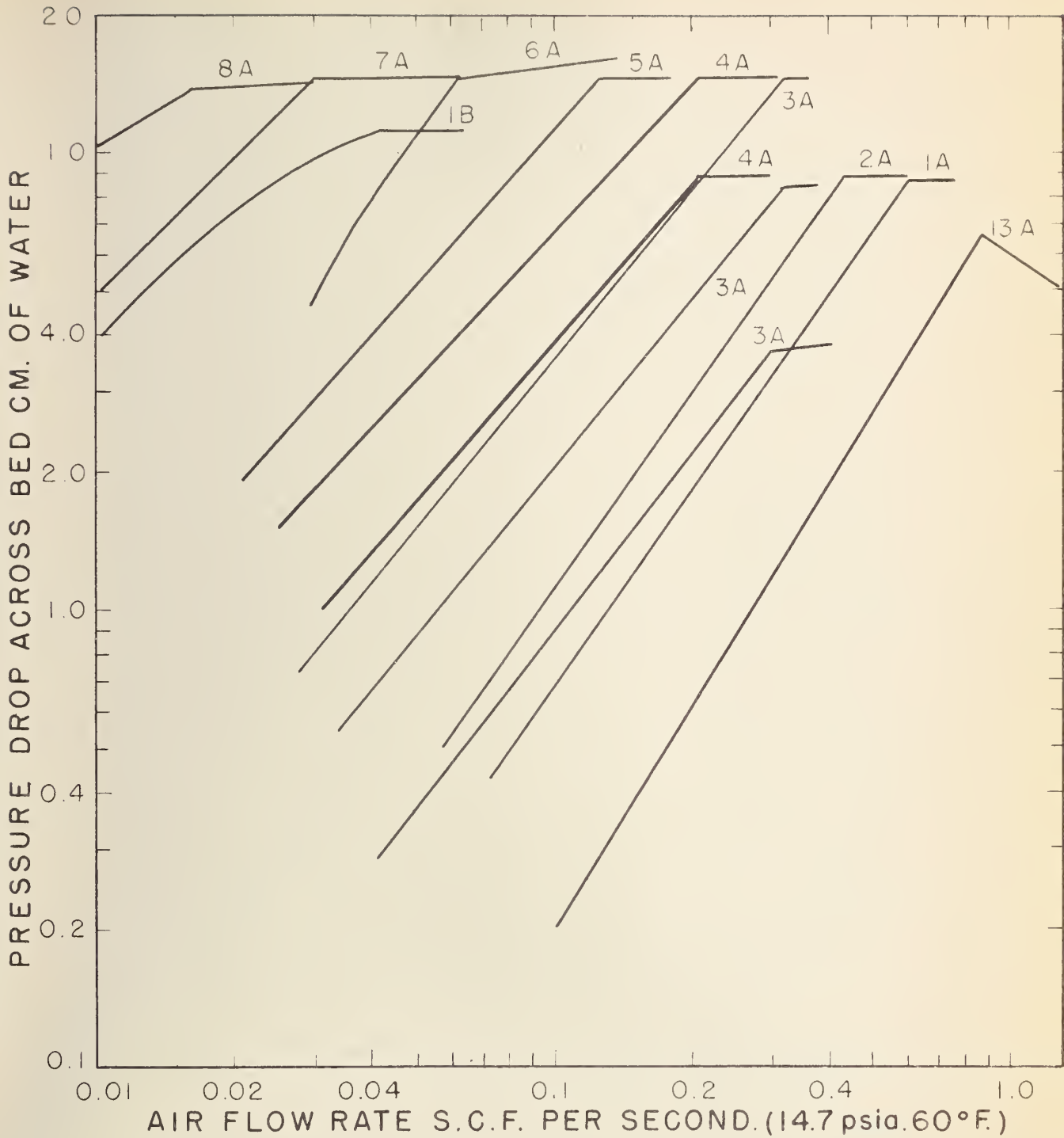
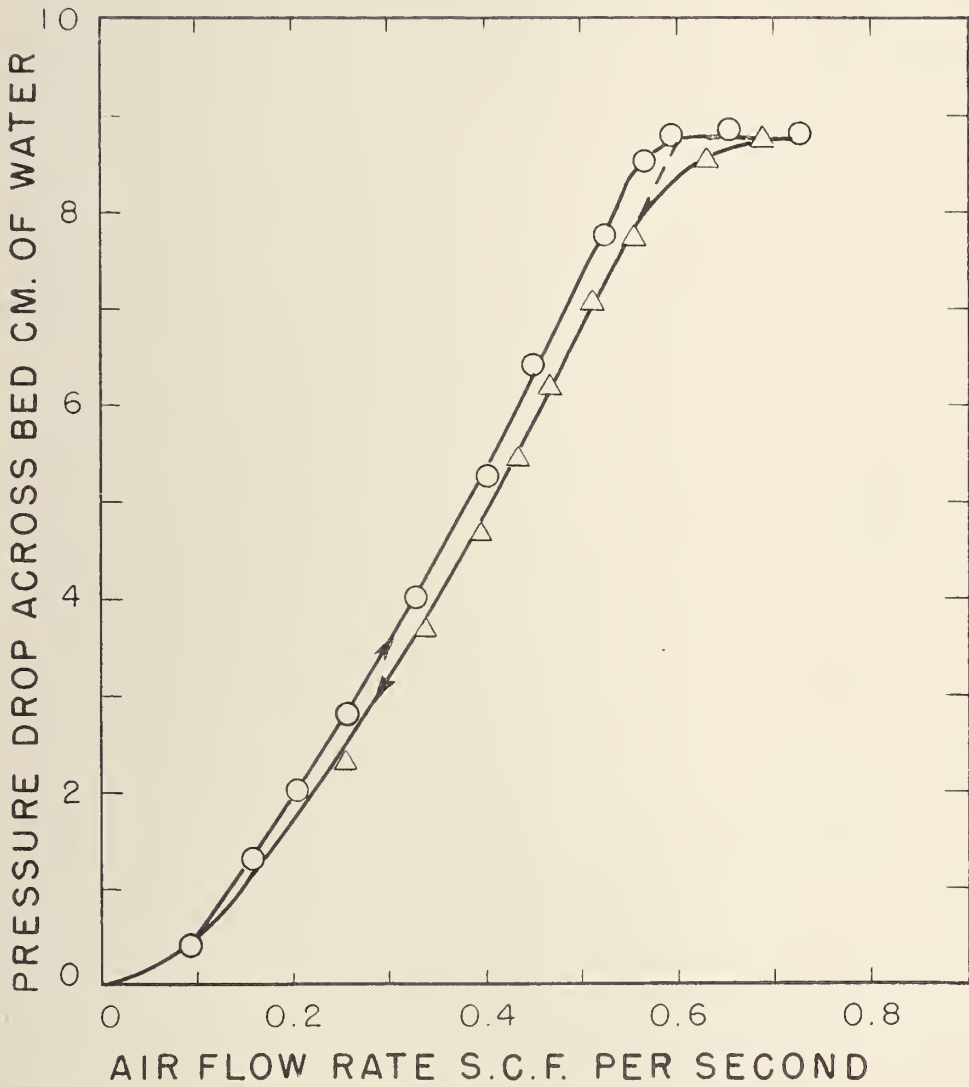
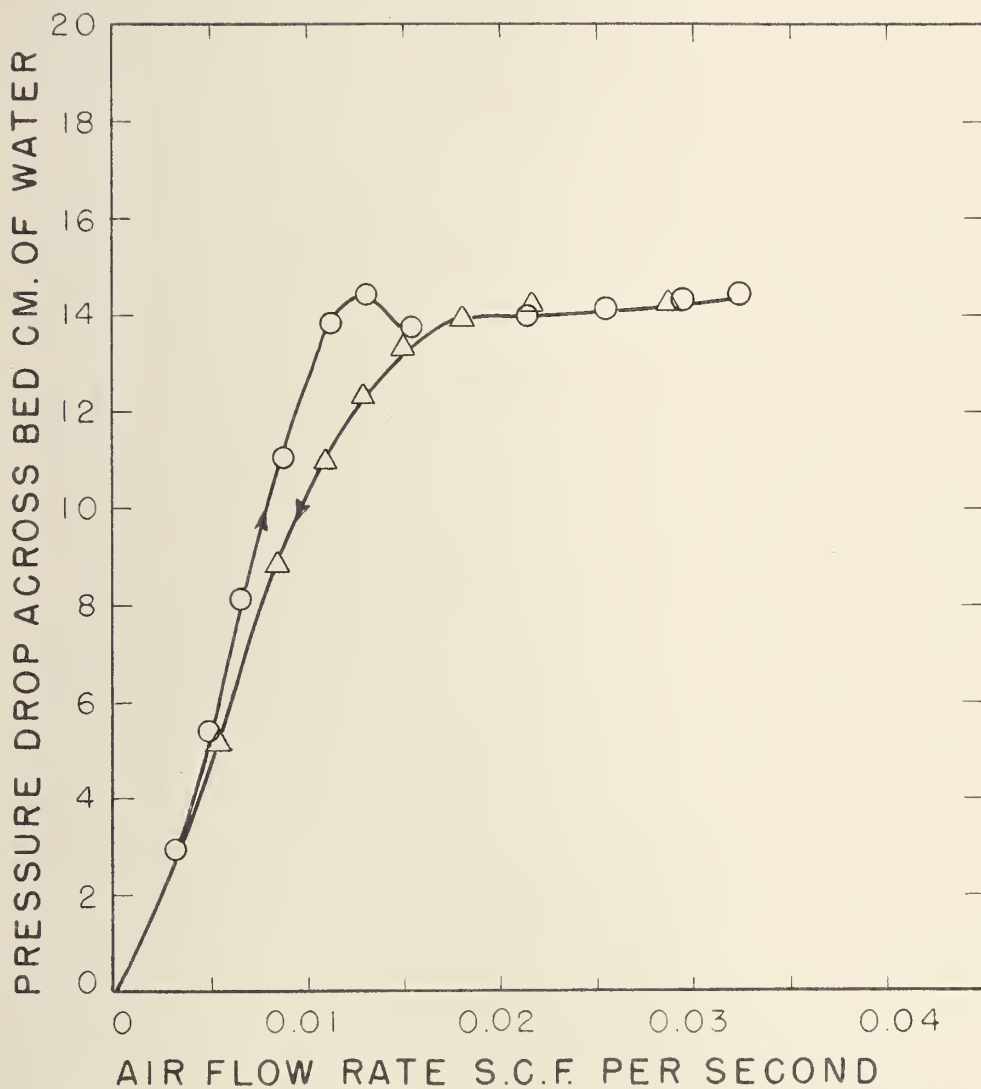


FIGURE 6. ALL RESULTS PRESSURE DROP VS. AIR FLOW RATE AS AIR FLOW RATE IS BEING REDUCED.



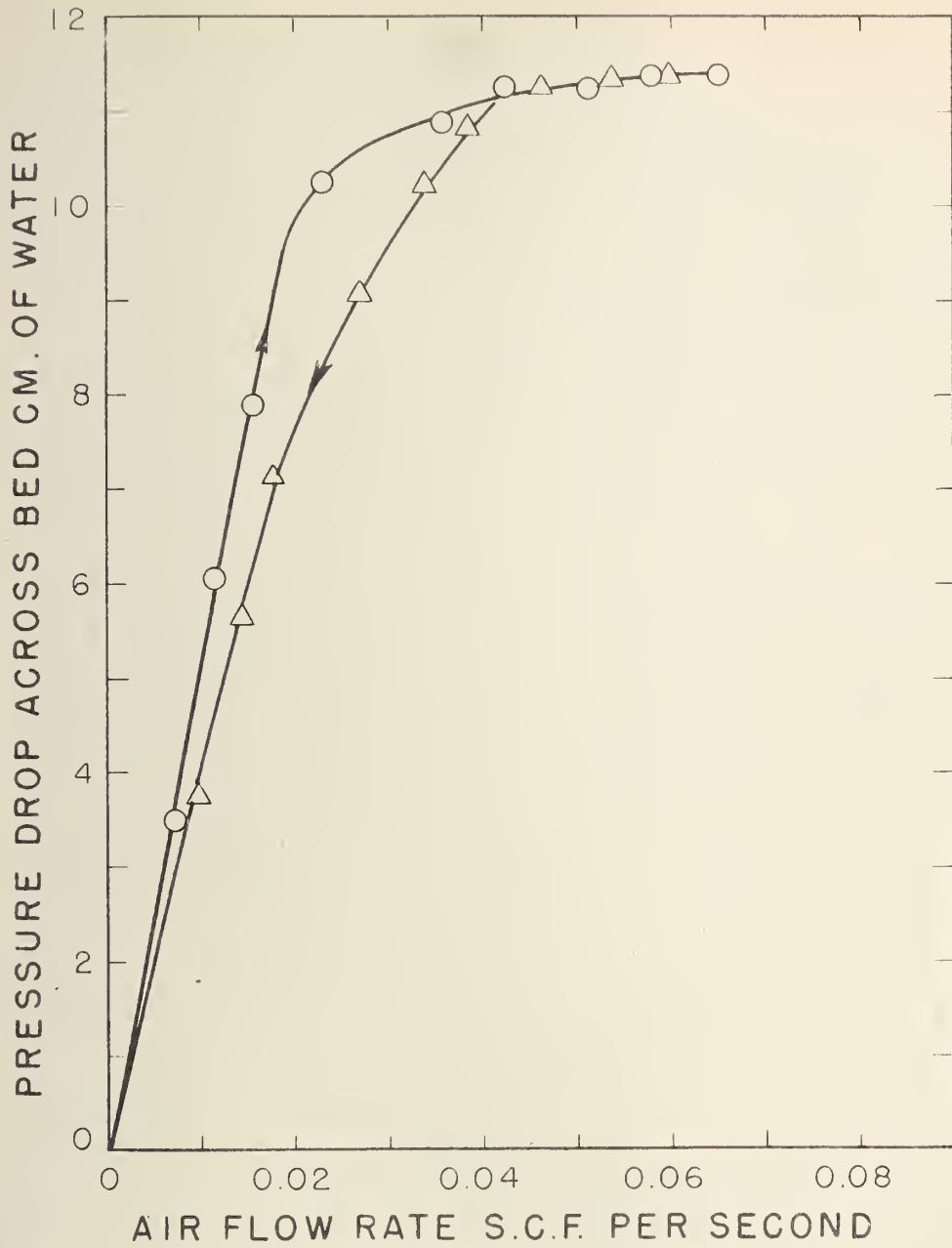
COAL SAMPLE 1A TYLER SCREEN -4 + 8

FIGURE 7. PRESSURE DROP VS. AIR FLOW RATE



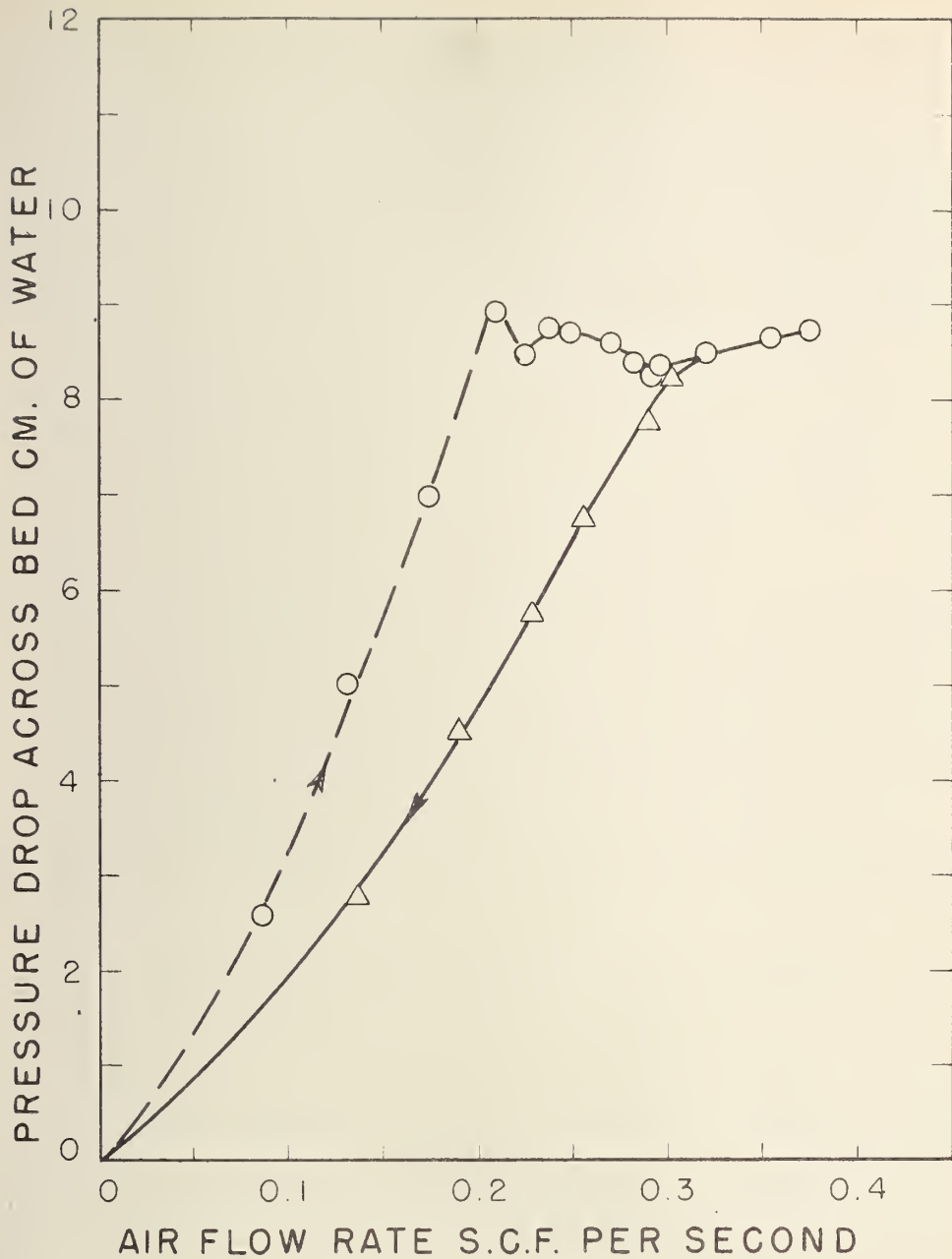
COAL SAMPLE 8A TYLER SCREEN -48 + 65

FIGURE 8. PRESSURE DROP VS. AIR FLOW RATE



COAL SAMPLE 1B TYLER SCREEN -10 ($-\frac{1}{16}$ IN.)

FIGURE 9. PRESSURE DROP VS. AIR FLOW RATE



COAL SAMPLE 3A TYLER SCREEN -10+14
RUN AS POURED IN FLUIDISATION TUBE

FIGURE 10. PRESSURE DROP VS. AIR FLOW RATE

curve for the bed as poured. The successive orientations of the bed to present a greater cross-sectional area for flow can be seen as sudden breaks in the plot.

As well as the critical gas velocity, several other properties of the particles and air were determined for the narrow size range samples. These were:-

1. Density of the bed at the critical gas velocity.
2. Bulk density of the particles.
3. True density of the particles.
4. Arithmetic mean diameter of the particles.
5. Equivalent diameter of the particles after Van Heerden et al. (10).
6. Density of the air.

The procedure for determining each was as follows:-

1. Density of the bed at the critical gas velocity.

The bed height was plotted against the gas velocity as the velocity was being decreased. The bed height at the critical point was then selected, and knowing the cross-sectional area of the bed and the mass of material in it, this quantity was easily evaluated.

2. Bulk density of the particles.

The coal sample was poured slowly into a 500 cc.

previously weighed measuring cylinder tilted at 30° to the vertical until almost 300 ccs. were in. The cylinder was then tilted slowly the opposite way until the surface was at right angles to the axis of the cylinder. Whilst holding it vertically the coal was sprinkled on to bring the level to the 300 cc. mark, it was then weighed and the bulk density calculated.

3. True density of the particles.

This was determined by the usual displacement method using toluene as the displaced liquid. It was constant for all samples within 1%.

4. Arithmetic mean diameter of the particles.

This was obtained from the arithmetic mean of the largest screen opening on which the sample was retained and the smallest through which it would pass.

5. Equivalent diameter of the particles.

Van Heerden defines this as being equal to the diameter of those spheres for which the number per unit volume of packed bed is the same as for the particles, both counted at maximum porosity. He has also shown that the maximum porosity of a bed of spheres equals 0.406. It follows then that if n is the number of particles per unit volume of bed at maximum porosity and D_e the equivalent diameter of the particles in inches then:-

$$n \pi D_e^3 / 6 = 1 - 0.406$$

i.e. $D_e = 1.04/n^{1/3}$

also letting

ρ_{bm} = density of the bed at maximum porosity, lbs/cuft.

and

m = number of particles in

x = grams of sample

then,

$$453.59 m \rho_{bm} / x = \text{number of particles / cuft.}$$

and,

$$D_e/12 = 1.04(453.59 m \rho_{bm} / x)^{-1/3}$$

which reduces to,

$$D_e = 1.623(x/m \rho_{bm})^{1/3} \dots\dots\dots(22).$$

Equation 22 was used to determine D_e . The number of particles in a certain weight were counted, (repeated three times for each sample) and knowing ρ_{bm} , D_e was calculated. The difficulty in the method (which is most tedious) is in deciding when a particle should be neglected due to its being very much smaller than the average particle. For instance a very small percentage of fine dust while having a negligible effect

on the fluidising properties, will decrease the magnitude of De considerably. In general particles which seemed to be less than one tenth of the average diameter were overlooked.

6. Density of the air.

This was evaluated assuming the air to be dry using the ideal gas law and the known pressure and temperature.

These properties together with the critical gas velocities are collected in Table 6 following. The critical gas velocity is expressed in various units. The actual velocity was calculated from the volume flowing knowing the temperature and pressure at the time of the test. Particle Reynolds numbers are also calculated at the critical, basing them on the two different mean diameters.

The critical gas velocity in ft/sec. is plotted against the arithmetic mean diameter of the particles in inches on log-log paper in Fig. 11. The slope of the curve varies from 2.0 to 0.5, i.e. we have,

$$V \propto D_p^n \quad 2 \geq n \geq 0.5$$

This same range of the exponent is found when V is the free fall velocity of a sphere having diameter

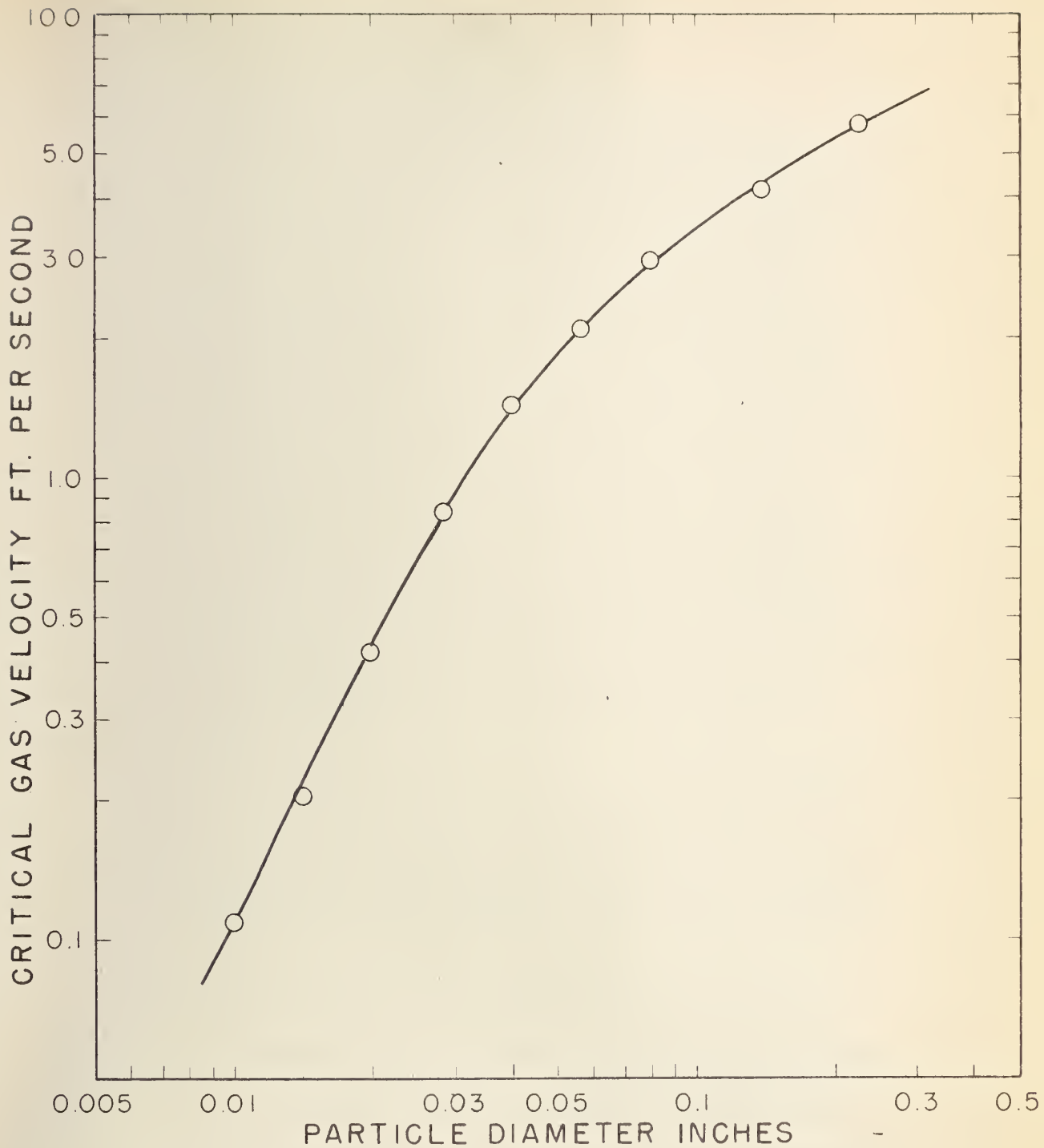


FIGURE II. CRITICAL GAS VELOCITY OF COAL PARTICLES
VS. PARTICLE DIAMETER.

Dp. The exponent 2 is for purely streamline flow, and the 0.5 is for fully turbulent flow. This graph then, lends itself to some measure of linear extrapolation at either end.

For comparison with other work, critical gas velocities have been evaluated for the narrow sized coal fractions by the method of Leva et al. (15), Eqn. 4; Baerg, Klassen and Gishler (2), Eqn. 10; and Van Heerden et al. (9) (10), Eqn. 7. They are the only investigators who have covered this range of particle sizes. No prior knowledge was assumed other than the arithmetic mean particle diameter, fluidising gas properties, particle density, bulk density of the particles and the bulk density at maximum porosity. The results of these computations, plotted in Fig. 12, indicate that the method of Van Heerden gives the closest check.

It was not thought advisable to attempt further treatment of this critical gas velocity data in view of the uniqueness of the system (coal particles/air) chosen.

The three other coal samples prepared namely -1/16 in., -1/8 in., and -1/4 in. screen were checked to see the closeness of the comparison between experimental and calculated critical fluidising velocities.

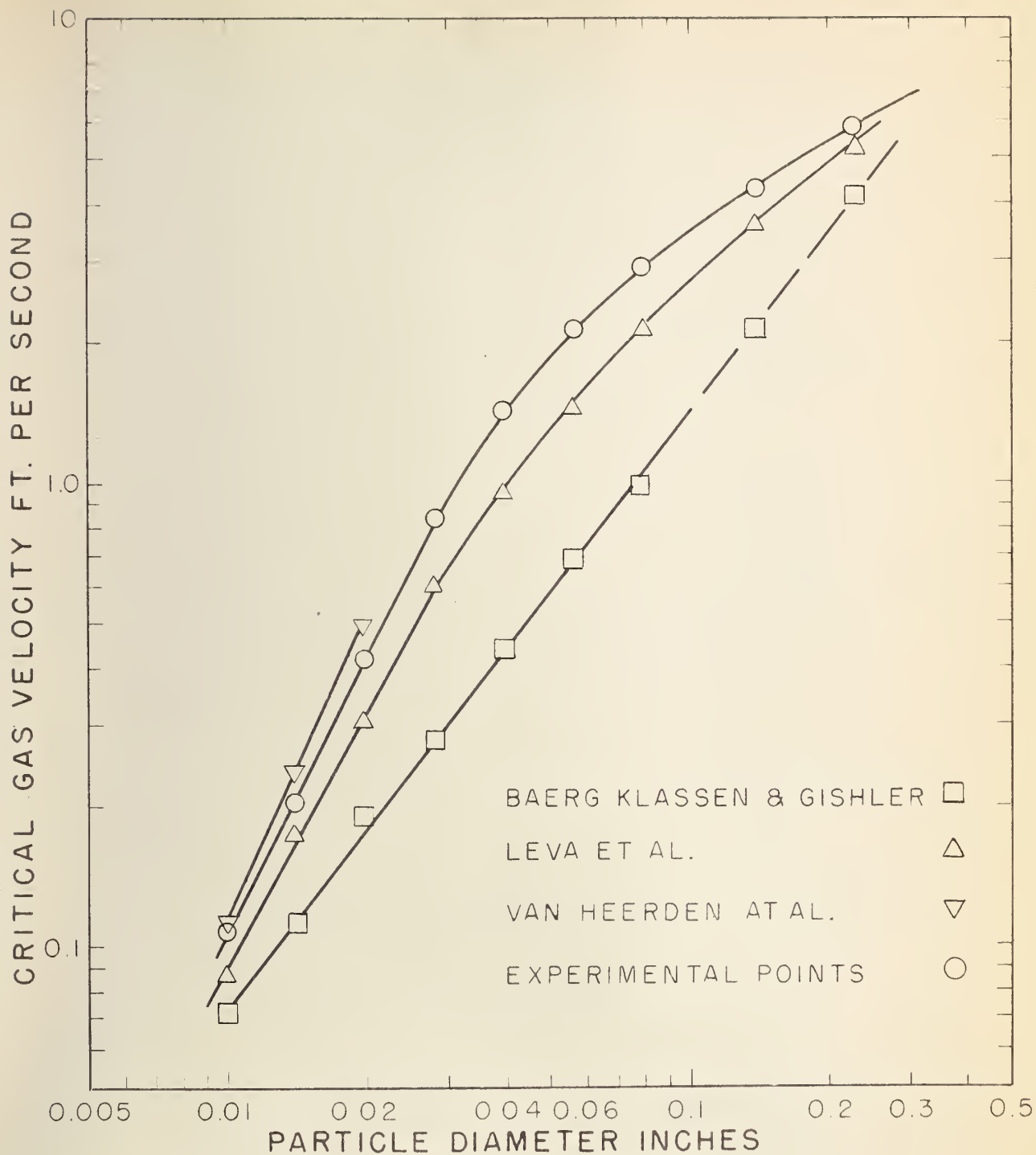


FIGURE 12. COMPARISON OF PRESENT WORK WITH THAT OF OTHER INVESTIGATIONS.

The difficulty with samples of such a wide size range is that during the course of fluidisation fine material is entrained at such a rate as to materially alter the average diameter, and unless provision is made (as was not done) for returning entrained material to the bed, the critical fluidising velocity will depend on the time taken to complete the test. This effect was so pronounced in the $-1/4$ in. and $-1/8$ in. sizes that no results could be taken. For the $-1/16$ in. size coal the following results were determined:-

A.M. mean diameter	=	0.0173 in.
Predicted critical gas velocity.	=	0.33 ft./sec.
Actual critical gas velocity.	=	0.28 ft./sec.

Since the bed density at the critical point, the true density of the coal, and the bulk density of the coal are known it is possible to work out the fraction voids as a function of particle diameter. The reasoning is as follows:-

$$\rho_{mf} = (1 - \epsilon_{mf})\rho_s + \epsilon_{mf}\rho_f$$

$$\rho_b = (1 - \epsilon_b)\rho_s + \epsilon_b\rho_f$$

that is:-

$$\epsilon_{mf} = \frac{\rho_s - \rho_{mf}}{\rho_s - \rho_f} \quad \text{and} \quad \epsilon_b = \frac{\rho_s - \rho_b}{\rho_s - \rho_f}$$

we can neglect ρ_f in comparison with ρ_s so we have:-

$$\epsilon_{mf} = 1 - \rho_{mf}/\rho_s$$

$$\epsilon_b = 1 - \rho_b/\rho_s$$

These computations have been performed for each particle size and are presented in Table 7 below, and plotted in Fig. 13. The usefulness of these figures depends upon the fraction voids penetrated by the toluene in obtaining ρ_s . It is a moot point whether the voids available for gas flow would be the same quantity, and increased penetration of toluene into the coal would increase the value of the fraction voids calculated. On the other hand the use of mercury as the liquid in the determination of ρ_s would lead to low values due to air being trapped with the coal particles.

TABLE 7. Void fractions in coal.

A.M. Particle diameter in.	ρ_{mf} lbs/cuft	ρ_b lbs/cuft	ρ_s lbs/cuft	ϵ_{mf}	ϵ_b
0.224		44.1	87.6		0.497
0.139	39.8	43.5	87.6	0.546	0.504
0.079	39.65	42.0	87.6	0.548	0.521
0.056	39.5	41.1	87.6	0.550	0.532
0.0394	39.0	40.2	87.6	0.555	0.541
0.028	39.4	39.5	87.6	0.551	0.550
0.0198	38.9	38.8	87.6	0.556	0.558
0.0140	37.6	38.0	87.6	0.571	0.567
0.0099	35.3	37.2	87.6	0.598	0.576

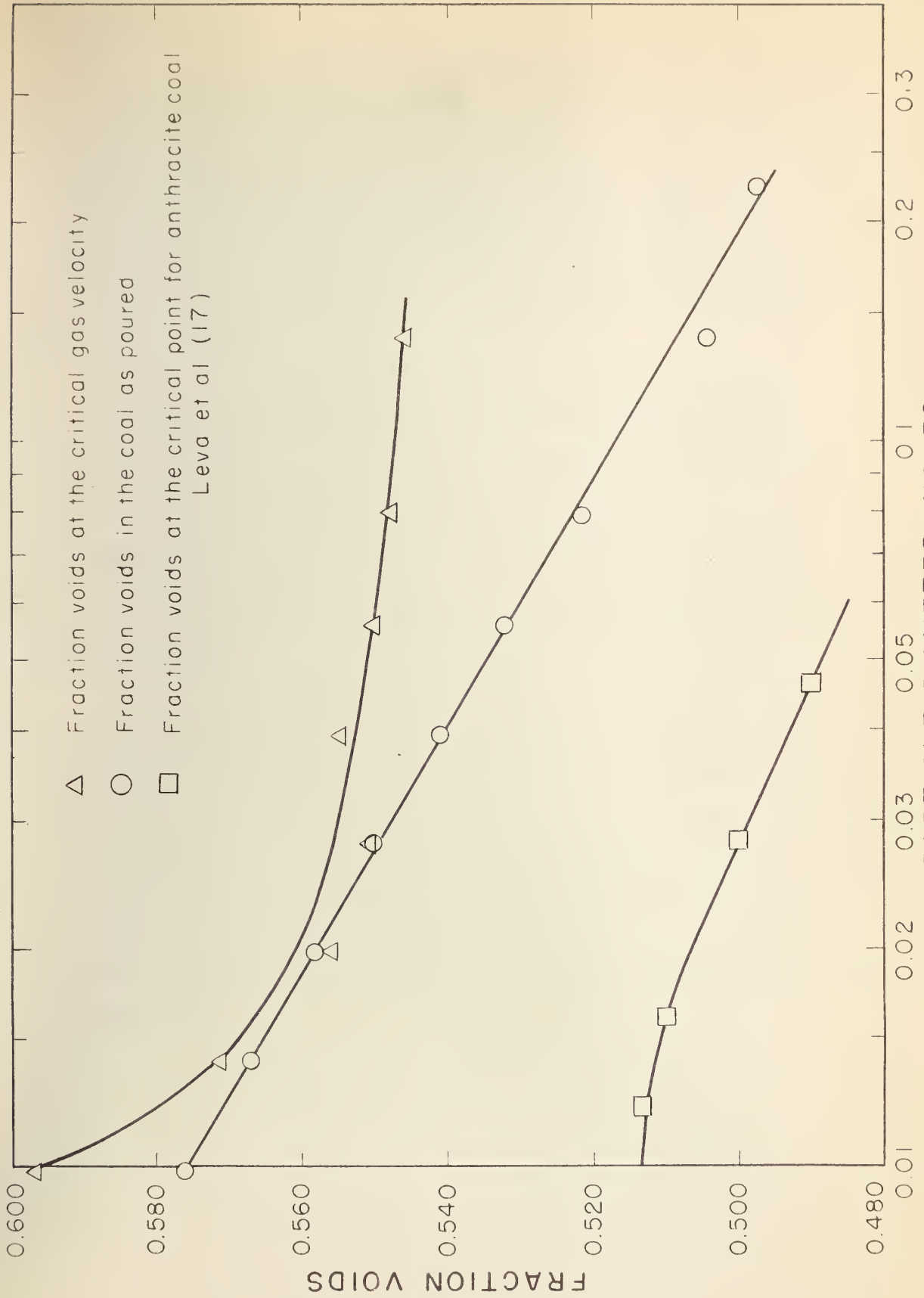


FIGURE 13. VOID FRACTIONS IN COAL.

G. Conclusions.

1. The discrepancies between the experimental curve of critical gas velocity against particle diameter and those obtained from the published correlations (page 61) are quite serious and indicate the inadvisability of using the correlations for systems other than those studied by their authors.
2. As indicated on page 63, the experimental value of the true density of the solid particles depends upon the method of determining it. Since this density is used to determine the void fraction in the fixed and fluidised beds, the absolute values of voidage so obtained are of doubtful significance.
3. The influence of the initial bed packing on the point at which the pressure drop vs. gas flow rate curve abruptly changes slope is shown in Fig. 10, page 53. This illustrates the necessity of defining the critical gas velocity as the velocity at the abrupt change in slope when the velocity is being reduced, since this does not depend upon the initial bed packing.

Table of Nomenclature for Part 1, Sections B, C and F.

A	Cross-sectional area of the fluidised bed.	ft. ²
B	Particle shape factor.	No dimensions
D _p	Particle diameter.	ft.
f	Friction factor.	No dimensions
f _F	Friction factor for fixed bed.	No dimensions
f _B	Friction factor for fluidised bed.	No dimensions
G	Superficial mass velocity.	lb./ft. ² sec.
G _{mf}	Superficial mass velocity at the critical point.	lb./ft. ² sec.
g	Gravitational acceleration.	ft./sec. ²
k	Constant in equation of Leva et al.	No dimensions
L	Height of bed.	ft.
M	Mass of fluidised bed.	lb.
n	State of flow factor.	No dimensions
S	Specific surface of the particles.	ft. ² /ft. ³
V	Superficial gas velocity.	ft./sec.
V _{mf}	Superficial gas velocity at the critical point.	ft./sec.
V _{ts}	Free fall velocity of a particle.	ft./sec.
ΔP	Pressure drop.	lb./ft. ²
Δp	Pressure drop.	poundals/ft. ²
ε	Void fraction (voidage, fraction voids).	No dimensions
ε _p	Void fraction in a stationary bed.	No dimensions
ε _{mf}	Void fraction at the critical gas velocity.	No dimensions
λ	Particle shape factor.	No dimensions

μ	Fluid viscosity.	lb./ft. sec.
ρ_b	Bulk density of particles.	lb./ft. ³
ρ_{bm}	Bulk density of fluidised particles at the critical velocity.	lb./ft. ³
ρ_f	Density of fluid.	lb./ft. ³
ρ_s	True density of solid.	lb./ft. ³
ϕ_s	Shape factor of particles.	No dimensions.

Dimensionless groups.

B ₁	Blake number.	$\frac{\rho_s - \rho_f}{\rho_f} \frac{D_p g}{V^2}$
$K_{\Delta P}$	Dimensionless group used by Wilhelm and Kwauk. (26).	$\frac{D_p^3 \rho_f g (\Delta P/L)}{2 \mu^2}$
$K_{\Delta P}$	Dimensionless group used by Wilhelm and Kwauk. (26).	$\frac{D_p^3 \rho_f g (\rho_s - \rho_f)}{\mu^2}$
Re _c	Reynolds number as modified by Carman(4).	$\frac{\rho_f V}{\mu_s}$
Re _o	Reynolds number at the critical fluidising velocity.	$V_{mf} \rho_f D_p / \mu$
Re _p	Reynolds number of the particles.	$V \rho_f D_p / \mu$

PART 2. CARBONISATION OF COAL IN A FLUIDISED BED.

A. The low temperature carbonisation of coal.

When coal, which though classed as a rock is of organic origin, is heated in the absence of air it is partially decomposed into a number of volatile materials. The nature of these materials and the solid carbonaceous material remaining depends upon the type of coal, the temperature to which it is heated, and the rate at which it is heated. In general two types of carbonisation, as this process is termed, are recognised, viz. low temperature, in the range 450-700°C and high temperature in the range 900-1200°C. The important products from high temperature carbonisation are the solid residue (coke) which is suitable for smelting and the gas which is important as a fuel. The liquid products are usually classed as a by-product.

In low temperature carbonisation on the other hand the object usually is to upgrade a low heating value coal and at the same time produce a higher yield of liquid compounds than is obtained from the high temperature process. However, the yield of gas is much lower and in general is not sufficient to provide the heat necessary for carbonisation. The liquid products other than water from low temperature carbonisation consist

mainly of aromatic and **naph**thenic compounds which form a useful starting point for an organic chemical industry. The solid residue (semi-coke) is usually of high reactivity and is more suitable as a fuel than the parent coal.

From an engineering stand-point the problem in low temperature carbonisation has been to supply heat to the coal charge at a sufficiently high rate without at the same time overheating a part of the coal. This has led in the past to a multiplicity of designs for mechanically stirring and moving the coal charge over the heat transfer surfaces, which have not been too successful. The use of a fluidised bed is an apparent solution to this problem and is at present being studied extensively.

B. Properties of Alberta Coals.

As shown by the accompanying coal map, Fig. 14, the coals of Alberta fall into several different classifications, and each type is distributed in a band roughly parallel to the Rocky Mountains. Coal is material of organic origin which has been changed by the loss of hydrogen and oxygen. The main factors which bring about this change are age, heat and pressure. The latter

FIGURE 14.

Coal Map of Alberta

COAL AREAS OF ALBERTA



KEY MAP

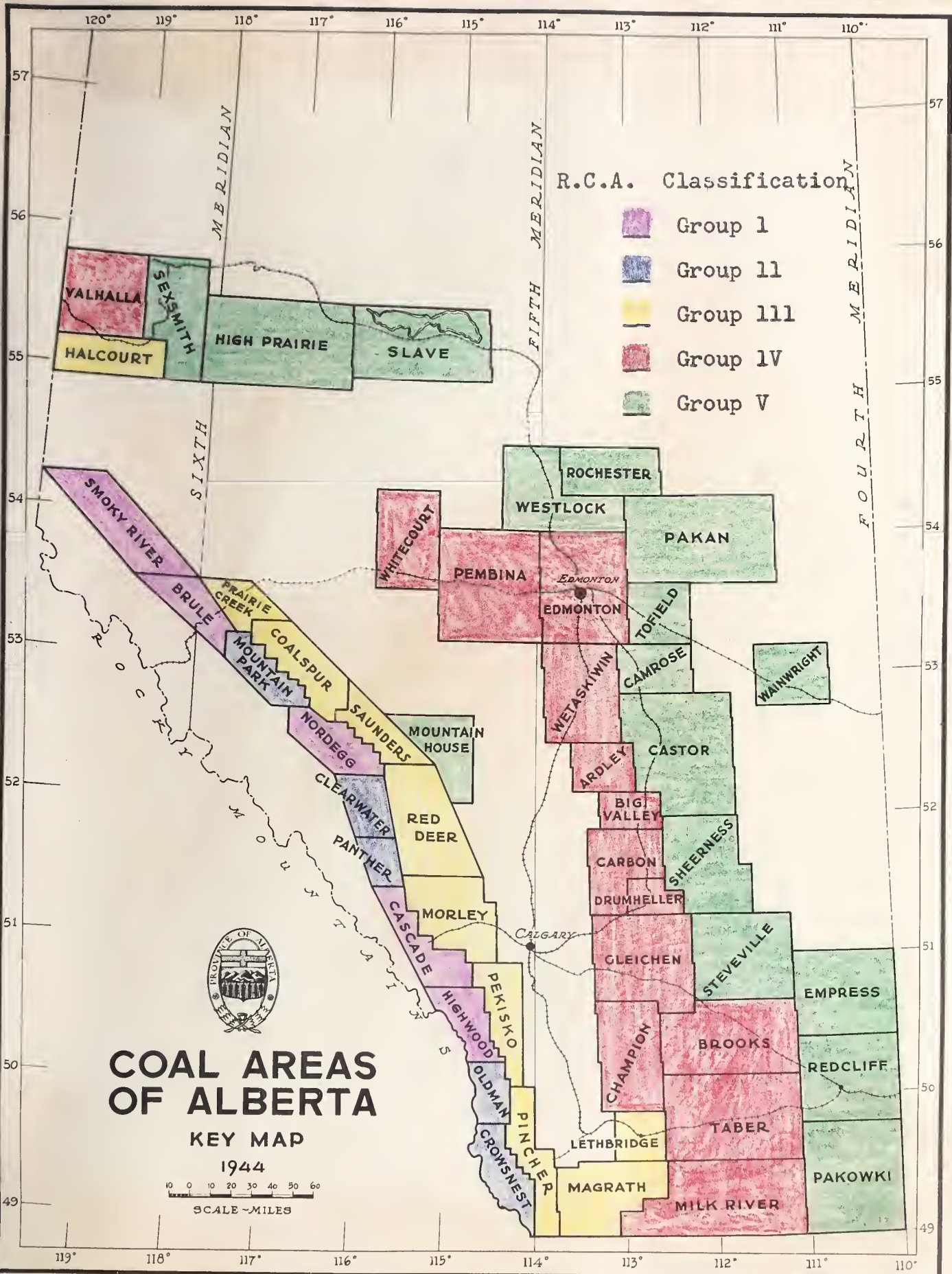
1944

0 10 20 30 40 50 60
SCALE - MILES



R.C.A. Classification

-  Group 1
-  Group 11
-  Group 111
-  Group 1V
-  Group V





are more important in the maturing, as it is called, than the former. It will be appreciated then that the nearer a coal lies to the Rocky Mountains the more pressure it has been subjected to. It is for this reason that the coals lie in bands and that the rank, which is the degree of transformation of the coal from plant material to the present day limit of anthracite increases from east to west.

The system of classification adopted in Canada is that outlined in A.S.T.M. D388-38 and is a classification by rank. In this classification, high rank coals are ranged in order of the percentage of fixed carbon in the dry mineral matter free coal. The greatest carbon is the highest rank. In the lower ranks the classification is based on the calorific value of the mineral matter free coal, but with water as it occurs in the seam. There are secondary classifications based on the weathering and coking properties of the coal.

The greatest coal production in the province occurs in the north south region running through Edmonton, Drumheller, and Taber. These coals are not the highest quality mined in the province but are the most accessible. In the A.S.T.M. classification they are subbituminous B i.e. they have a moist calorific value between 9,500 and 11,000 B.T.U./lb. and are weathering and non-agglomerating (non-coking). Some typical analyses of this type

X

of coal are given below, Table 8 taken from (24).

Table 8. Typical properties of Alberta subbituminous B coals.

District	Moisture %	Ash %	V.M. %	F.C. %	C.V. gross B.T.U./lb.
Edmonton B	25.0	6.2	28.4	40.4	8,860
Drumheller A	18.0	6.6	31.2	44.2	10,020
Taber A	15.3	10.2	31.5	43.0	9,500

These coals do not coke on heating and lend themselves admirably to upgrading by low temperature carbonisation. They also have poor weathering properties but since they have to be crushed before fluidised carbonising, this is no disadvantage. Accordingly these subbituminous coals as mined near Edmonton were chosen for the initial runs of the carboniser.

For an exhaustive treatment of the occurrence, analysis and utilisation of Alberta coals, the appropriate reference (24) should be consulted.

C. Equipment Design.

The design details concerning the carboniser, carboniser heater, and related equipment appear in Appendix B. The following discussion concerns only

the flow plan and significant dimensions.

The unique properties of the fluidised bed which lend themselves to the low temperature carbonisation of coal are, ease of solids handling permitting continuous operation, and high heat transfer rates. For small scale plants such as this the solids handling techniques of oil catalytic cracking, involving fluidised transfer lines, specially designed slide valves, and a multiplicity of gas injection points etc. are not easily scaled down. It was therefore decided to use a screw feeder to inject coal into the base of the fluidised bed and to allow the carbonised coal to overflow down a central pipe into a hopper below.

There are four possibilities for transferring heat to the bed, firstly in the fluidising gas, secondly by injection of heated particles, thirdly by partial combustion of the coal charge, and fourthly through the walls of the retaining vessel. The first was rejected because of the low rates which could be obtained with practical fluidising velocities and the second because of the solids handling problem, though in a commercial plant this would be quite feasible. It is not known whether the third method affects the tar and light oil yields, it will certainly affect the gas composition, the fourth method was therefore decided upon. The heat transfer coefficients from a fluidised

bed to the wall are quite high ranging from 20 to 100 B.T.U./ft.² hr. °F. It was decided to take advantage of this fact not only for heat transfer from the wall to the carbonising fluidised bed but also from a fluidised bed supplying heat to the wall. Before proceeding with this design, however, it was decided to determine the ease with which a fluidised bed could be used as a source of heat, and the fuel chosen was naturally coal or coke. A furnace was accordingly constructed as in Fig. 15, from 3 in. pipe. Two pounds of -20 + 30 Ottawa sand were first charged to the bed and fluidised with air. The bed was then heated through the wall below the lagging using a welding torch. It was found after some experimentation that after the temperature of the fluidised bed reached 1200°F, -1/16 in. mesh coal could be injected and the outside heat source removed. The bed remained fluidised, the coal burnt practically instantaneously and the temperature could be controlled by the amount of coal added. This particular furnace was kept at 1500 - 1600°F. for a considerable length of time. It was therefore decided to adopt this method to heating the carbonisation reactor and to use natural gas to bring the sand bed to temperature before commencing coal injection. Previous studies had shown that coal crushed to -1/16 in. mesh would be most suitable for fluidisation. The only other major decision was

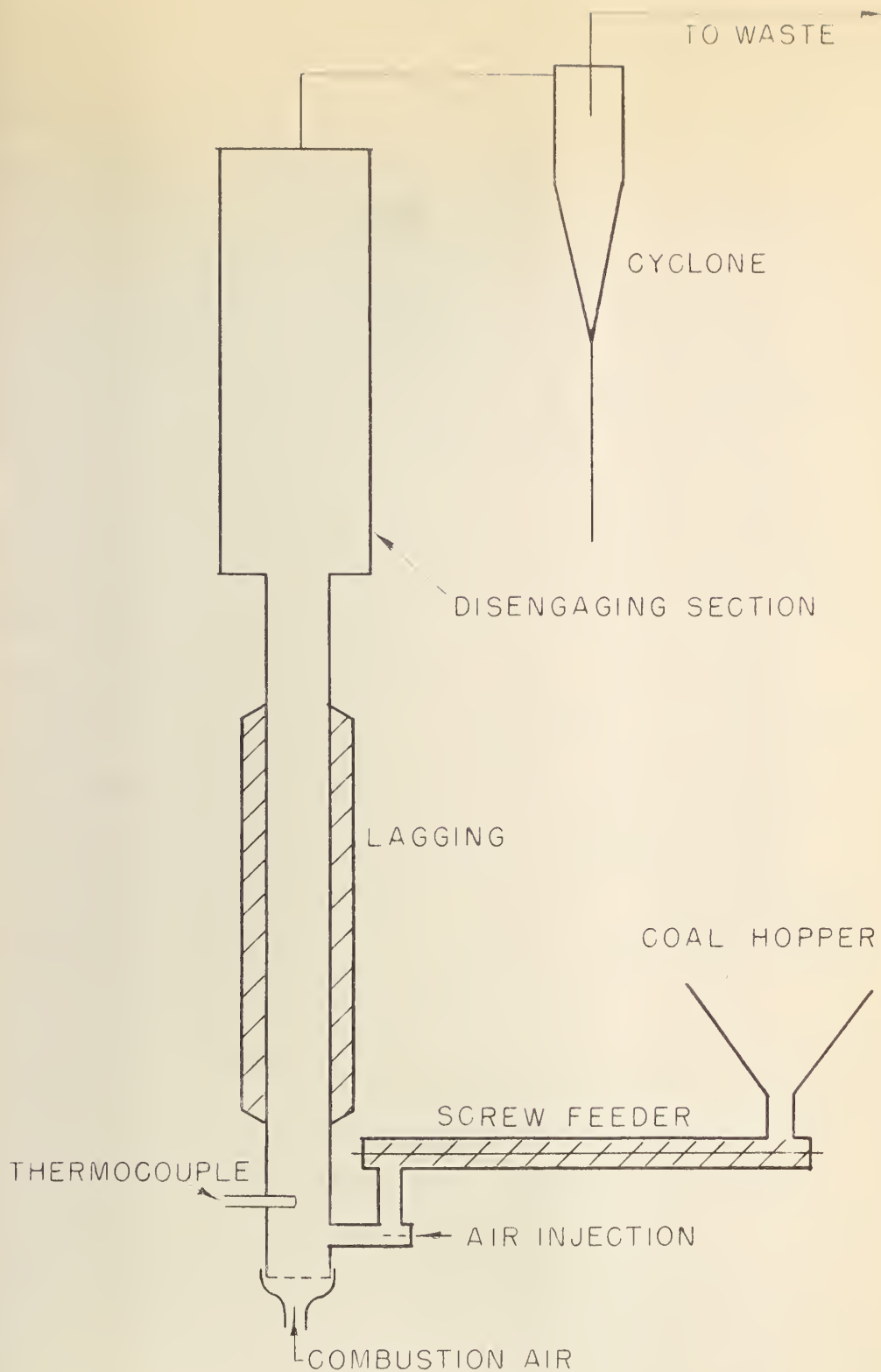


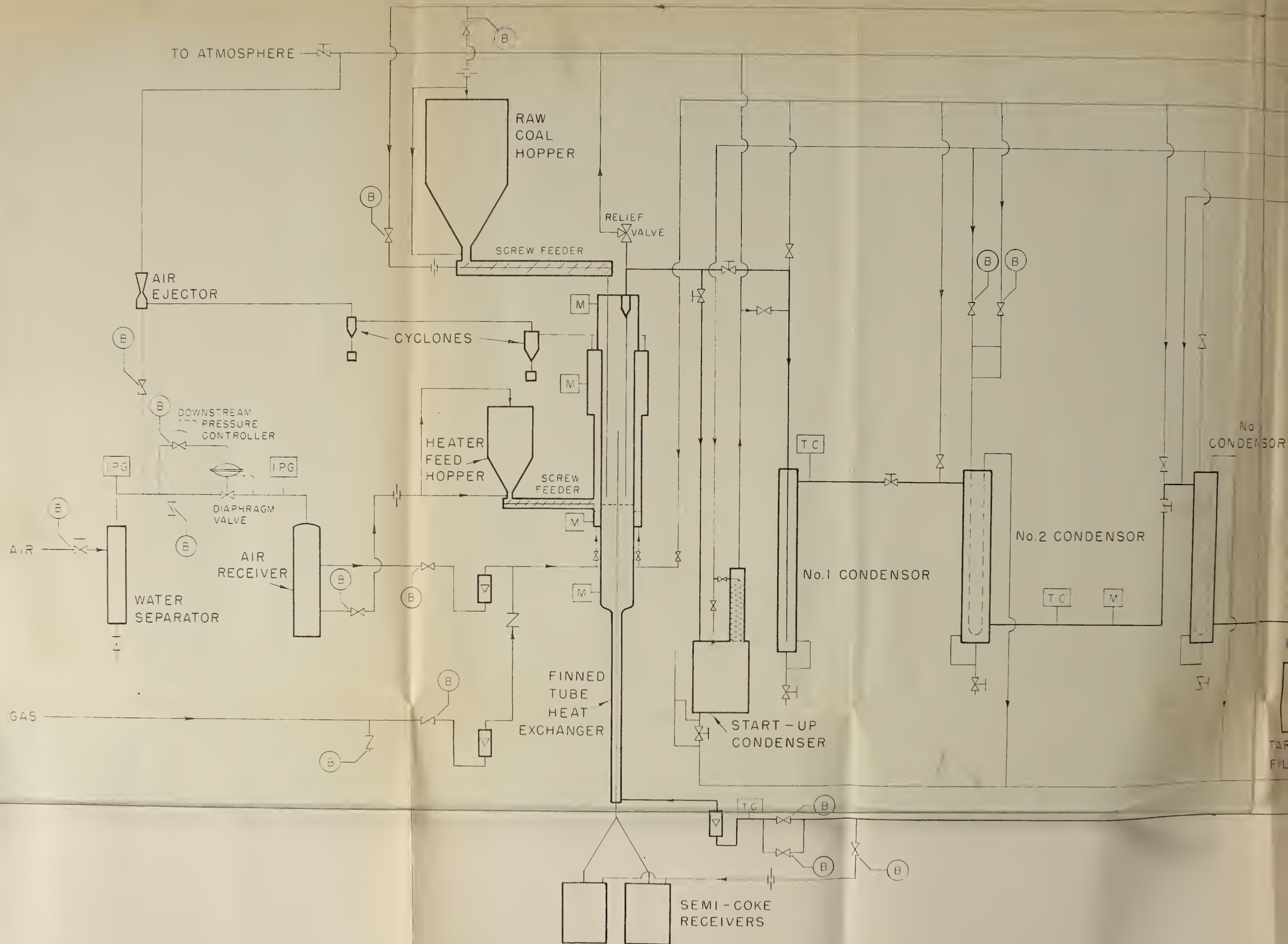
FIGURE 15. FLUIDISED COAL BURNER.

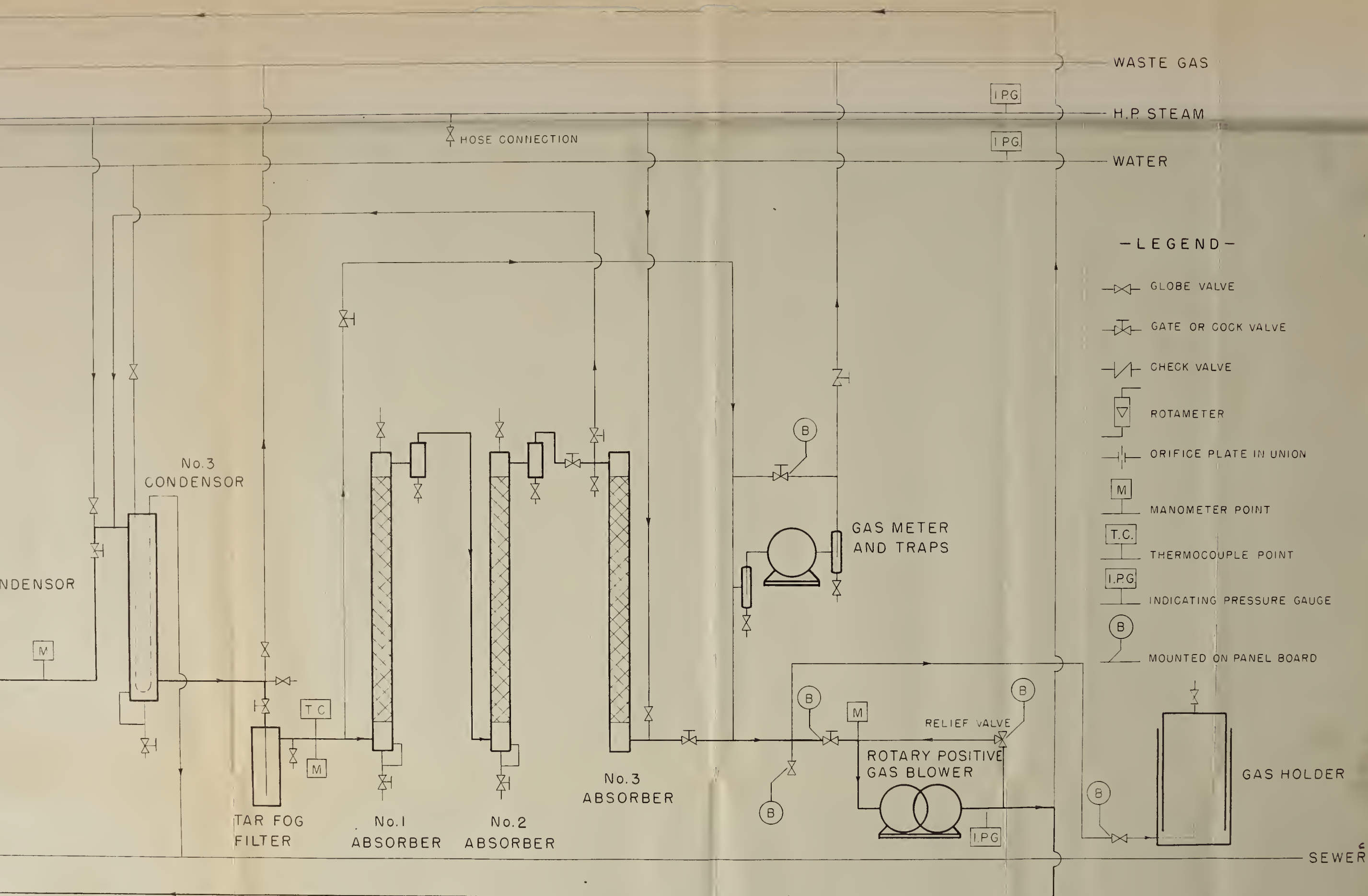
the nature of the gas to be used to fluidise the coal and the proposed through-put. It was agreed that 60 lb./hr. of coal as received would yield sufficient quantities of products for extensive tests, this was accordingly adopted, and it was decided to use the dry gas from the carbonisation after product recovery to fluidise the coal, which would minimise losses of low boiling liquids from the system. However, this does not preclude the use of air involving actual heat release by combustion in the fluidised bed, or the use of an inert gas such as nitrogen, at a later date. The complete flow sheet of the equipment is indicated in the attached Fig. 16. Some photos, plates 1 to VI, give an idea of the physical layout, and an enlarged drawing of the carboniser and heater appears in Fig. 17. In discussing the equipment reference will be made to this last figure and the simplified flow sheet of Fig. 18.

Referring to Fig. 17, the carboniser and carboniser heater are built as a unit constructed of two sections bolted together. The inner 6 in. diameter tube with a 10 in. disengaging section above is the carboniser proper. Both the carboniser and the outer shell are constructed of 3/16 in. type 316 stainless steel. The two cover plates are mild steel. The raw coal hopper and screw feeder are connected to the carboniser through a flexible bellows so they may be continuously weighed on a platform scale.

FIGURE 16

Complete Flow Sheet.





RESEARCH COUNCIL OF ALBERTA

FLUIDISED COAL CARBONISER

FLOW SHEET

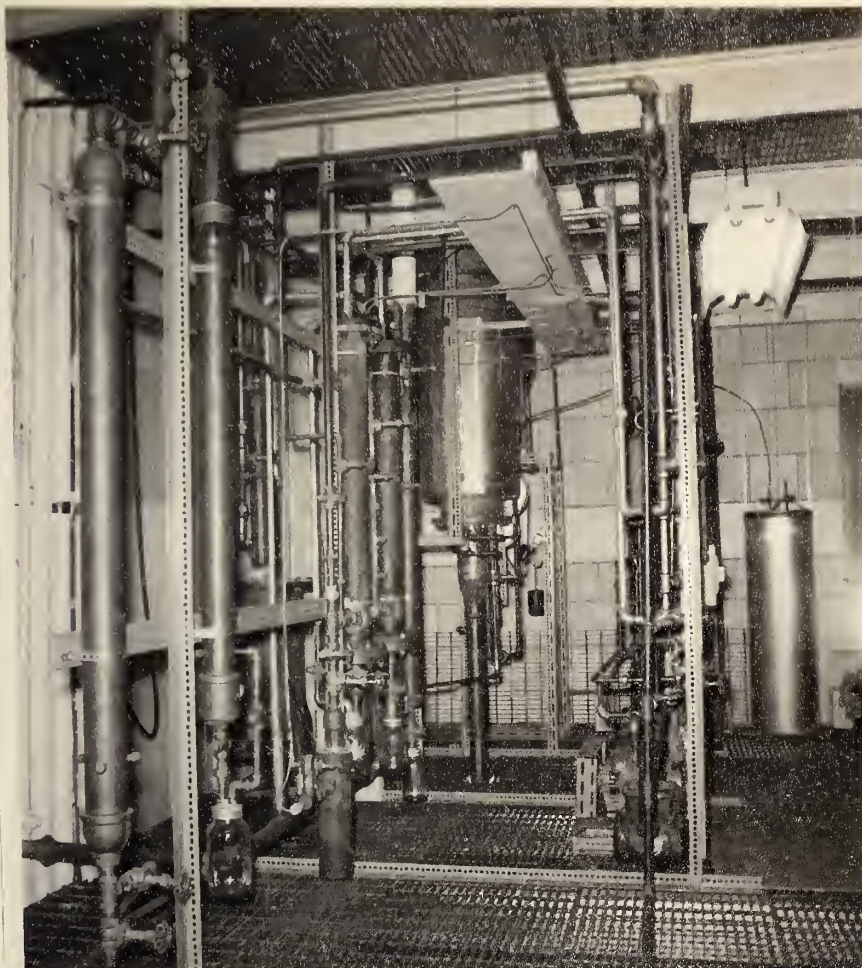


PLATE 1. General view of the Equipment.

From centre to left are seen, the carboniser and heater, nos. 1, 2 and 3 condensers, the tar fog filter, and nos. 2 and 3 absorbers. On the extreme right is the gas holder with the panel board between it and the carboniser.

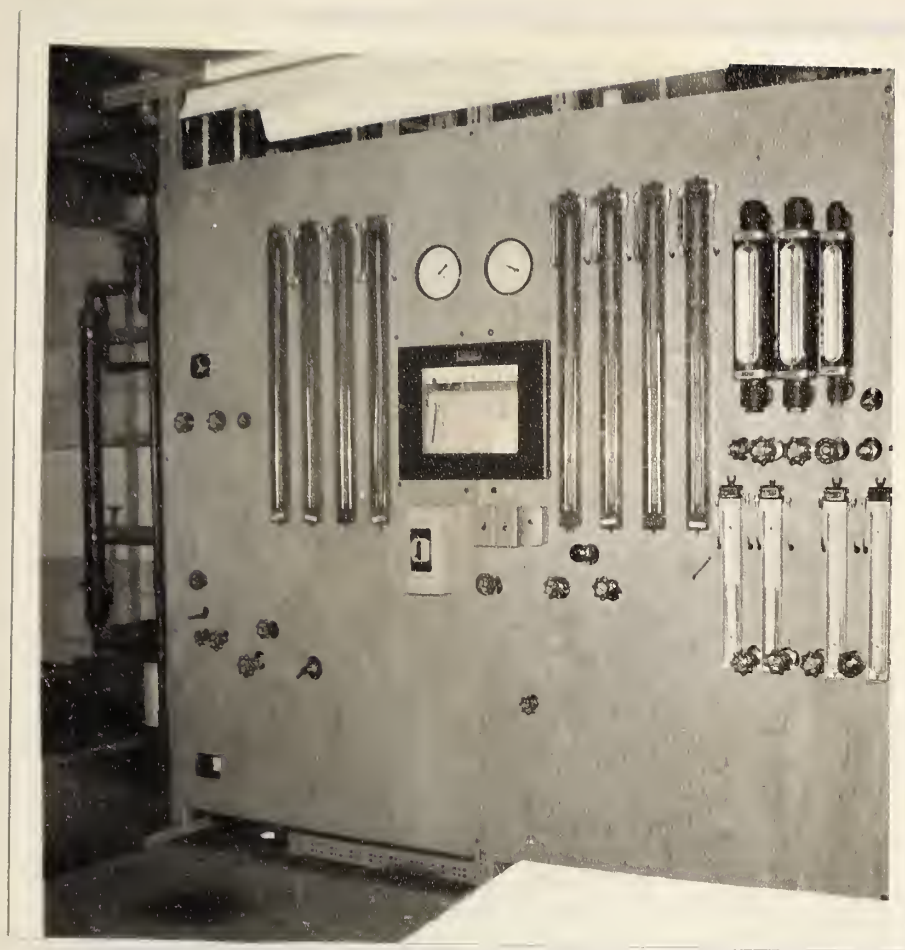


PLATE 11. General view of the Panel Board.

The right hand side is devoted to the carboniser and heater control, the left hand side to product recovery control.

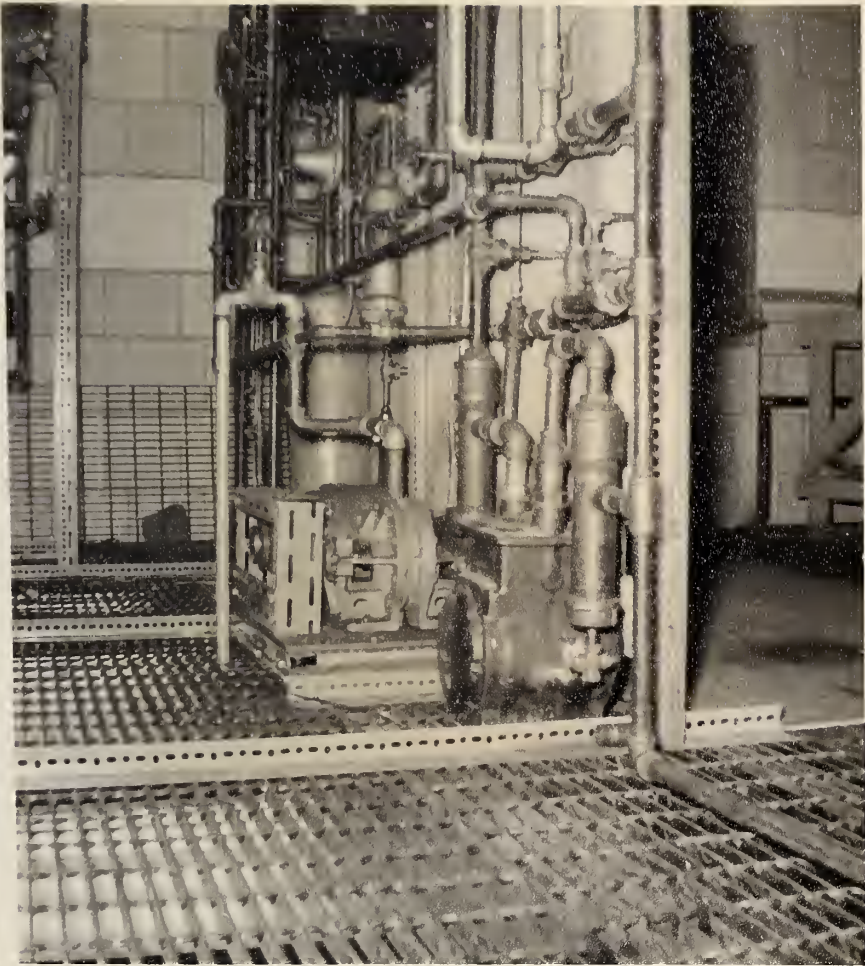


PLATE 111. Rear of Panel Board.

In the centre is the fluidising gas recirculating blower, on the right are the gas meter and traps. The line on the right comes from no. 3 absorber.

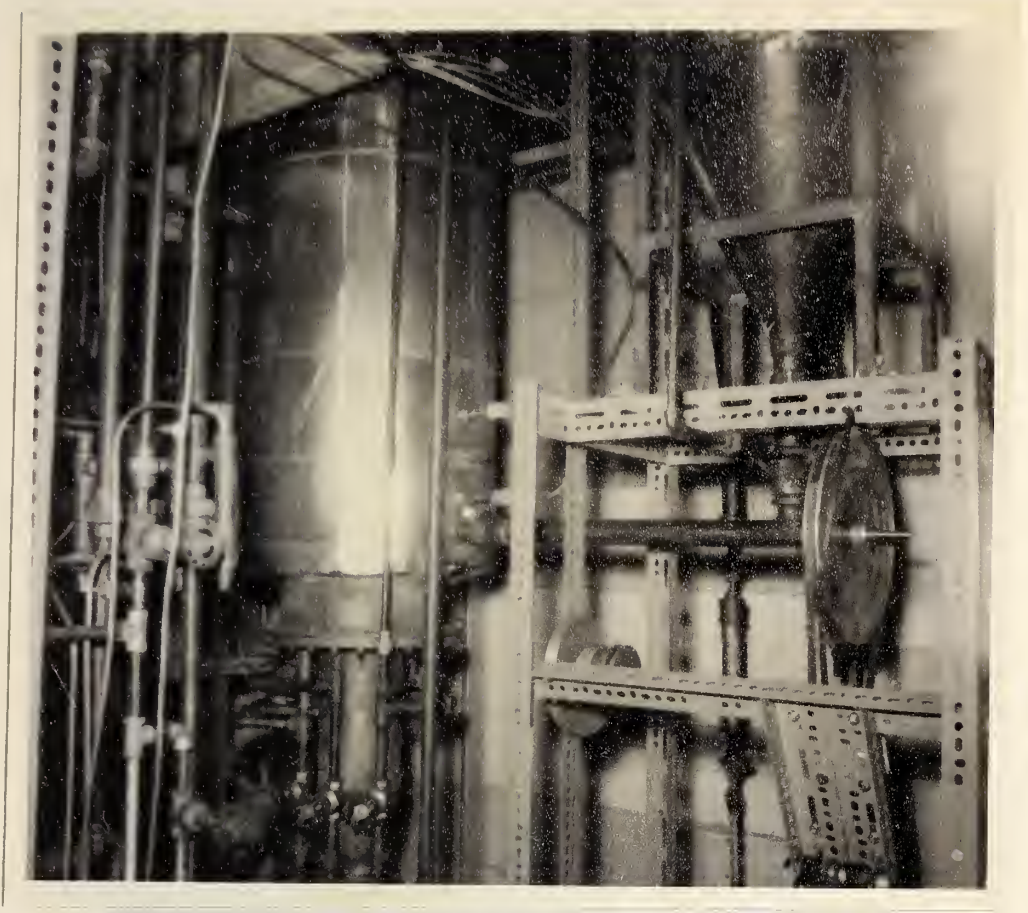


PLATE IV. Heater and Heater Feed Hopper.

The lower part of the heater feed hopper can be seen on the right, joined by the screw feeder to the carboniser heater.

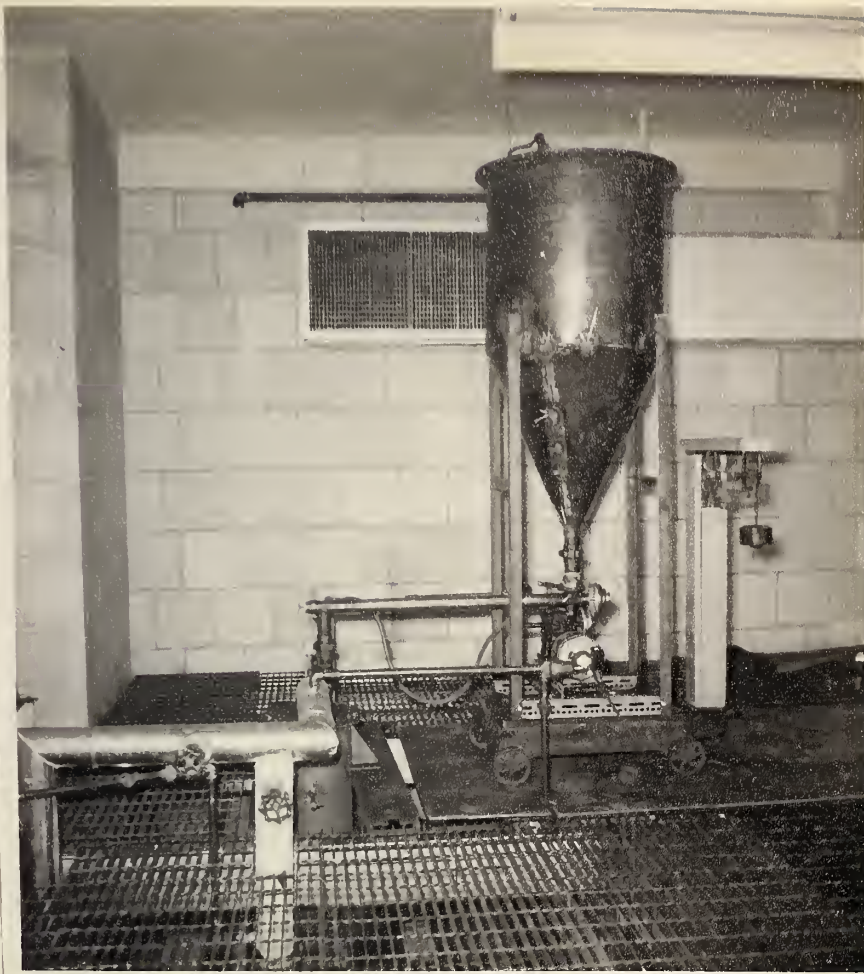


PLATE V. Coal Feed Hopper.

The coal feed hopper, screw feeder and its drive are all mounted on the platform scale. The flexible metal coupling can just be seen below the union at the left. In the foreground are the product transfer lines.

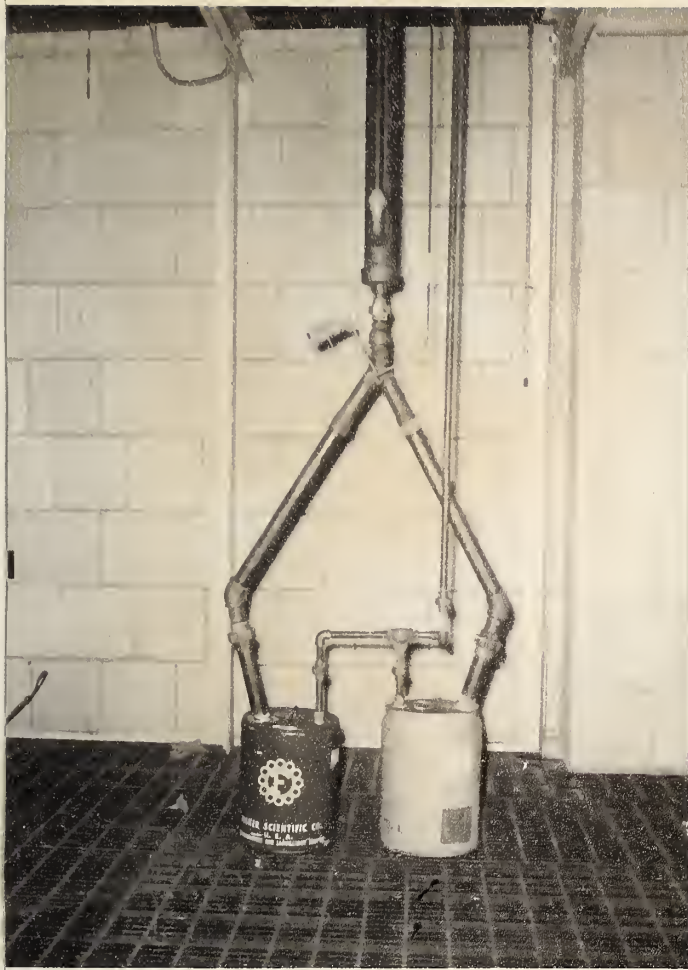


PLATE VI Semi-coke receivers.

At the top can be seen the lower half of the semi-coke/gas heat exchanger extending from the carboniser above. Below this is the two way flap valve leading to the semi-coke receivers.

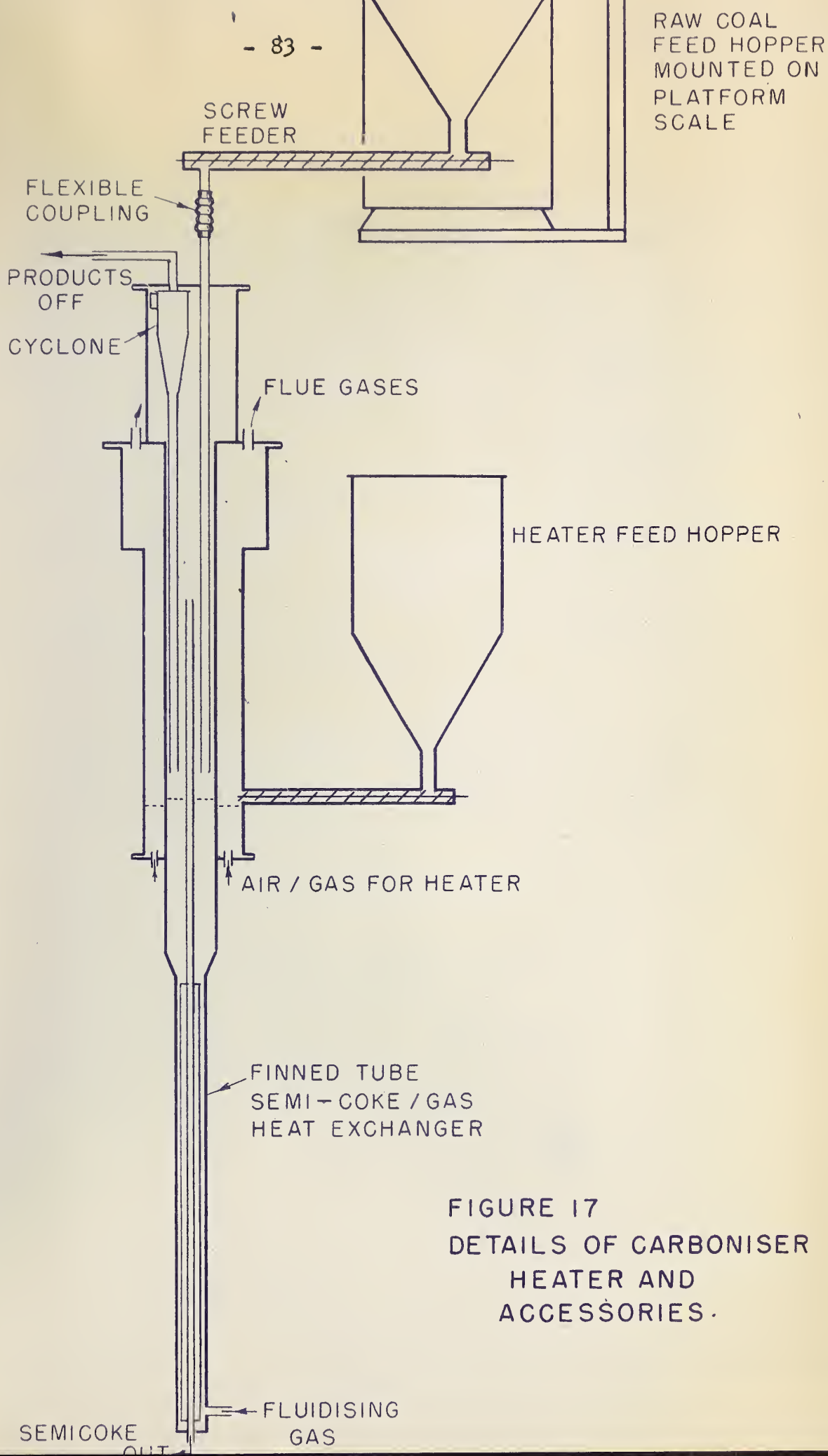


FIGURE 17
DETAILS OF CARBONISER
HEATER AND
ACCESSORIES.

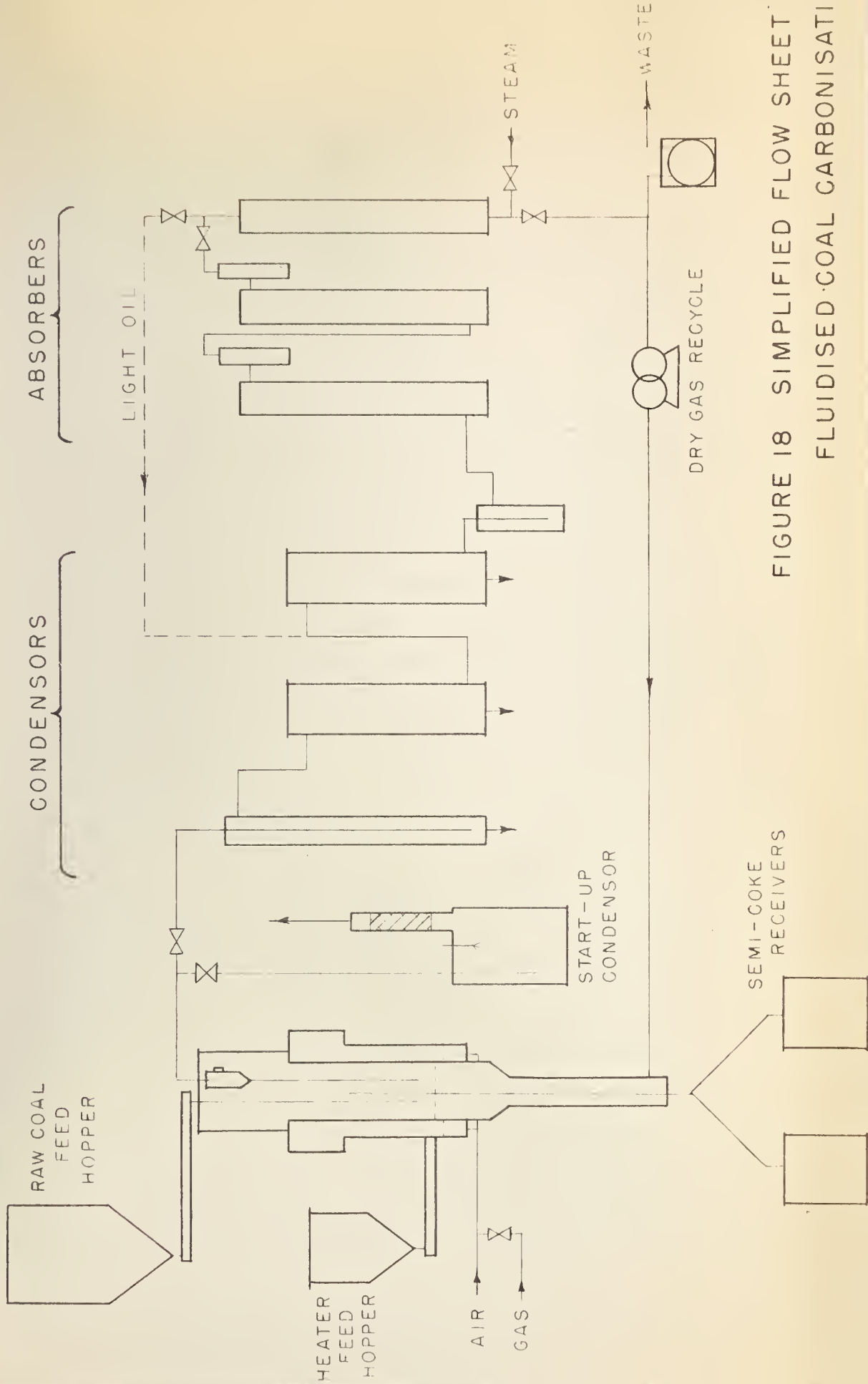


FIGURE 18 SIMPLIFIED FLOW SHEET
FLUIDISED COAL CARBONISATION

The coal ground to $-1/16$ in. mesh drops from the screw feeder down a 1 in. pipe to about 3 in. above the supporting screen for the fluidised bed. Sufficient gas is injected into the coal hopper and the screw feeder to prevent flow of carbonisation products back along the feed line, and to ensure that the coal is not carbonised in the feed inlet pipe. The coal is carbonised in the fluidised bed and the semi-coke flows down through the central 1 in. pipe which is also sealed by an upward flow of gas. This pipe which is attached at its lower end to a finned tube heat exchanger terminates just above the screen supporting the bed in a screwed coupling, different length sections can then be screwed in from the top to vary the height of the bed. From the base of the heat exchanger the semi-coke passes through a two way flap valve to one of two semi-coke receivers. The fluidising gas passes up the outside of the finned tube which is supported in a 3 in. standard pipe screwed into the base of the carboniser. It is heated by the hot semi-coke passing down through the centre, and passes up through the supporting screen which consists of a lower $3/8$ in. stainless steel plate drilled with $1/4$ in. holes to which is wired a 100 mesh stainless steel screen. The whole assembly rests on a stainless ring welded to the inside of the 6 in. tube. The products of carbonisation pass up through the disengaging section and a cyclone

where the remaining entrained solids are removed. The solids are returned to the bed and the products pass out to the recovery section.

The heater, which consists of a 12 in. diameter shell with a 16 in. diameter disengaging section above it, is concentric with the carboniser. The base is a $3/4$ in. mild steel plate sealed around the 6 in. tube with packing and a packing follower ring. Six $1/4$ in. air/gas inlet ports are mounted in the base. The supporting screen for the heater is, like the carboniser screen, constructed of a $3/8$ in. stainless steel plate drilled with $1/4$ in. holes with a 100 mesh stainless screen. The assembly is forced up against a ring welded around the outside of the shell by threaded stainless rods projecting through and up from the bottom cover plate. Wear plates of $1/8$ in. stainless steel, $1\frac{1}{2}$ in. diameter, are mounted 3 in. above each burner port. Semi-coke for fuel is injected directly into the fluidised bed by a screw feeder which is also sealed by a flow of air. The products of combustion pass up through the disengaging space where sand and unburnt coke are separated, through two cyclones to waste.

Temperatures are measured by two thermocouples in the fluidised bed of the carboniser and one in the disengaging space, three in the heater bed and one in its disengaging space.

The products of carbonisation can take two routes. During start up and when a run is not in progress they pass to the start-up condenser where the tars are condensed by direct contact with a water spray. The gases are further washed with water in a 2 ft. bed of $1/4$ in. Raschig rings before going to waste.

During a run the carbonisation products pass in series through an air cooled condenser consisting of a two inch tube inside a 6 ft. length of 3 in. pipe and two water cooled condensers consisting of a shell made from 4 ft. of 4 in. pipe, and tube bundles made from 20 ft. of $1/2$ in. copper tube in a 6 pass trombone arrangement. Water is on the tube side. Provision is made for heating the water on the first of these condensers so as to effect a partial separation of the constituents.

Provision is made to pass the uncondensed gases from the last condenser through a glass wool tar fog filter to a series of three absorbers. The first together with its liquid trap is constructed of Lucite and is packed with $1/4$ in. carbon Raschig rings and is designed for treating the gas with acid solution to remove ammonia; the second is of 3 in. diameter steel pipe and is packed with about 3 ft. of $1/4$ in. carbon Raschig rings and is for use with caustic soda solution for removing acid gases; the third is 5 ft. of 3 in. steel pipe packed with silica gel to absorb light oil vapours from the gas. This last absorber

can be steamed out and the products recovered in the third condenser.

The dry gas from the last absorber is recycled with a gas pump through the semi-coke heat exchanger and the fluidised carboniser. Provision is made for taking continuous and spot samples of the dry gas and the excess is exhausted through a meter to waste.

D. Results.

Runs 1 to 4 are described in Appendix C attached to this thesis. No attempt was made in these four runs to collect samples or obtain a material balance. In runs 5 and 6, this was attempted, and the results though not entirely satisfactory are presented in this section.

The complete runs are described, the analyses of feed and products are tabulated, the operating variables are summarized and the material balance for each run is presented. In both runs the coal feed from the Edmonton beds had been crushed to $-1/16$ in. mesh, and the carboniser bed height was set at 2 ft.

Run 5. March 20, 1956, 10.45 am. to 4.07 pm.

The carboniser heater was brought up to 600°C . in $2\frac{1}{2}$ hours, using natural gas and air. The gas was then shut off and semi-coke injected into the fluidised sand bed. Some oxygen was also used. The coal feed to the carboniser was started at 1.45 pm. but the inlet line filled with coal due to the purge gas line into the coal inlet pipe being plugged with coal dust. The coal inlet pipe was cleaned out using a compressed air lance and coal feed resumed satisfactorily at 2.05 pm. Both the carboniser and heater temperatures dropped by about 100°C . but after half an hour they had steadied out. The

equipment ran steadily for a further half hour and a timed run, which lasted one hour, was started at 3.07 pm. By the end of the run the pressure drop from the outlet of the carboniser to the outlet of no. 2 condenser had risen to 5 in. of mercury, indicating blocking in the lines. The equipment was therefore shut down.

During the one hour run, the coal feed and semi-coke, liquid, and gas products were all measured. There was a build up of semi-coke in the carboniser as indicated by an increase in the pressure drop across it during the one hour run. This was easily allowed for knowing the cross-sectional area of the carboniser bed. Temperature conditions during this run can be seen in Fig. 19.

Shut down.

The product transfer lines and condenser train were full of coal dust and tar, they were washed clean with steam and water followed by air. Provision was made to record the semi-coke temperature at the outlet from the semi-coke/gas heat exchanger.

Run 6. March 23, 1956, 9.00 am. to 1.56 pm.

Heating proceeded smoothly and the burner port was shut at 10.45 am. when the sand bed fluidised evenly with an average temperature of 550°C . Semi-coke feed was started at 10.55 am. and the natural gas shut off. The bed increased from 575 to 680°C . in 15 minutes without

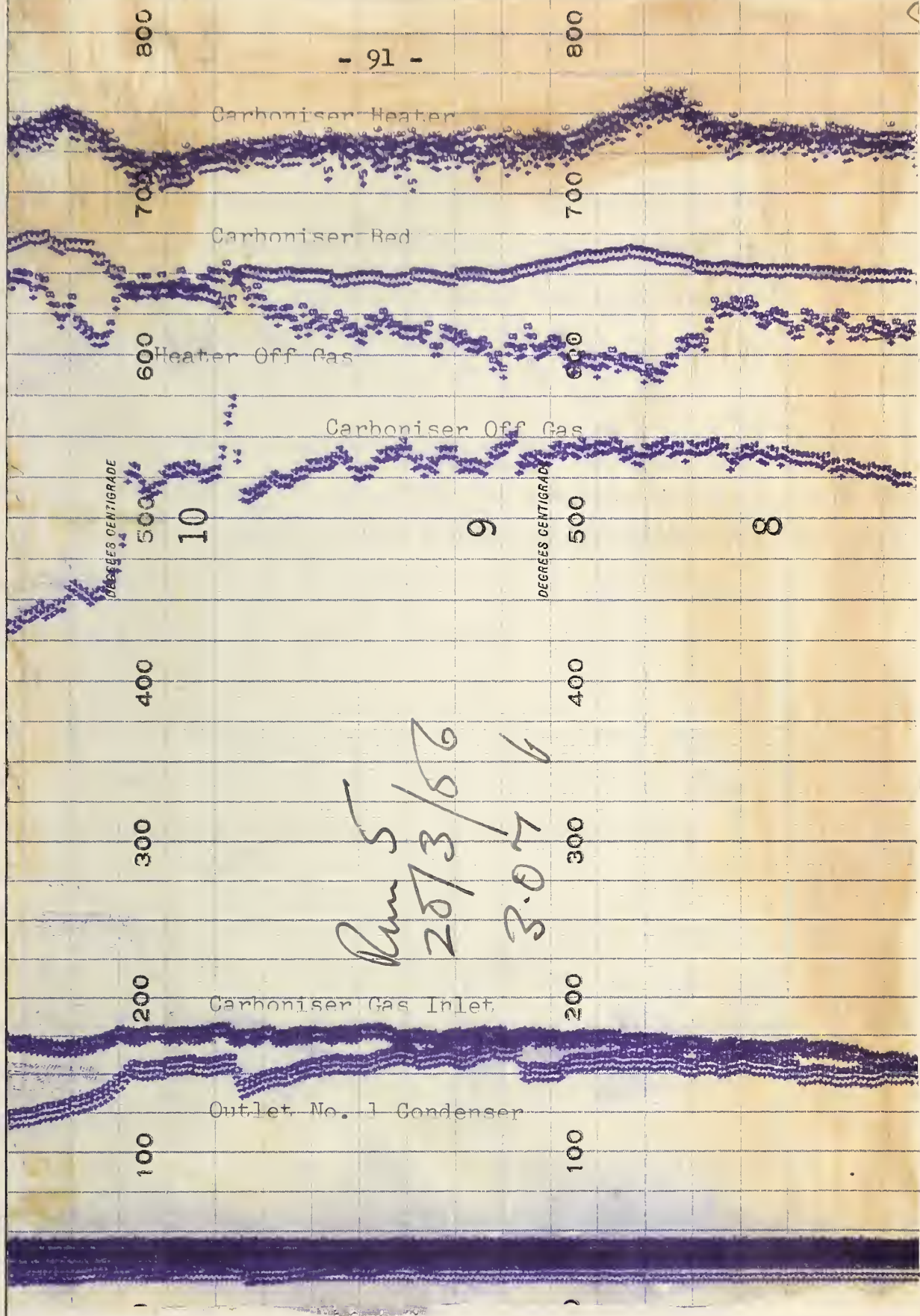


FIGURE 19 Temperature Conditions during Run 5.



the aid of oxygen, and at this point coal feed was introduced into the carboniser. From 11.10 am. until the end of the run conditions were steady with the exception of two surges of coal into the carboniser which decreased temperatures temporarily. During all this time, however, the pressure drop from the outlet of the carboniser to the outlet of no. 2 condenser would build up and then suddenly decrease due to intermittent blocking of some line. The first timed run was started at 12.10 pm. but was abandoned owing to the first surge in the coal feed which brought the carboniser temperature down from 675 to 510 °C.

After the temperatures had remained steady for one hour, a second timed run was started at 1.22 pm. There was a surge in the coal feed at one point resulting in the carboniser temperature dropping from 625 to 590°C. This run was terminated at 1.56 pm., since the pressure drop from the outlet of no. 2 condenser was in danger of blowing the manometer. The temperature conditions during Run 6 are presented in Fig. 20.

Shut down.

As was expected the product transfer line and the condensers were full of coal dust and tar. It was decided to clean each section separately and determine the weight of material in each. This was done and the following amounts found:-

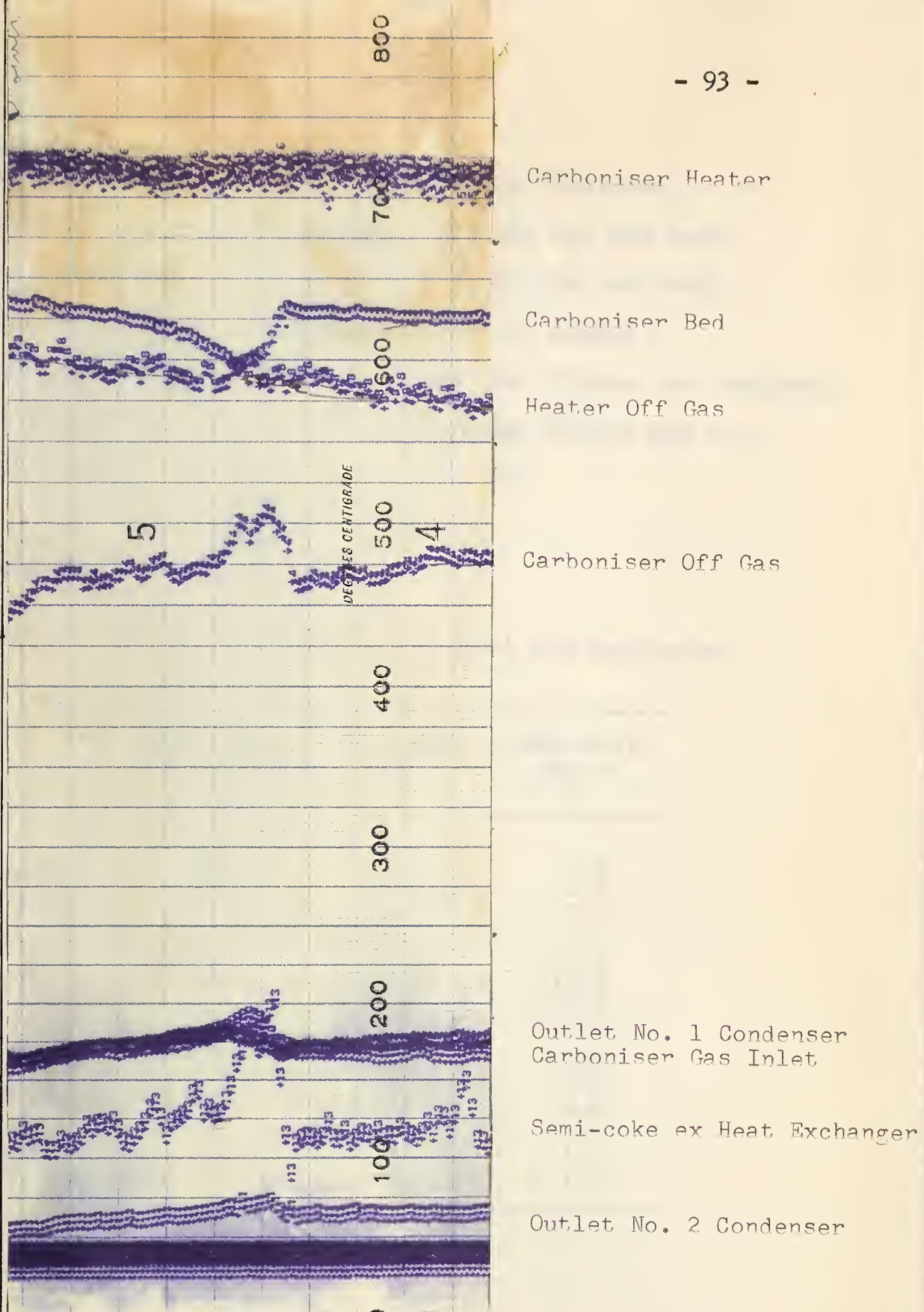


FIGURE 20 Temperature Conditions during Run 6.

Product transfer line and no. 1 condenser	3.5 lb. Coal dust
Line no. 1 to no. 2 condenser	0.7 lb. Tar and coal
No. 2 condenser	7.3 lb. Tar and coal
Line no. 2 to no. 3 condenser	0.6 lb. Liquid
No. 3 condenser	0.7 lb. Liquid, tar and coal
Tar fog filter	<u>1.7 lb.</u> Liquid and tar.
Total weight	14.5 lb.

Analyses

Table 9. Screen analyses of coal feed and semi-coke.

Tyler Mesh	Coal Feed Runs 5 and 6 %	Semi-coke Run 5 %	Semi-coke Run 6 %
+10	0.4	0.2	0.4
-10 +14	1.6	1.0	1.5
-14 +20	18.1	14.0	15.4
-20 +28	18.5	22.0	22.1
-28 +35	15.1	18.3	18.9
-35 +48	13.5	14.1	15.3
-48 +65	8.8	10.3	9.5
-65 +100	7.1	6.9	7.5
-100 +150	6.0	6.0	6.0
-150 +200	2.5	3.2	1.9
-200	8.3	4.0	1.5

1944 July 10 - 10.1
1944 July 11 - 10.2
1944 July 12 - 10.3
1944 July 13 - 10.4
1944 July 14 - 10.5
1944 July 15 - 10.6
1944 July 16 - 10.7
1944 July 17 - 10.8
1944 July 18 - 10.9
1944 July 19 - 11.0

TABLE 1

Summary of the data for the period July 10 to July 19, 1944

Time	Latitude	Longitude	Altitude
10.1	10.1	10.1	10.1
10.2	10.2	10.2	10.2
10.3	10.3	10.3	10.3
10.4	10.4	10.4	10.4
10.5	10.5	10.5	10.5
10.6	10.6	10.6	10.6
10.7	10.7	10.7	10.7
10.8	10.8	10.8	10.8
10.9	10.9	10.9	10.9
11.0	11.0	11.0	11.0

Table 10. Proximate analyses of Coal Feed and Semi-coke

	Ash %	V.M. %	F.C. %	Moisture %
Coal Feed Runs 5 and 6 as received	9.07	33.33	39.69	17.91
Coal Feed Runs 5 and 6 dry basis	11.0	40.6	48.4	21.8
Semi-coke Run 5 as received	15.34	7.31	76.68	0.69
Semi-coke Run 5 dry basis	15.45	7.35	77.2	0.70
Semi-coke Run 6 as received	14.29	9.40	75.65	0.66
Semi-coke Run 6	14.39	9.46	76.15	0.67

Table 11. Gross Calorific Value of Coal Feed and Semi-coke. B.T.U./lb.

	Dry Basis	As Received
Coal Feed, Runs 5 and 6	11,450	9,400
Semi-coke, Run 5	12,640	12,550
Semi-coke, Run 6	12,500	12,400

Table 12. Analysis of liquid product, run 5.

Tar (by decantation)	4%	Specific gravity	1.036
Aqueous liquor	96%	Specific gravity	1.01
Tar distilled to 350°C	65%		
OH content of the tar	4.4%		
Composition of the tar			
Saturates	3.2%		
Olefins	8.6%		
Aromatic	45.0%		
Others	44.0%		

Table 13. Orsat analyses of gaseous products.

	Run 5		Run 6	
	3.14 pm.	3.27 pm.	1.25 pm.	1.50 pm.
CO ₂	23.8	13.5	25.2	27.0
Unsaturation	26.6	34.9	36.0	41.4
O ₂	2.7	4.8	4.4	3.8
CO	2.7	2.7	0.5	0.8
H ₂	26.8	19.0	8.6	4.4
Paraffins	10.7	21.2	10.8	11.3
Paraffin H/C ratio	3.72	3.71	3.82	3.81
N ₂ by difference	6.7	3.9	14.5	11.3

Table 14. Operating variables, runs 5 and 6

	Run 5	Run 6
Duration of run	60 min.	34 min.
<u>Temperatures</u> °C		
Heater	725	710
Heater off gas	610	585
Carboniser	650	620
Carboniser off gas	535	475
Gas inlet heat exchanger	35	38
Gas outlet heat exchanger	165	175
Semi-coke outlet heat exchanger	-	125
Outlet no. 1 condenser	150	165
Outlet no. 2 condenser	35	60
<u>Pressures</u> in. Hg		
Inlet carboniser	4.0	9.0
Inlet heater	6.0	4.0
Suction gas recirculating blower	0.4	0.2
<u>Pressure Drops</u> in. Hg		
Carboniser bed	0.75	0.7
Heater bed	2.1	1.8
Outlet carboniser to outlet no. 2 condenser	2.3	7.5
Outlet no. 2 condenser to outlet tar fog filter	0.2	0.8
Outlet tar fog filter to suction of blower	0.1	0.5
<u>Flows</u>		
Carboniser fluidising gas	0.67	0.71
cuft./min. at 15.6 psia		18.0 psia
and 35°C		37°C

Table 14. Operating variables. (continued)

	Run 5	Run 6
Duration of run	60 min.	34 min.
<u>Flows.</u>		
Air to heater scfm. (70°F. and 14.7 psia)	21.2	15.8
Gas through meter cuft. (700 mm. and 20°C.)	27.7	35.3
Purge gas cuft./min. @ 700 mm. and 80°F.		
Coal inlet	0.75	0.84
Semi-coke outlet	0.15	0.12
Heater feed	0.25	0.25
Coal feed rate	40 rpm. 42 lb.	40 rpm. 24 lb.
Heater feed rate	9.6 rpm.	5.5 rpm.

Material Balances.

Using the previous tabulated data the following material balances have been drawn up.

Run 5.

1 hour basis

Coal Feed	42.0 lb.	Semi-coke	15.8 lb.
		Liquids	5.5 lb.
		Gas	2.0 lb.
	<u>42.0 lb.</u>		<u>23.3 lb.</u>
	23.3 lb.		
Unaccounted for	18.7 lb.		

Notes: The semi-coke product is composed of 12.5 lb. recovered in the receivers and a 3.3 lb. build

up in the carboniser bed. The residues of tar and coal dust in the condenser train were not weighed after this run. They would probably account for the 18.7 lb.

Run 6.

1 hour basis

Coal Feed	42.5 lb.	Semi-coke	10.6 lb.
		Liquids	6.5 lb.
		Gas	<u>4.4 lb.</u>
	<u>42.5 lb.</u>		21.5 lb.
	21.5 lb.		
Unaccounted for	21.0 lb.		

Notes: After the end of this run, 14.5 lb. of material were removed from the condenser train and transfer line. This was collected in an indeterminate time, but it is more probable that the major portion was deposited there, during the timed portion of the run since the pressure drop from the outlet of the carboniser to the outlet of no. 2 condenser was fluctuating more severely at this time. Had 11.9 lb. of this material been deposited during the 34 minutes of run 6, this would account in full for the 21.0 lb. discrepancy.

In view of the uncertainties connected with the material balances no attempt has been made to check the heat balances.

322

1950

737

• १४८०

E. Conclusions.

1. The data obtained on the low temperature carboniser indicate in a qualitative way that the equipment will work satisfactorily. One encouraging feature of these runs has been the ease of control of the heater, which responds rapidly to changes in the air rate, and which seems to have sufficient capacity to smooth out rapid changes in the heat load.

2. The semi-coke/gas heater has demonstrated the feasibility of indirect solid gas heat exchange in small scale units of this type. It is felt that the quantity of purge gas which flows countercurrently to the semi-coke and in contact with it will have an appreciable effect on the amount of heat recoverable from the semi-coke by virtue of its effect on the hold up of semi-coke in the exchanger.

3. The approximate overall heat transfer coefficient between the heater and carboniser was $60 \text{ BTU/hr.}^{\circ}\text{F ft}^2$. This is based on the assumption that all the coal fed to the carboniser was raised to the temperature of the bed.

F. Future work.

The heater could be made fully automatic either by controlling the air rate when running with excess fuel, or with a more complicated arrangement, by controlling both

the fuel and air inlets.

The problem of unsteady feeding of coal to the carboniser can be solved by connecting a balance line from the top of the coal inlet pipe to the top of the coal feed hopper, since during these runs the fluctuations in carboniser pressure caused corresponding fluctuations in the pressure above the coal feed hopper which would lag behind those in the carboniser. Thus there was a fluctuating pressure drop across the coal screw feeder with consequent variation in coal delivery.

During these runs there was only a single stage 3 in. diameter cyclone to remove coal from the carboniser off gases. However with the solution of the unsteady coal feed problem and possibly an increased diameter disengaging space, this may still be adequate. If it is not, a two stage cyclone will have to be specially designed for the equipment when some data on the size analysis and flow rate of the entrained material has been collected. During these runs also, the amount of gas injected through the coal inlet pipe was approximately equal to that used for fluidisation through the screen. This would obviously lead to a poor distribution of gas across the carboniser cross-section with consequent instabilities. It can easily be remedied by reducing the diameter of the coal inlet pipe and so the amount of purge gas to give the same velocity in it.

BIBLIOGRAPHY

1. Agarwal, O.P., and Storrow, J.A., Chemistry and Industry, 278, (1951).
2. Baerg, A., Klassen, J., and Gishler, P.E., Can. J. Research, 28F, 287, (1950).
3. Brown, Unit Operations, John Wiley and Sons, Inc., New York, 160.
4. Carman, P.C., Tr. Inst. Chem. Engrs., 15, 150, (1937).
5. Ergun, S., and Orning, A.A., Ind. Eng. Chem., 41, 1179, (1949).
6. Hancock, R.T., Coke and Gas, 11, 386, (1949).
7. Hancock, R.T., Mining Mag., 55, 90, (1936).
8. Hancock, R.T., Ibid., 67, 179, (1942).
9. Van Heerden, C., J. App. Chem., 2, S7, (1952).
10. Van Heerden, C., Nobel, A.P.P., and Van Krevelen, D.W., Chem. Eng. Sci., 1, 37, (1951).
11. Hirst, A.A., Tr. Inst. Min. Engrs., 85, 236, (1932-33).
12. Johnson, E., Inst. of Gas Engrs., Pub. 378/179.
13. Jolley, L.J., and Stanton, J.E., J. App. Chem., 2, S62, (1952).
14. Jottrand, R., Ibid., 2, S17, (1952).
15. Leva, M. et al., Chem. Eng. Prog., 44, 511, (1948).
16. Leva, M. et al., Ibid., 44, 619, (1948).
17. Leva, M. et al., Ind. Eng. Chem., 41, 1206, (1949).
18. Leva, M., Chem. Eng. Prog., 47, 39, (1951).
19. Lewis, W.K., Gilliland, E.R., and Bauer, W.C., Ind. Eng. Chem., 41, 1104, (1949).
20. Matheson, G.L., Herbst, W.A., and Holt, P.H., Ibid., 41, 1099, (1949).

21. Miller, C.O., and Logwinuk, A.K., Ibid., 43, 1221, (1951).
22. Morse, R.D., Ibid., 41, 1117, (1949).
23. Parent, J.D., Yagol, N., and Steiner, C.S., Chem. Eng. Prog., 43, 429, (1947).
24. Stansfield, E., and Lang, W.A., Coals of Alberta, Their Occurrence, Analysis, and Utilisation, Report 35, Research Council of Alberta, (1944).
25. Toomey, R.D., and Johnstone, H.F., Chem. Eng. Prog., 48, 220, (1952).
26. Wilhelm, R.H., and Kwauk, M., Ibid., 44, 201, (1948).
27. Young, R.J., J. App. Chem., 2, S55, (1952).
28. Grohse, E.W., A.I.Ch.E. Journal, 1 358, (1955).

APPENDIX A

In this appendix the air flow rates and pressure drops across the fluidised bed are tabulated for each run. The pressure drops as read have been corrected for the pressure drop across the empty tube and screen and are presented as centimetres of water manometer differential. The air flow rates are in s.c.f. per second (14.7 psia and 60°F). The cross-sectional area of the fluidisation tube was 0.165 ft.²

Run 1 3A	Run 2 3A	Run 3 3A
Tyler Mesh -10+14	Tyler Mesh -10+14	Tyler Mesh -10+14
Wt. Charged 5 lbs.	Wt. Charged 3 lbs.	Wt. Charged 1.5 lbs.
T = 530°R, P = 703mms.	T = 529°R, P = 706mms.	T = 540°R, P = 704mms.

Air Flow Rate	Pressure Drop	Air Flow Rate	Pressure Drop	Air Flow Rate	Pressure Drop
0.068	2.25	0.088	2.60	0.107	2.00
0.128	2.95	0.132	5.00	0.159	2.25
0.139	5.30	0.178	7.05	0.198	2.30
0.206	9.50	0.215	8.90	0.224	2.65
0.232	11.20	0.225	8.45	0.250	2.95
0.255	12.75	0.238	8.75	0.279	3.50
0.266	13.40	0.248	8.70	0.292	3.60
0.274	13.70	0.258	8.85	0.304	3.65
0.282	13.95	0.269	8.65	0.325	3.70
0.289	14.10	0.279	8.40	0.350	3.75
0.296	14.05	0.289	8.30	0.380	3.95
0.307	14.15	0.297	8.35	0.376	3.65
0.329	14.50	0.314	8.45	0.309	3.90
0.359	14.60	0.332	8.45	0.277	3.45
0.319	14.25	0.356	8.65	0.229	2.65
0.292	13.65	0.374	8.70	0.187	2.00
0.261	11.50	0.325	8.50	0.139	1.40
0.208	8.75	0.307	8.25	0.125	1.20
0.144	5.50	0.300	8.10	0.188	2.10
0.160	6.15	0.288	7.70	0.224	2.80
0.225	9.85	0.276	7.30	0.259	3.15
0.264	12.45	0.255	6.55	0.282	3.50
0.278	13.40	0.228	5.75	0.302	3.65
0.286	14.00	0.189	4.50	0.328	3.75
0.290		0.134	2.75	0.363	3.80
0.294	14.55	0.092	1.70	0.397	3.95
0.301	14.50	0.146	3.10	0.112	1.85
0.306	14.45	0.188	4.60	0.171	3.20
0.312	14.25	0.236	6.20	0.216	3.90
0.321	14.35	0.265	7.40	0.250	3.85
0.346	14.60	0.277	7.90	0.270	3.80
		0.296	8.35	0.283	3.75
		0.298	8.55	0.297	3.80

Run 4 4A
Tyler Mesh -14+20
Wt. Charged 5 lbs.
T = 541°R, P = 703mms.

Run 5 4A
Tyler Mesh -14+20
Wt. Charged 3 lbs.
T = 534°R, P = 711mms.

Run 6 4A
Tyler Mesh -14+20
Wt. Charged 5 lbs.
T = 537°R, P = 713mms.

Air Flow Rate	Pressure Drop	Air Flow Rate	Pressure Drop	Air Flow Rate	Pressure Drop
------------------	------------------	------------------	------------------	------------------	------------------

0.037	2.40	0.099	4.05	0.0308	3.50
0.074	4.80	0.139	5.85	0.0527	6.28
0.099	6.95	0.166	7.45	0.0700	8.65
0.127	9.30	0.194	8.45	0.0836	10.55
0.151	11.70	0.223	8.65	0.0992	12.80
0.171	13.65	0.246	8.85	0.115	14.07
0.187	14.50	0.267	8.95	0.132	14.48
0.201	14.50	0.288	8.95	0.148	14.60
0.212	14.60	0.307	8.90	0.172	14.58
0.246	14.70	0.291	9.00	0.202	14.60
0.272	14.75	0.272	9.00	0.188	14.64
0.314	14.80	0.247	8.95	0.164	14.58
0.291	14.80	0.224	8.85	0.142	14.54
0.253	14.75	0.204	8.60	0.125	14.32
0.219	14.60	0.178	7.50	0.113	13.07
0.203	14.40	0.145	5.85	0.0875	10.09
0.162	11.70	0.119	4.75	0.0706	7.80
0.107	7.30	0.088	3.30	0.0519	5.53
0.081	5.30	0.128	5.25	0.0351	3.29
0.108	7.35	0.173	7.45	0.0339	3.85
0.134	9.60	0.199	8.40	0.0579	6.80
0.153	11.50	0.211	8.40	0.0823	10.05
0.174	13.40	0.248	8.90	0.110	13.85
0.187	14.35	0.274	8.90	0.143	14.58
0.190	14.60			0.179	14.65
0.201	14.30				
0.210	14.55				
0.257	14.75				
0.295	14.85				

Run 7 6A
Tyler Mesh -28+35
Wt. Charged 5 lbs.
T = 539°R, P = 711mms.

Run 8 2A
Tyler Mesh -8+10
Wt. Charged 3 lbs.
T = 543°R, P = 709mms.

Run 9 1A
Tyler Mesh -4+8
Wt. Charged 3 lbs.
T = 538°R, P = 702mms.

Air Flow Rate	Pressure Drop	Air Flow Rate	Pressure Drop	Air Flow Rate	Pressure Drop
0.0169	2.85	0.127	1.50	0.094	0.40
0.0239	5.05	0.226	3.75	0.157	1.30
0.0338	8.09	0.267	5.20	0.207	2.00
0.0441	11.06	0.314	6.45	0.263	2.80
0.0541	13.42	0.361	7.85	0.329	4.05
0.0671	14.67	0.422	8.65	0.404	5.30
0.0831	15.00	0.476	8.90	0.453	6.40
0.111	15.49	0.535	8.75	0.521	7.75
0.216	15.81	0.600	8.85	0.561	8.50
0.144	16.12	0.482	8.95	0.592	8.70
0.125	15.72	0.455	9.00	0.649	8.75
0.111	15.44	0.387	7.95	0.724	8.60
0.0950	15.15	0.360	7.05	0.758	8.80
0.0739	14.65	0.330	6.15	0.686	8.75
0.0638	13.88	0.295	5.25	0.627	8.60
0.0521	11.33	0.252	4.10	0.551	7.80
0.0421	8.52	0.189	2.55	0.522	7.10
0.0329	6.04	0.264	4.95	0.469	6.20
0.0262	3.27	0.345	7.35	0.431	5.45
0.0267	6.17	0.392	8.55	0.393	4.70
0.0439	11.80	0.414	8.70	0.339	3.75
0.0488	14.44	0.494	8.95	0.256	2.35
0.0718	14.70			0.335	3.95
0.0971	15.30			0.480	6.80
0.128	15.85			0.676	8.75
				0.738	8.60

Run 10 7A
Tyler Mesh -35+50
Wt. Charged 5 lbs.
T = 536°R, P = 702mms.

Run 11 8A
Tyler Mesh -48+65
Wt. Charged 5 lbs.
T = 534°R, P = 702mms.

Run 12 1B
Tyler Mesh -10
Wt. Charged 3.8 lbs.
T = 542°R, P = 707mms.

Air Flow Rate	Pressure Drop	Air Flow Rate	Pressure Drop	Air Flow Rate	Pressure Drop
0.00517	2.75	0.00331	2.90	0.00583	1.20
0.00852	4.98	0.00496	5.39	0.00729	3.58
0.0134	8.06	0.00670	8.08	0.0115	6.06
0.0185	10.85	0.00878	11.03	0.0163	7.95
0.0239	13.72	0.0112	13.82	0.0230	10.28
0.0281	14.56	0.0131	14.46	0.0358	10.89
0.0326	14.30	0.0153	13.76	0.0424	11.26
0.0386	14.42	0.0185	13.85	0.0514	11.23
0.0465	14.60	0.0215	13.99	0.0582	11.40
0.0549	14.62	0.0255	14.17	0.0645	11.38
0.0696	14.71	0.0294	14.30	0.0595	11.40
0.0800	14.72	0.0348	14.45	0.0533	11.32
0.0654	14.73	0.0310	14.45	0.0467	11.25
0.0574	14.70	0.0286	14.36	0.0386	10.87
0.0513	14.68	0.0256	14.32	0.0338	10.19
0.0434	16.61	0.0236	14.33	0.0272	9.12
0.0351	14.44	0.0217	14.24	0.0144	7.14
0.0294	13.55	0.0197	14.04	0.0144	5.66
0.0260	12.72	0.0179	13.85	0.00974	3.67
0.0210	10.39	0.0149	13.26		
0.0132	6.61	0.0131	12.36		
0.00875	4.58	0.0109	10.92		
0.0152	8.15	0.00855	8.88		
0.0221	11.83	0.00539	5.19		
0.0275	14.27	0.00355	2.00		
0.0323	14.15				
0.0438	14.41				
0.0571	14.66				

Run 13 2B
Not calculated
because of
excessive
entrainment

Run 14 13A
Tyler Mesh -3+4
Wt. Charged 3 lbs.
T=532°R, P=704 mms.

Air Flow Pressure	
Rate	Drop
0.253	0.77
0.440	2.10
0.573	3.12
0.684	4.05
0.860	5.85
0.997	5.70
1.084	5.50
1.153	4.75
1.250	4.95
1.400	4.60
1.533	4.30
1.402	4.50
1.235	5.55
1.139	5.65
1.012	6.20
0.860	6.60
0.669	4.50
0.431	2.20

Appendix B. Equipment Design.

1. Specifications
2. Carboniser design.
3. Material balance.
4. Heat balance.
5. Experimental heater results.
6. Heater design.
7. Accessories.

In this appendix the design of the carboniser, carboniser heater and accessories only are considered. Results on an experimental heater are included. The logical sequence of design steps is indicated by the table of contents. Design of the product recovery section is conventional. It was tailored to use only standard pipe and fittings and is therefore not included. Technical data were taken from standard sources on the subject.

1. Specifications.

Coal feed rate 60 lb./hr. as delivered.

Coal analysis	Moisture	16%
	Ash	10%
	Volatile matter	30%
	Fixed Carbon	44%

Product yield	Tar & light oil	20 imp. galls/ ton dry coal
	Gas	3500 scf./ton. dry coal
	Semi-coke	15% V.M.

Fluidising conditions Coal ground to -1/16 in. mesh

Arithmetic mean diameter	0.0173 in.
-----------------------------	------------

Critical gas velocity	0.32 ft./sec.
--------------------------	---------------

Fluidising velocity	0.64 ft./sec.
------------------------	---------------

Temperatures	Carboniser	1100°F.
--------------	------------	---------

	Carboniser heater	1500-1600°F.
--	----------------------	--------------

Heater fluidised bed	-20 + 28 in. Ottawa sand.
----------------------	------------------------------

2. Carboniser Design.

Residence Time:-

The standard decay curve for material having an initial concentration C_0 in an ideally mixed mass M lb. with constant inflow and outflow P lb./hr. is

$$M \ln \frac{C}{C_0} = -Px$$

where C is the concentration after time x hours.

Let x denote the coking time for the particular coal in hours and z the fractional complete coking required

$$\text{then:- } \frac{C}{C_0} = 1 - z$$

If A = area of bed ft.²

L = height of bed ft.

and ρ = density of bed lb./ft.³

then $M = AL\rho$

and $AL\rho \ln(1 - z) = -Px$

$$\text{i.e. } A = \frac{-Px}{L\rho \ln(1 - z)} \dots\dots\dots(1).$$

The following results on coking times in a fluidised

bed are taken from Stone, Batchelor and Johnstone,
Ind. Eng. Chem. 46, 274-8. (1954).

Temperature °F	% Completion	Time sec.	Coal Type
800	55	600	non-coking Colorado
900	70	120	"
1000	75	75	"
770	68	300	Coking Pittsburgh
850	84	120	"
950	82	60	"

Assuming that at 1100°F. the coal will be properly
coked after 600 seconds = 1/6 hours, then setting

$$z = 0.95$$

$$\rho = 30 \text{ lb./cuft. from previous work (Part 1)}$$

$$L = 1 \text{ ft.}$$

$$P = 60 \text{ lb./hr. specified}$$

we have

$$A = \frac{-60 \cdot 1/6}{30 \ln(0.05)} = 0.111 \text{ ft.}^2$$

Therefore the diameter of the carboniser should be
4.524 in. To allow for internal fittings the diameter is
increased to 6 in. The height of the carboniser is set
at 3 ft. 6 in. above the screen to allow for a bed up to
2 ft. 6 in. deep. The disengaging section above the

carboniser would be 8.5 in. in diameter in order to double the cross-sectional area, so this is set at 10 in. to allow for fittings and its height is set at 1 ft. 6 in. to accommodate a cyclone.

3. Material balance.

a. Fluidising gas

Velocity = 0.64 ft./sec. in 6 in. dia. tube

S.G. = 0.62, Temperature = 1100°C.

whence mass rate = 6.9 lb./hr.

b. Coal feed = 60 lb./hr., 16% H₂O
= 50.4 lb. dry coal/hr.
and 9.6 lb. water/hr.

c. Gas liberated in carboniser

= 3,500 cuft./ton dry coal S.G. = 0.62
= 3.7 lb./hr.

d. Tar and light oil

= 20 imp. gal./ton. S.G. = 1.0
= 4.5 lb./hr.

e. Semi-coke V.M. = 15%

therefore mass rate = 38.1 lb./hr.

The first of these is the fact that the
the first of these is the fact that the
the first of these is the fact that the
the first of these is the fact that the

the first of these is the fact that the
the first of these is the fact that the
the first of these is the fact that the
the first of these is the fact that the

the first of these is the fact that the
the first of these is the fact that the
the first of these is the fact that the
the first of these is the fact that the

the first of these is the fact that the
the first of these is the fact that the
the first of these is the fact that the
the first of these is the fact that the

the first of these is the fact that the
the first of these is the fact that the
the first of these is the fact that the
the first of these is the fact that the

the first of these is the fact that the
the first of these is the fact that the
the first of these is the fact that the
the first of these is the fact that the

f. Difference 1.1 lb./hr.

assume this is water vapour from constitutional water.

The material balance around the carboniser is then on a 1 hr. basis:-

Entering Streams		Exit Streams.	
coal	60.0 lb.	Semi-coke	38.1 lb.
Fluidising gas	6.0 lb.	Tar & light oil	4.5 lb.
		H ₂ O	13.7 lb.
		Gas	10.6 lb.
	<hr/>		<hr/>
	66.0 lb.		66.9 lb.

h. Heat Balance.

Thermal Properties.

The specific heat of the coal and semi-coke is calculated using a weighted arithmetic average of the specific heats of the ash, water, coal and semi-coke as follows:-

Ash	0.165 B.T.U./lb. ^o F.
Water	1.000 " "
Coal (ash and water free)	0.250 " "
Semi-coke (ash and water free)	0.36 " "

The calculations yield an average specific heat for the coal feed of 0.354 B.T.U./lb.^oF., and for the semi-coke product of 0.33 B.T.U./lb.^oF.

Tar and light oil.

Average Liquid specific heat 60-212°F. 0.5 B.T.U./lb°F

Average Vapour specific heat 0.25 "

Latent heat (212°F.) 135 B.T.U./lb.

Mean specific heat of gas between 32 and 1100°F is equal to 0.676 B.T.U./lb°F.

Since the data on heats of carbonisation at these temperatures is very scanty it is assumed to be zero, although figures of 40 B.T.U./lb. coal have been quoted for high temperature carbonisation. Using a temperature base of 32°F., a pressure base of 14.7 psia, the following energy quantities have been calculated for a period of one hour.

Heat out with exit streams		Heat in with entering stream	
B.T.U.		B.T.U.	
4.5 lb.	Tar and gas 2,000	60 lb. coal	1,100
10.6 lb.	gas 7,700		
13.7 lb.	water 21,700		
38.1 lb.	semi-coke <u>13,400</u>		
	44,800		<u>1,100</u>
Less heat in	<u>1,100</u>		
	43,700		
12.5% losses	<u>6,300</u>		
	50,000		

Based on these figures the heat requirements are 50,000 B.T.U./hr. It will be noticed that no heat input is mentioned for the fluidising gas. This was omitted because the entering temperature of the gas depends upon the performance of the semi-coke/gas heat exchanger which could not be assessed at this time. It was felt that this error would cancel any error in omitting the heat of carbonisation.

5. Experimental Heater Results.

The experimental heater in its final form is shown in Fig. 15 which is taken from Part 2 of this thesis. It was constructed from 33 in. of 3 in. standard pipe above which was mounted a 7 in. by 20 in. disengaging section. Air, dried and metered in the experimental fluidising equipment Fig. 3, Part 1, was passed through a 100 mesh stainless steel screen pressed into a 3 in. by $1\frac{1}{2}$ in. reducer screwed to the 3 in. pipe and a chromel/alumel thermocouple was mounted in the bed just above this point. The products of combustion passed from the disengaging section through a cyclone to the atmosphere. The 3 in. pipe was lagged with standard magnesia insulation except at the base.

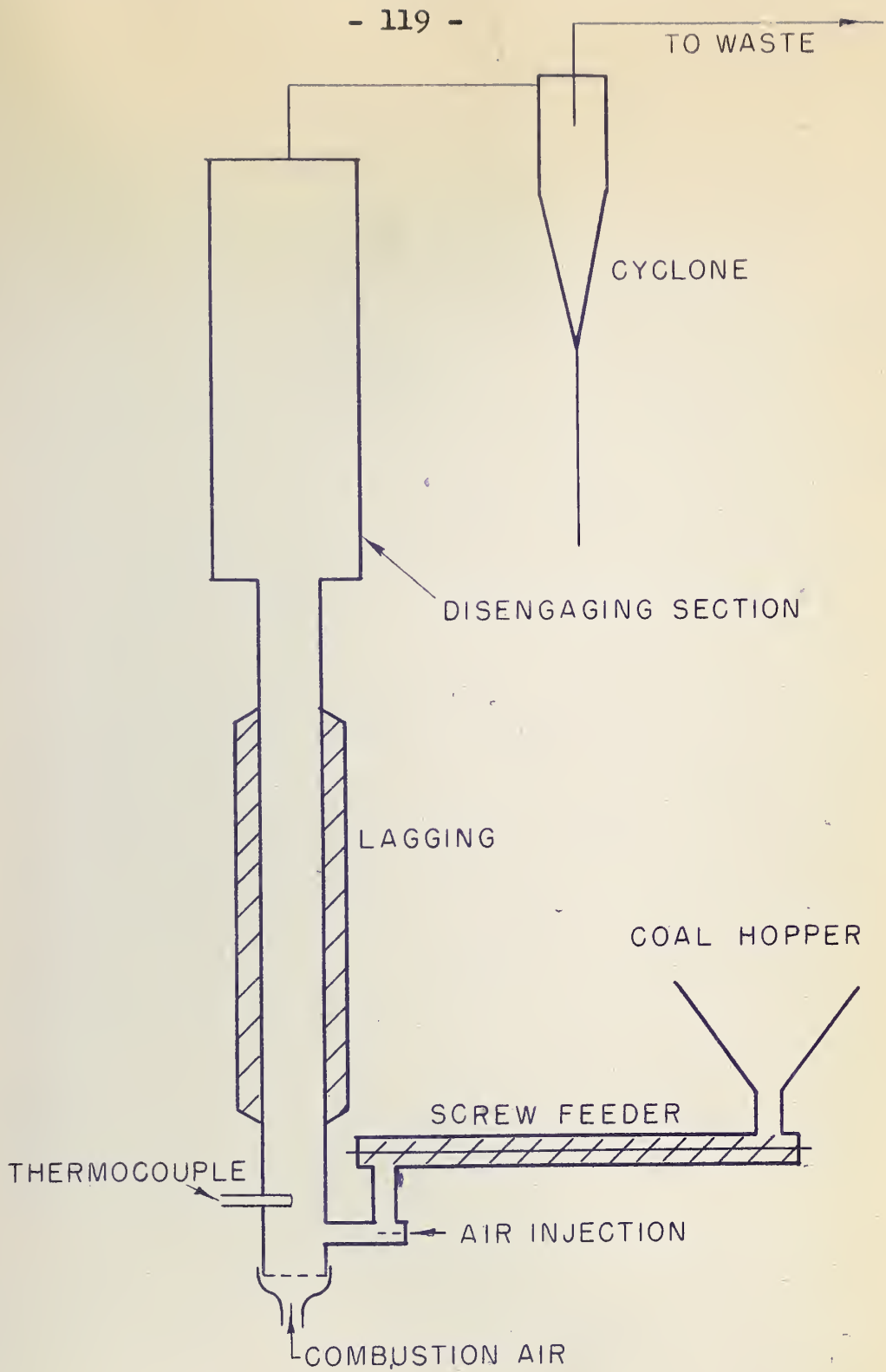


FIGURE 15. FLUIDISED COAL BURNER.

Three different designs of heater based on the 3 in. pipe had been previously tried, but were not satisfactory. The object of the work was only to establish the feasibility of the idea and so the results are not meant to be quantitative.

Using an oxy-acetylene flame applied to the base of the heater, it took approximately 1 hour to raise the temperature of 2 lb. of fluidised -20 +28 Ottawa sand to 1400°F. Coal was then injected at a rate of 2 to 3 lb./hr. and for the next two hours the temperature of the fluidised bed was maintained between 1400 and 1650°F with an air rate of 121 scf/hr. The temperature was not raised any higher to avoid failure of the mild steel. The test was discontinued when the thermocouple burnt out. The pressure drop across the bed stayed reasonably constant indicating that the bed weight did not increase i.e. that ash and unburnt coal were rapidly removed from the bed. A sample of the combustion gases was taken and analysed as follows:-

CO ₂	16.1 %	
O ₂	1.0 %	
CO	2.2 %	
CH ₄	2.7 %	Hydrocarbon as CH ₄
N ₂ by difference	78.0 %	

Taking the diameter of the bed as 3 inches the air rate is calculated as

1.3 lb./in.² bed cross section/hr.

This is the figure used in the carboniser heater design.

6. Heater Design.

The heater is required to burn sufficient semi-coke to liberate 50,000 B.T.U. per hour at 1500°F. The design is based on the following specifications:-

Calorific value of semi-coke 14,500 B.T.U./lb.

Theoretical air 10.6 lb./lb.

Specific heat of waste gases 0.260 B.T.U./lb.°F.

The available heat per lb. of semi-coke at 1500°F. is then

$$14,500 - 11.6(0.26)(1500 - 60)$$

which is approximately 10,000 B.T.U. per hour.

The weight of semi-coke required per hour is therefore 5 lb. and the theoretical air requirements are

$$5(10.6) = 53 \text{ lb./hr.}$$

In the experimental heater the air rate was 1.3 lb./in²/hr. The required bed area is therefore 41 sq. in., and the dimensions of the annular heating bed would be

6.325 in. minimum diameter

9.6 in. maximum diameter

However, in order to allow for a reasonably thick fluidised bed and for lower heating value fuels, a maximum diameter of 12 in. was chosen.

The diameter of the disengaging space around a 6.325 in. diameter tube to give double the cross-sectional

area for flow would be 15.6 in. This was accordingly fixed at 16 in.

With the leading dimensions of the carboniser and the heater fixed, the most logical design was evolved and the final drawing is reproduced in Fig. 21. The question of heat transfer from the heater to carboniser arose but on working out the bed to wall heat transfer coefficients by the different correlations proposed in the literature, values ranging from 20-110 B.T.U./hr. ft.² °F. were obtained. With a bed height of 1 ft. and an overall temperature difference of 500°F. the overall coefficient would have to be 64 B.T.U./hr. ft.² °F. This figure would be reduced by half if the bed height were doubled and so it was considered that the heat transfer rates would be adequate.

7. Accessories.

The accessories considered here are a gas recirculating pump and rotameter for the fluidising gas to the carboniser, and an air and natural gas rotameter for the carboniser heater.

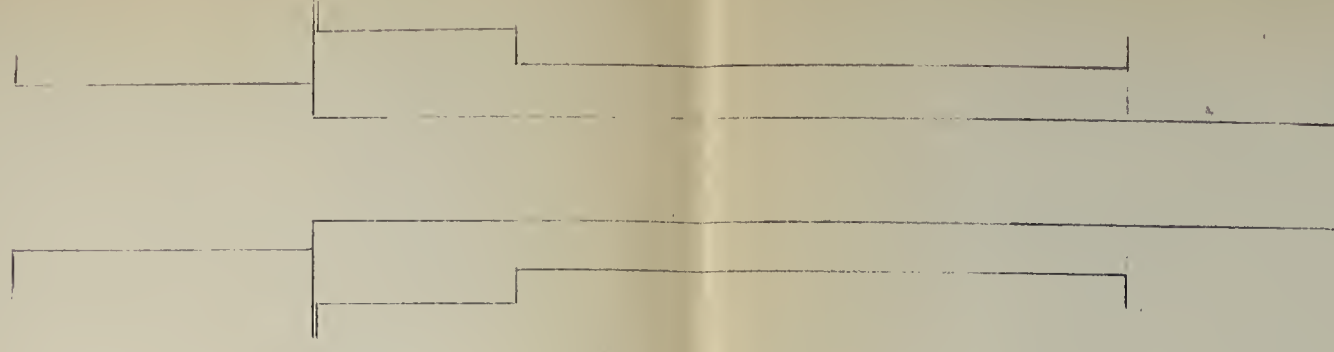
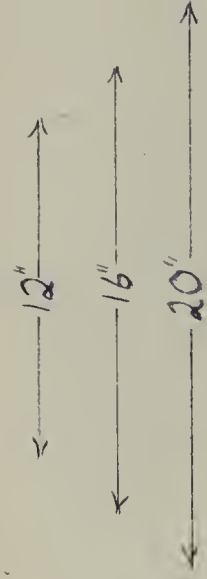
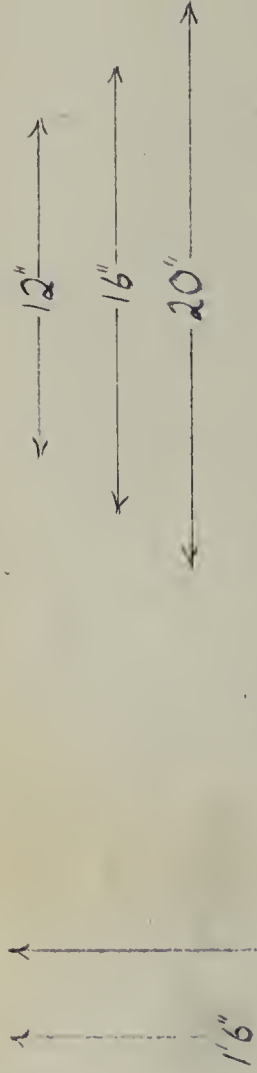
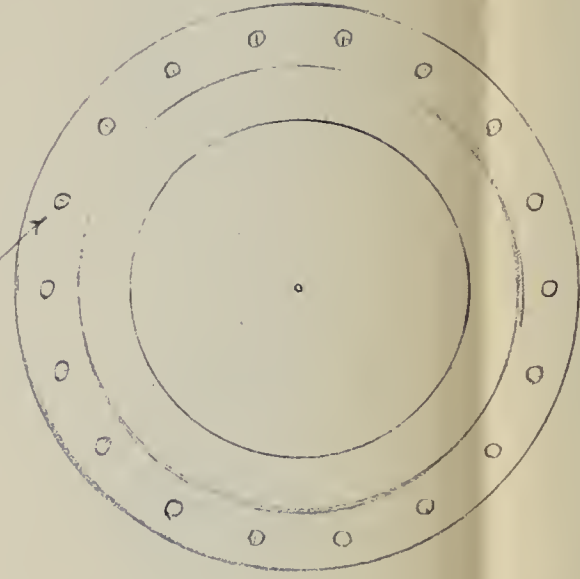
The velocity in the 6 in. diameter tube is 0.64 ft./sec. This corresponds to a rate of 7.6 cuft./min. This is the maximum capacity of the pump when the bed is to be

FIGURE 21

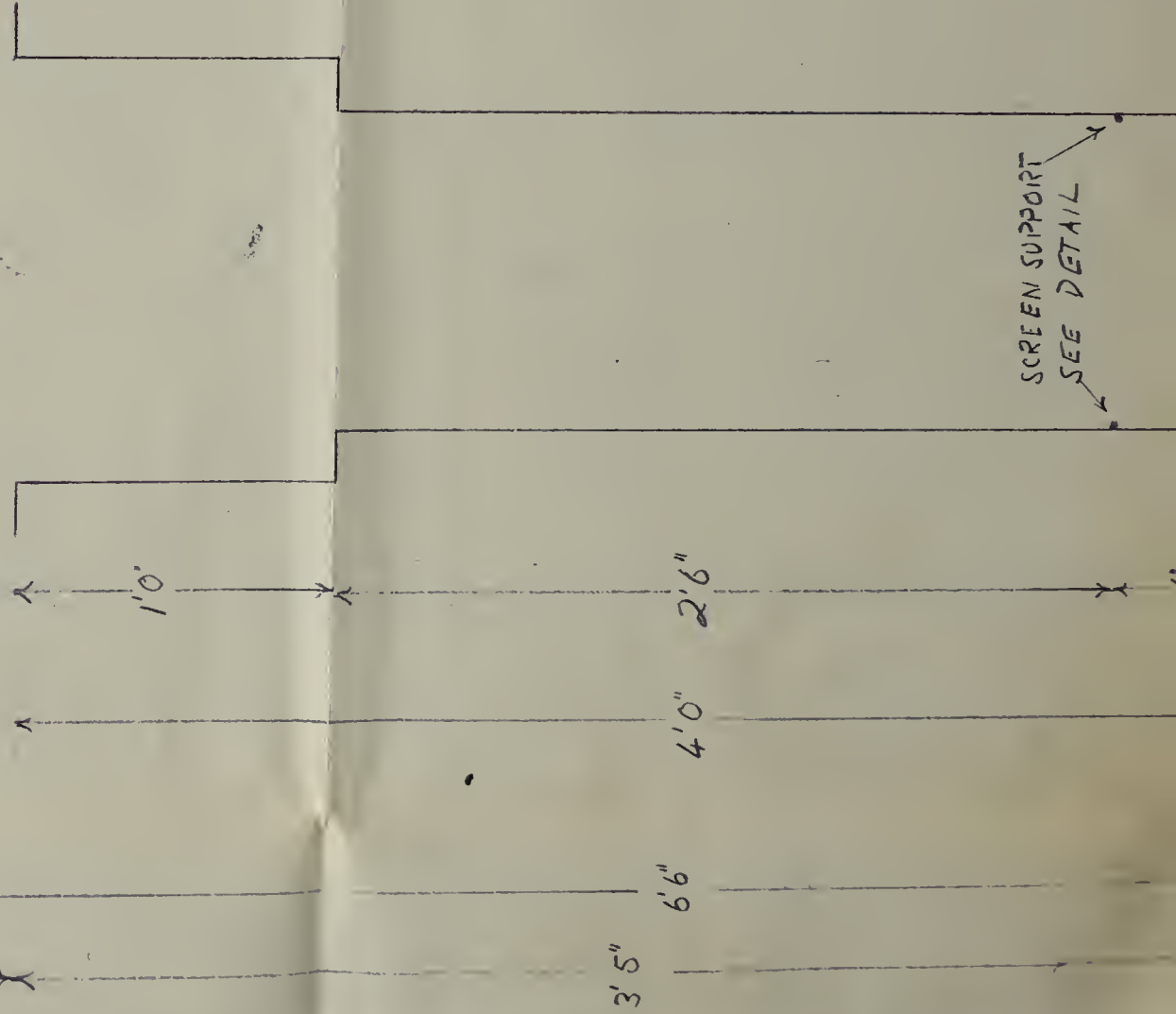
Detailed Drawing of Carboniser and Heater.

DRILL 24 HOLES $\frac{7}{16}$ " DIA. EQUALLY
SPACED ON 9" RADIUS

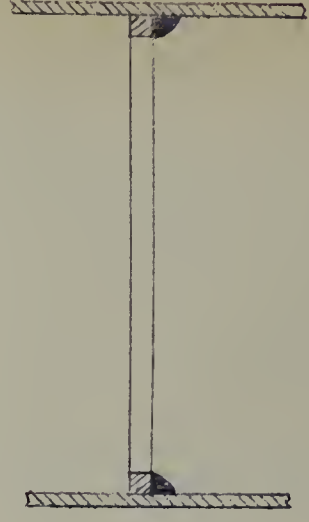
DRILL 20 HOLES $\frac{7}{16}$ " DIA
EQUALLY SPACED
ON 6" RADIUS

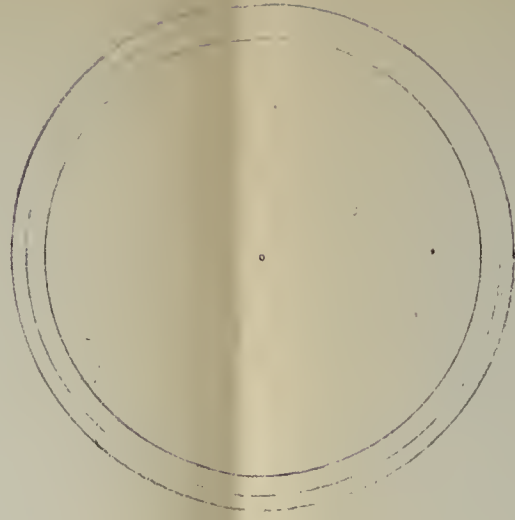
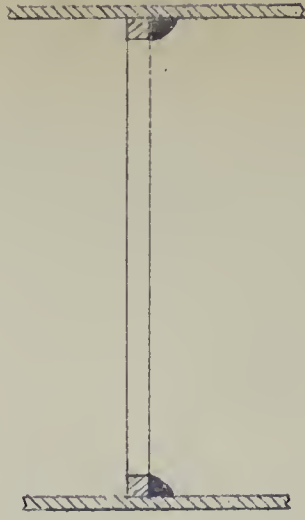
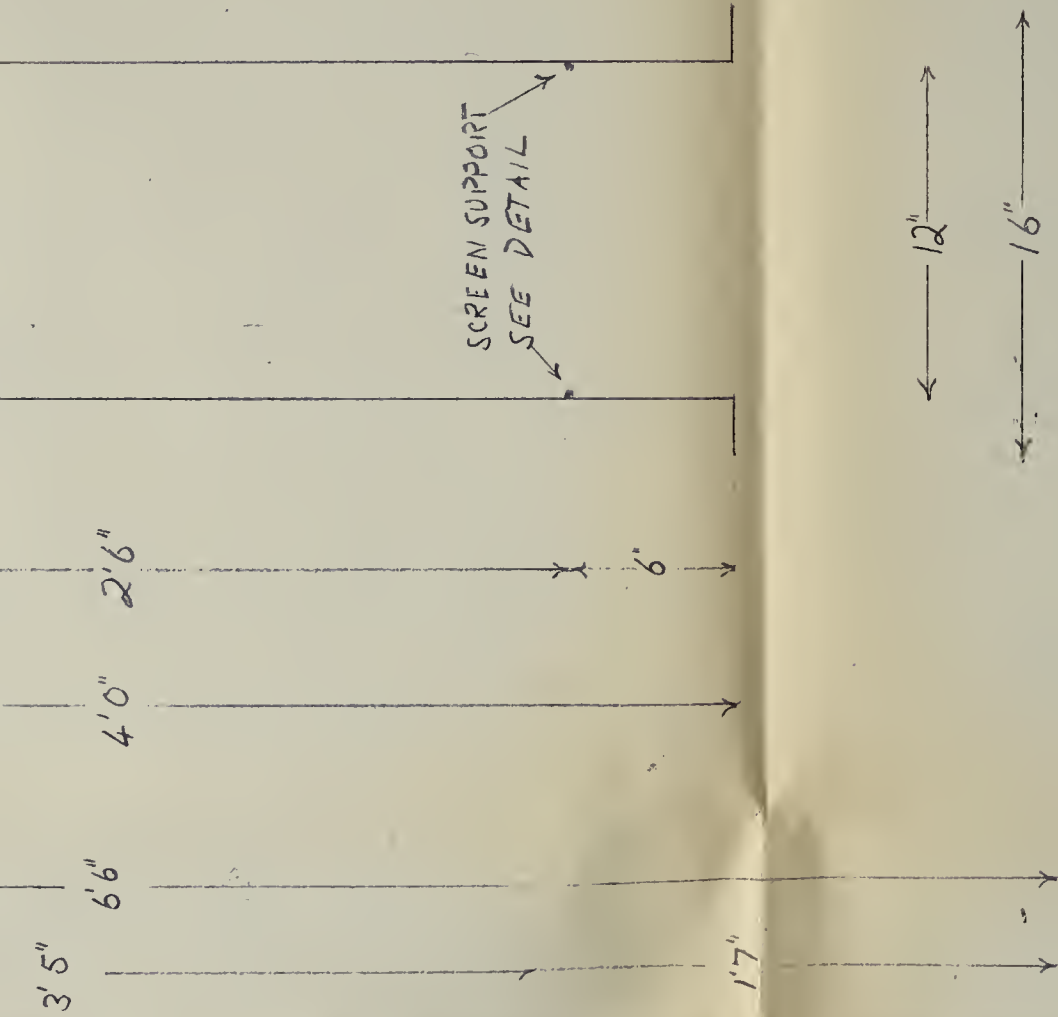


THE TWO SECTIONS WILL
BE ASSEMBLED AS
SHOWN



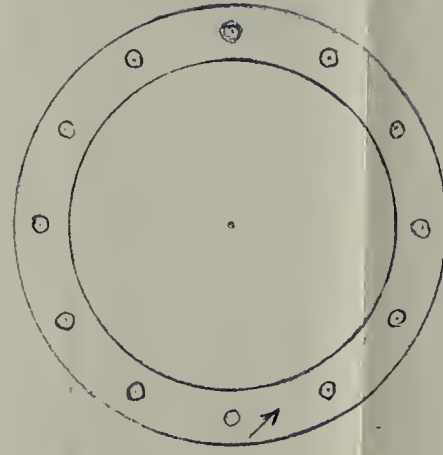
SCREEN SUPPORT
SEE DETAIL





TYPE M.S.

24 HOLES $\frac{7}{16}$ " DIA. EQUALLY
ON 7" RADIUS



DETAIL SCREEN SUPPORT
WELD $\frac{1}{4}$ " SQUARE OR ROUND
SECTION ROD TO INSIDE OF
TUBES

CARBONISATION REACTOR

DRAWN BY C.S.S.

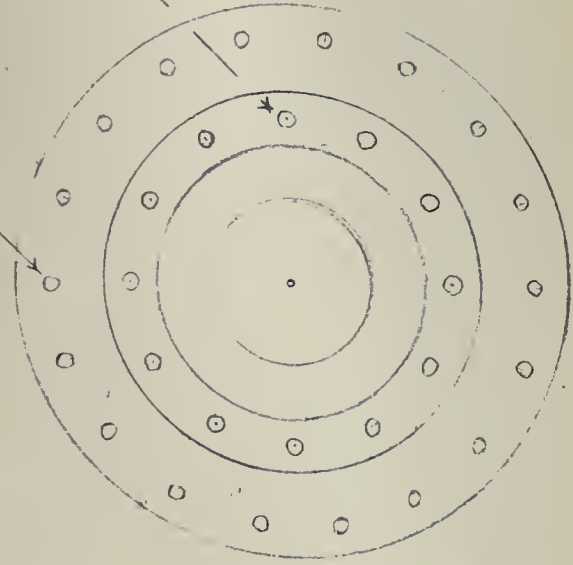
DATE 28/10/1955

SCALE 2" = 1 FOOT

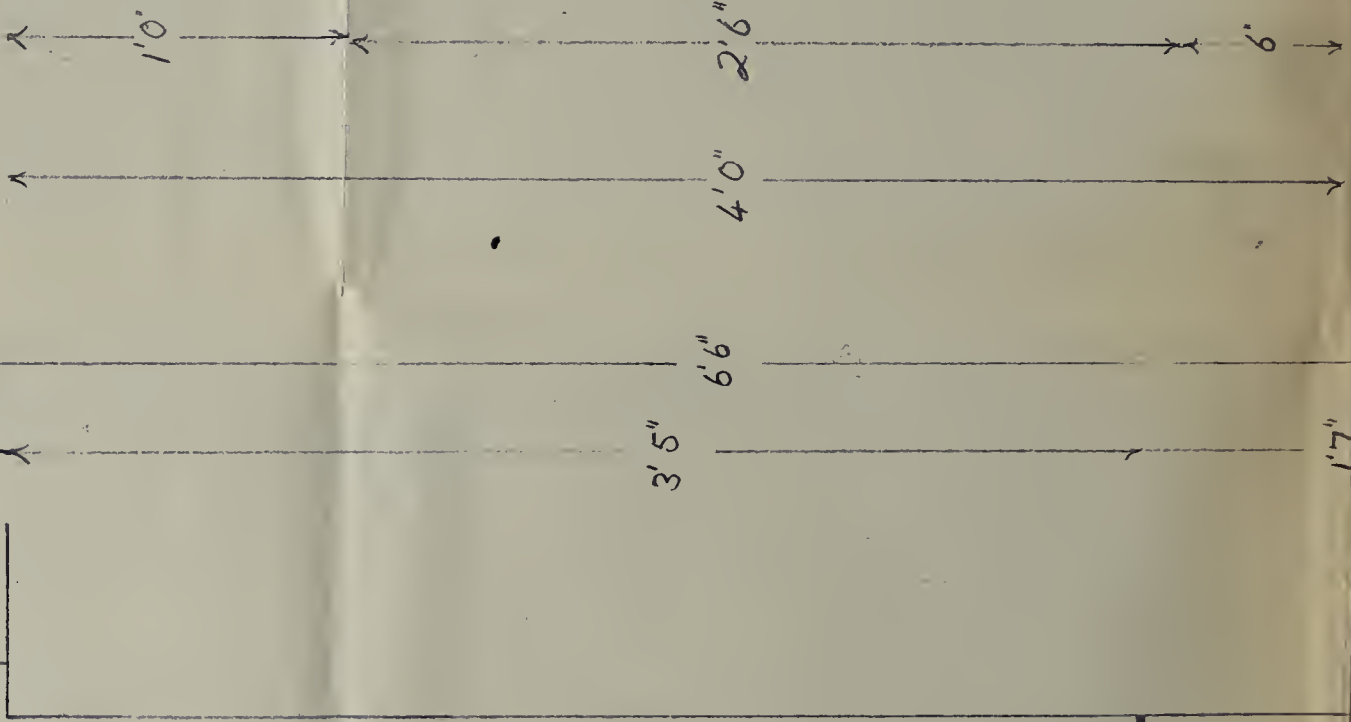
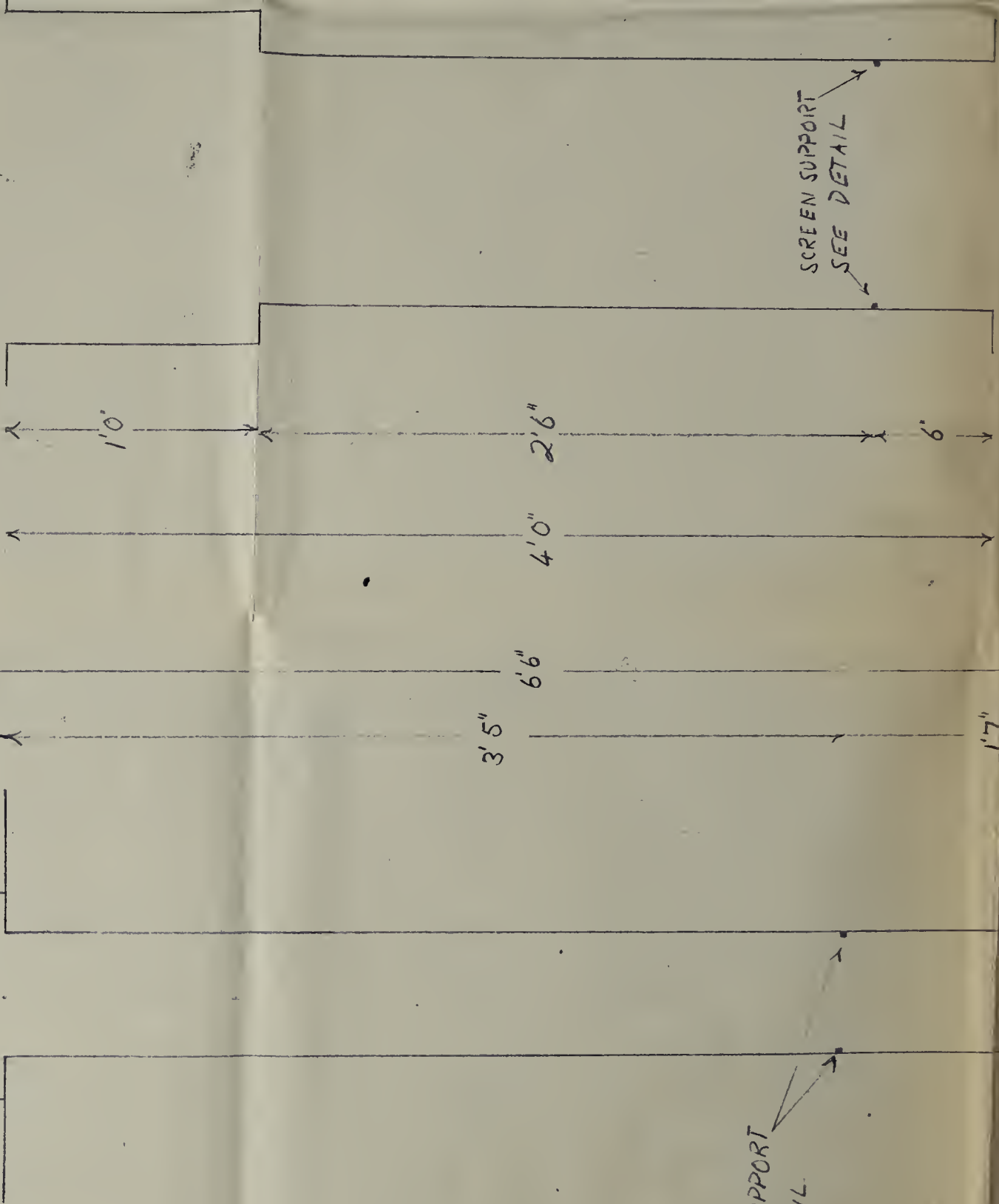
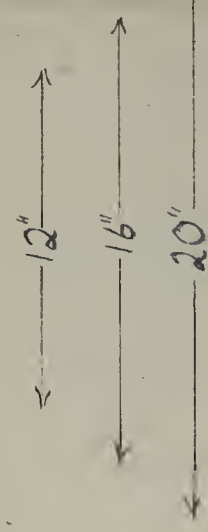
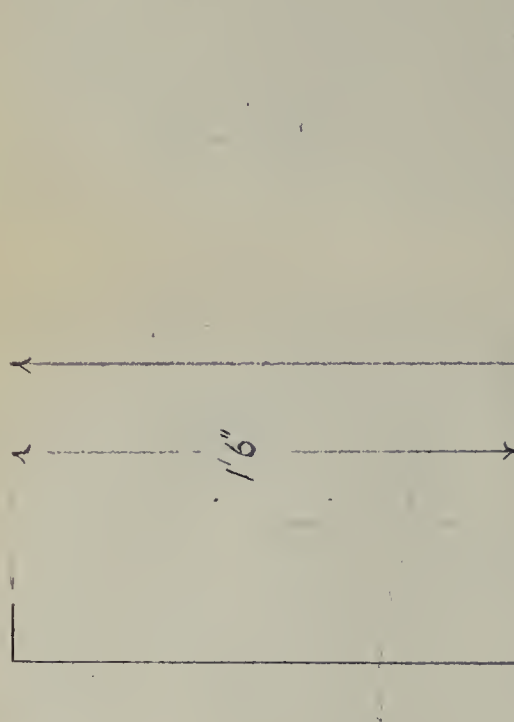
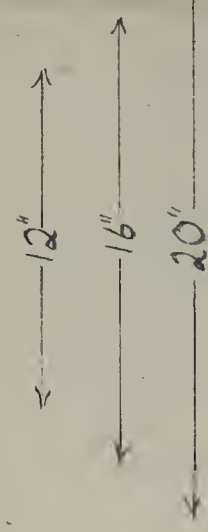
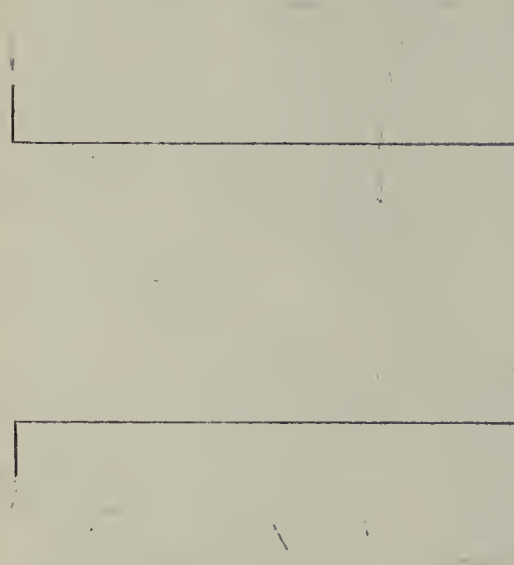
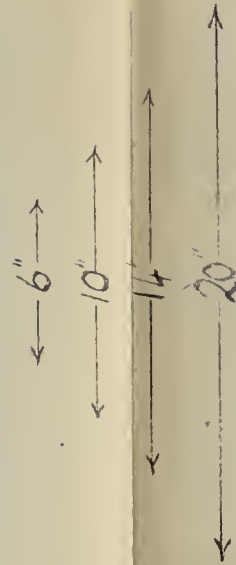
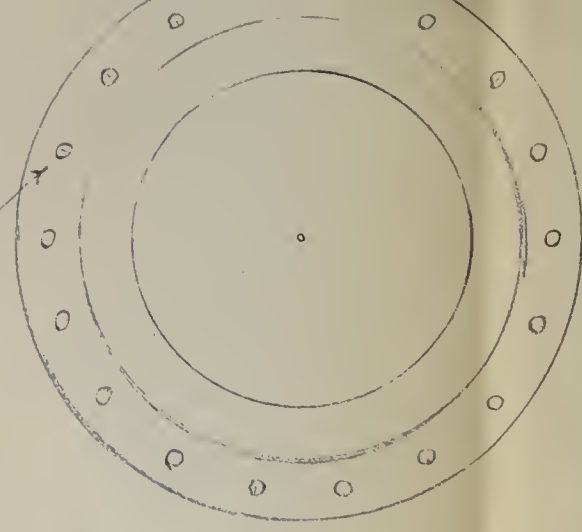
NO. FL-B-1

UNLESS OTHERWISE INDICATED,
FOR DETAIL OF FITTINGS

DRILL 24 HOLES $\frac{7}{16}$ " DIA. EQUALLY
SPACED ON 9" RADIUS



DRILL 20 HOLES $\frac{7}{16}$ " DIA.
EQUALLY SPACED
ON 6" RADIUS



SCREEN SUPPORT
SEE DETAIL

SCREEN SUPPORT
SEE DETAIL

SCREEN SUPPORT
SEE DETAIL

SCREEN SUPPORT
SEE DETAIL

6"

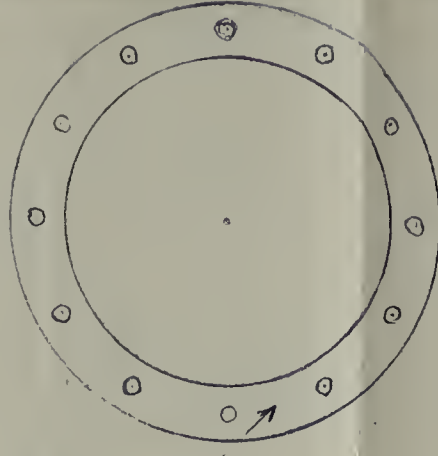
17"

12"

16"

WELD ON 6x3 STANDARD WEIGHT M.S.
REDUCER, WELDED FITTING TYPE

DRILL 24 HOLES $\frac{7}{16}$ " DIA. EQUALLY
SPACED ON 7" RADIUS



MATERIALS OF CONSTRUCTION: $\frac{3}{16}$ " STAINLESS STEEL
TYPE 316
UNLESS OTHERWISE INDICATED.

SEE DRAWING NO. FL-B-2 FOR DETAIL OF FITTINGS.



fluidised at room temperature. The volume delivered by the pump will be decreased as the temperature of the bed is increased. The pressure drop from pump discharge to suction was calculated and found to be 4 lb./in.^2 . A Roots-Connersville blower delivering 9.5 cuft./min. of 0.5 S.G. gas at 5.5 lb./in.^2 above suction pressure was therefore specified and the only suitable rotameter available was rated at $1.1 - 11.1 \text{ scf./min.}$ of air.

The cross-sectional area of the heater is 82 sq. in. With an air rate of $1.3 \text{ lb./hr./in.}^2$ the total air requirements are 23.2 scf./min. Theoretical air requirements for natural gas are 10 cuft./cuft. which gives a natural gas rate of 2.32 scf./min. The rotameters selected to cover these ranges were for the air, $3.5 - 35 \text{ scf./min.}$, and for the natural gas $0.46 - 4.67 \text{ scf./min.}$

APPENDIX C. Equipment commissioning.

1. Introduction

2. Calibrations

3. Physical Constants

4. Runs on heater alone

5. Runs on carboniser alone

6. Commissioning runs.

1. Introduction.

This appendix includes all material concerning the commissioning of the fluidised coal carboniser. In designing a pilot plant such as this without previous experience of similar equipment it is obvious that every eventuality cannot be foreseen. Several of the initial runs on the equipment were terminated for one reason or another before data could be obtained. However, each of these runs resulted in modifications of the equipment and the elimination of weak points. For this reason they are described in detail in section 6.

2. Calibration.

The coal feed screw conveyer, heater feed screw conveyer and the orifice plates for the purge gas flows were calibrated and the manufacturers' calibrations for the rotameters were checked. The screw feeders will deliver different quantities of material according to the quantity of gas which is blown through them with the solid. For these calibrations no gas was passed through the feeders. The calibration curves are plotted in Fig. 22.

The four purge gas streams are metered with orifice plates. For convenience the same size orifice viz. 0.075 in. diameter in a $\frac{1}{2}$ in. standard pipe was chosen for each. The manometer taps were drilled the same for each in the supporting union. In view of this, only one orifice assembly was calibrated. Air was passed in series through the orifice and a wet test meter. The calibration curve is plotted in Fig. 23. The quantity as read off this curve is corrected for gases other than air by multiplying the value by $(29/M)^{\frac{1}{2}}$, where M is the molecular weight of the gas.

The rotameters were checked by passing air in series through them and a dry gas meter. The rate was kept constant at some percentage of the full scale reading and the quantity of air passing through the meter in a fixed time recorded. The rotameters are calibrated by the manufacturers and the 100% reading in scfm (70°F and 14.7 psia)

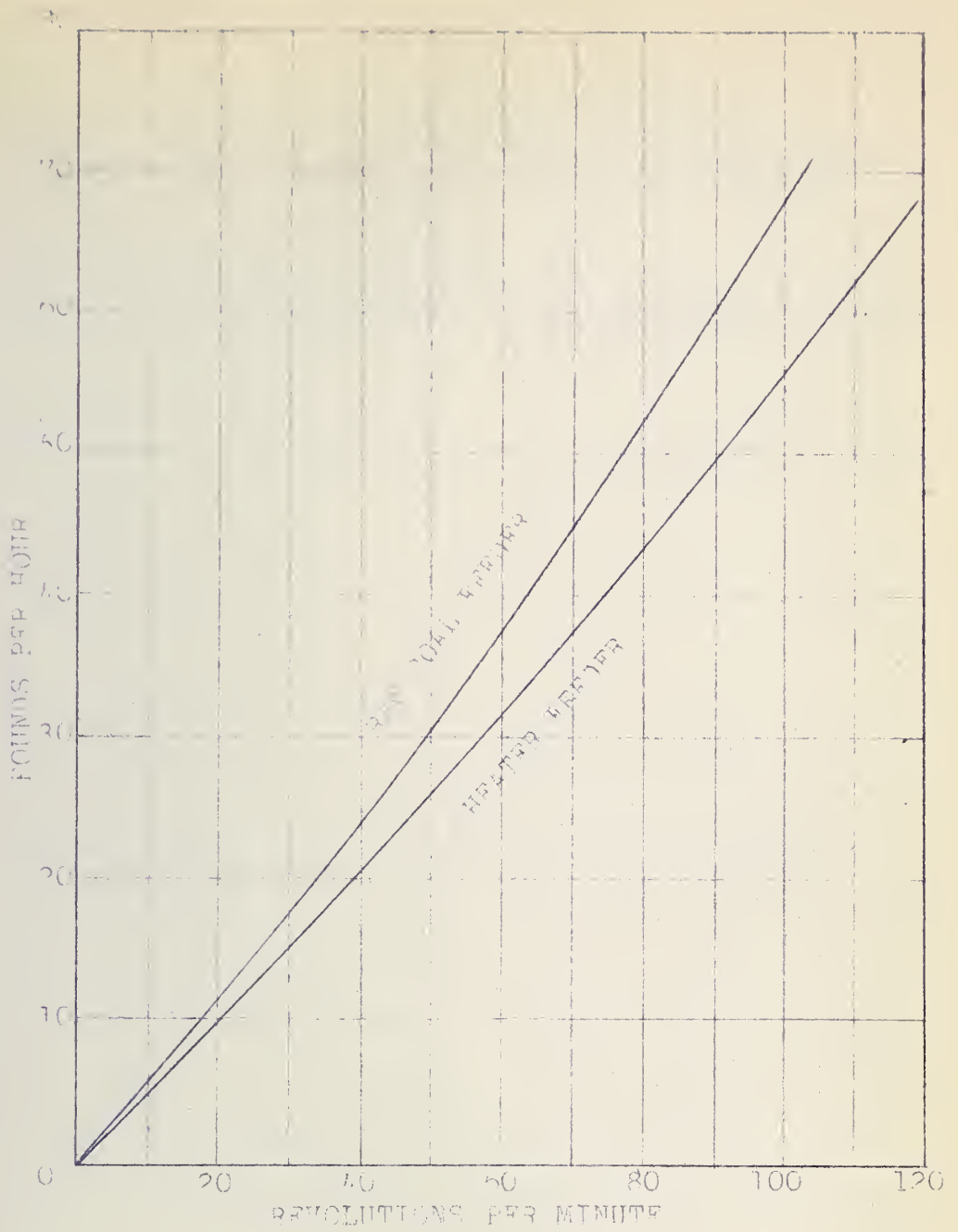


FIGURE 22 Calibration of Screw Feeders

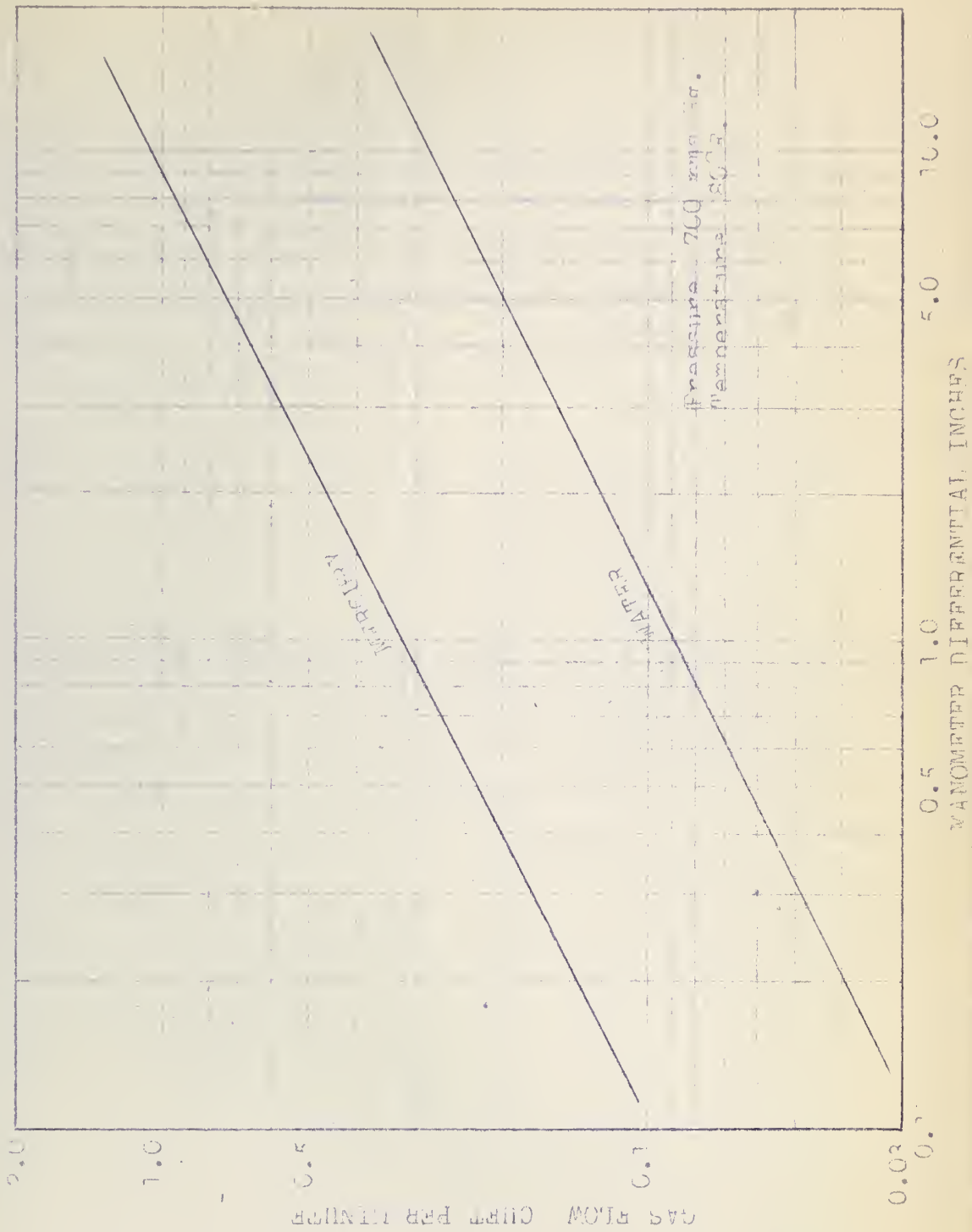


FIGURE 23 Calibration of Purge Gas Orifice Plates.

given. The value of the gas flow as read on the rotameter is corrected for density differences by multiplying it by $(0.075/\rho_f)^{\frac{1}{2}}$, where ρ_f is the density of the gas in the rotameter lb./cuft., or if it is required in scfm. (70°F and 14.7 psia) it should be multiplied by $(\rho_f/0.075)^{\frac{1}{2}}$. The results of these checks are tabulated below:- 9

Rotameter check calibration.

Rotameter	100% reading scf./min.	Volume as measured by rotameter cuft./min.	Volume as measured by dry gas meter cuft./min.
Fluidising gas	11.1	6.96	6.74
Air	36.3	11.14	11.18
Natural gas	4.62	2.44	2.30

These figures check within the accuracy of the dry gas meter ($\pm 5\%$), and so the manufacturer's calibrations for the rotameters were accepted.

3. Physical Constants.

It was thought advisable to determine the bulk density, fraction voids, and pressure drop against gas velocity curves for the coal in the carboniser and the sand in the heater before running the equipment. The results for the density and void fraction of the coal

and sand are tabulated below, and the curves for the coal and sand are plotted in Fig. 24 as pressure drop across the supporting screen and bed in in. of water against the gas flow rate in cuft./min.

Bulk Density and void fraction of coal and sand.

Material	Bulk Density lb./cuft.	Fraction voids as poured.
-20 + 28 Ottawa sand	103	0.377
-1/16 in. mesh coal	48	0.347

4. Runs on Heater alone.

The combustion chamber below the heater is an annular space 6 in. I.D. 12 in. O.D. and 6 in. deep. There are six 1/4 in. diameter burner ports projecting up from below, a 1 1/4 in. observation and lighting port, and a pilot light. Originally the pilot light was a circular pipe on the outside of the ring of burners drilled every half in. This did not prove satisfactory and was changed for a single 1/4 in. diameter burner after Run 4. Three runs were made on the heater alone using natural gas and air. The first was a failure due to flash backs while lighting. Accordingly an air ejector was fitted in the off-gas line to keep the heater under a slight vacuum

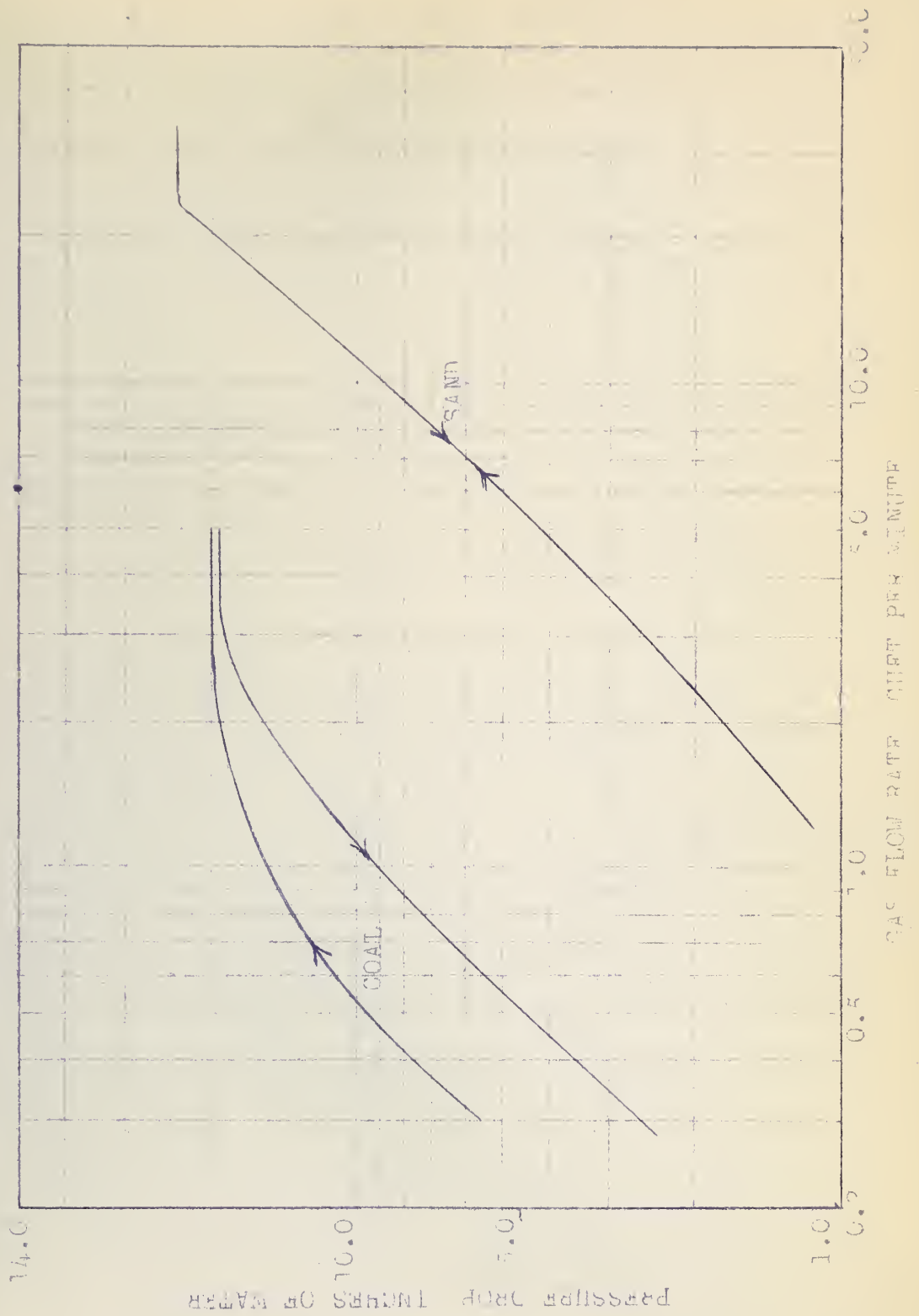


FIGURE 2/ Pressure Drop vs. Gas Flow Rate for Coal in the Carboniser and Sand in the Heater.

while the burners were being lit.

During the second run it was discovered that the flame would not remain stable unless the lighting port were open or the screen support were glowing red. The hot gases from the flame heated the bed which remained fixed for some time. This is indicated by the three thermocouples in the bed reading different temperatures. After two hours, temperatures were in the region of 400°C and suddenly two of the thermocouples on one side of the bed recorded and continued to record the same temperature. This was taken as evidence of fluidisation. However, since the thermocouple on the opposite side of the bed did not read the same temperature, it was assumed that this side was not fluidised. The run was discontinued due to an air failure at the power plant.

The final run in this series proceeded very smoothly. Two hours after lighting, the thermocouples on one side read 520 and 470°C respectively and the one on the other read 514°C . The one side fluidised and the two thermocouples read 495°C . Over the next hour the temperature on the fluidised side rose to 590°C while the other remained approximately constant. This side then fluidised and after fluctuating wildly its temperature became the same as the opposite side. During the next hour the temperature, constant throughout the bed, rose steadily to 725°C . The test was then discontinued. The air and

natural gas rates at the time when even fluidisation occurred were approximately 15 scfm. of air and 1.15 scfm. of natural gas. After complete fluidisation the inner wall was observed to be glowing evenly red for a depth of two feet, which was the approximate height of the bed.

The mild steel support originally used for the 100 mesh stainless steel screen in the heater was so buckled after this run that a new one was fabricated from 3/8 in. type 316 stainless steel. This has since shown no signs of deterioration.

5. Runs on the Carboniser alone.

The object of these runs was to test the solids circulating system of the carboniser proper. Coal was fed to the carboniser and removed from the semi-coke receivers while the bed was being fluidised with air.

The main difficulty was experienced with the coal screw feeder. The bearings (mild steel in brass) were not satisfactory due to binding with coal dust which resulted in stripping a speed reducer. The bearings were replaced with sealed ball bearings and a heavier speed reducer was used. No trouble has been experienced with this since. The bearing in the heater screw feeder was also replaced at this time.

Provision had been made for purge gas to be delivered to the end of the screw feeder where the coal enters the inlet pipe to the carboniser, to the base of the coal feed hopper and to the top of the coal feed hopper. A satisfactory run was made feeding coal to and removing it from the carboniser, except that the coal feed rates as measured by the platform scale on which the feed hopper rests did not correlate with the calibration of the screw feeder. During this run air was delivered to the three points previously mentioned. It has since been discovered that the feeder will deliver far more coal than the calibration would indicate if gas is blown through with it. This effect was masked in these runs since the coal supplied by the Research Council of Alberta was quite damp.

At the beginning only a very slight dust carry over was noticed at gas rates twice the critical (3 cuft./min.) when the equipment was dismantled the sealed leg of the cyclone was found to be blocked with fine damp coal. It was felt that this would not be a problem when running at temperature and in fact the cyclone has never been found plugged since.

6. Commissioning Runs.

The four commissioning runs will be dealt with sep-

arately. In all cases the coal feed from the Edmonton beds had been crushed to $\frac{1}{16}$ in. mesh and the fluidised bed height was 2 ft.

Run 1. March 2, 1956, 11.50 am. to 7 pm.

As the proposed feed for the heater was semi-coke manufactured in the carboniser, the object of this run was to produce semi-coke using natural gas only in the heater. However, since at 3 pm. the heater temperature (the heater was fully fluidised) was only 570°C , it was decided to start feeding raw coal to the heater. Some oxygen was also put into the bed through the pilot light and the temperature rose satisfactorily to 800°C , though there was a high carry over of fine coal to the heater cyclones. Coal feed was started at 4.30 pm. This caused the carboniser bed temperature to drop to about 650°C . All the products of the carbonisation were condensed in the start-up condenser. There was a sudden drop in the carboniser bed temperature from 650 to 500°C at 5.40 pm. indicating a sudden surge in the coal feed. After 6.00 pm. there was considerable difficulty in feeding coal at a steady rate. It seemed impossible to establish a bed (as indicated by a very low pressure drop across the carboniser) and the bed temperature rose steadily to the heater temperature. Feed was shut off at 7 pm. and the run

abandoned. During the run, the quantity of gas delivered to the coal hopper, feeder, and inlet pipe was about 0.6 cuft./min.

There was difficulty with manometers blowing and in keeping a water seal in the start-up condenser. The semi-coke/gas heat exchanger expanded making it difficult to change the semi-coke receivers, and one of the carboniser bed thermocouples read consistently about 300°C below the other.

Shut down.

When the carboniser was opened, only 3 in. of semi-coke were found in the bed. The cyclone was clean, but the coal inlet pipe was plugged with about 6 in. of damp coal. This could possibly have been due to manometer fluid. The coal screw feeder was also plugged with damp coal. The low reading thermocouple was checked and found faulty. The Raschig rings from the start-up condenser were found in the base of this condenser and also about 20 ft. away in the waste gas line. The recirculating gas blower had seized with coal tar.

Lines and equipment were cleared up and Raschig rings replaced in the start-up condenser. Mercury was used in all manometers and a permanent oxygen line fitted into the heater pilot feed. The purge gas line to the base of the hopper was removed. The semi-coke/gas heat exchanger was shortened.

Run 2. March 7, 1956. 7.30 a.m. to 1.30 p.m.

The heater was brought up to 420°C with natural gas and air in $3\frac{1}{2}$ hours. Semi-coke was then injected into the heater bed and the gas turned off. The heater temperature rose to 750°C in three quarters of an hour. Some oxygen was used. Within a quarter of an hour of feeding semi-coke to the heater, the carboniser which had been filled with coal before the run was at 600°C . It was kept at this temperature for about one hour by controlling the coal feed rate. The fluidising gas from the semi-coke heat exchanger remained reasonably constant at 160°C . It was found that the temperature of the heater could be very easily controlled by varying the air rate, i.e. there was excess semi-coke in the bed. After this reasonably steady period, the carboniser temperature rose and the pressure drop across the bed decreased and the coal feed could not be restarted so the equipment was shut down. During this run the quantity of purge gas delivered to the coal inlet pipe was approximately 0.85 cuft./min.

Shut Down.

A plug about 6 in. long was found near the top of the coal inlet pipe. It was evidently due to tar condensing at this point. Some dust was found in the product transfer line and only about 3 in. of coal were left in the carboniser.

The burner chamber beneath the heater was full of sand. When the heater was dismantled, it was found that the 100 mesh screen was burnt through above each of two burners.

The fluidising gas blower was stripped down and found to be coated with a black lacquer which was insoluble in the common solvents.

The stainless steel screen was replaced and protected by wear plates suspended over each burner. A steam line was connected to the inlet of the gas blower so that it could be steamed out at the end of each run, and an air blast was arranged to cool the coal inlet pipe. The 3 in. cyclone in the carboniser was replaced with one 2 in. in diameter in an attempt to cut down dust carryover.

Run 3. March 14, 1956, 8 am. to 1 pm.

On checking the equipment before the run, it was found that the start-up condenser was blocked. It was therefore decided to use the three condensers and the tar fog filter continuously. The absorber train was not used because it was not felt to be justified during these preliminary tests until everything else was working better. After the heater had been heated about $3\frac{1}{2}$ hr. with gas, semi-coke injection was started, and the heater

temperature was increased satisfactorily from 530 to 675°C. Coal was fed intermittently to the carboniser for about one hour, in order to keep its temperature around 525°C, then however, the coal inlet plugged. It was thought that 1.0 cuft./min. of gas was being passed through this pipe but a plug on a manometer trap had been inadvertently left off so that there could not have been more than half this quantity flowing. By shutting down the carbonising section the inlet pipe was cleared and coal feed started again. Unfortunately while this was being done the semi-coke feed to the heater had been shut off, since the heater temperature had risen to 800°C. With the sudden load in the carboniser zone the temperature in the heater dropped quickly. Even though the semi-coke feed was resumed, conditions showed no signs of becoming steady. Very little semi-coke was left so the heater was shut down and coal passed through the carboniser at a high rate until its temperature dropped below 400°C, to provide heater feed for the next run.

Shut down.

The pressure drop from the outlet of the carboniser to the outlet of No. 2 condenser had been increasing towards the end of the run. When the transfer lines were opened they were found to be coated with a 1/8 in. layer of coal dust and there was also a considerable amount of coal dust in No. 1 condenser. All the elbows in the

transfer line were replaced with crosses to facilitate future cleaning operations. Since the 2 in. cyclone seemed to have had no beneficial effect on the dust carry-over problem, the original cyclone was replaced.

There was still some sand in the burner chamber below the heater. When this was dismantled, the screen was found to be intact. It was therefore assumed that the sand had worked its way between the screen and screen support around the 6 in. carboniser. To remedy this, the 6 in. packing follower ring was replaced above the screen support instead of below so that the 100 mesh screen was held between it and the stainless steel screen. This prevented sand working its way between the two.

Run 4 March 16, 1956. 11.15 am. to 3.15 pm.

The critical gas velocity of semi-coke in the carboniser was checked and found to occur at the 18% reading on the rotameter when the bed was at room temperature. The gas velocity was accordingly set at this figure and as the temperature increased it was noticed that this setting decreased to about 8% without any adjustments on the operator's part. However, the bed always remained fluidised. The heater was brought up to temperature very smoothly. The lighting port was not shut until about two

hours after lighting in order to prevent the flame from going out. When the port was closed, the bed fluidised and its temperature averaged out at 500°C. After fluidising the bed, the temperature could not be raised above 575°C with semi-coke and oxygen. The heater screw feeder was checked twice but seemed to be working. Usually some unburnt semi-coke collected in the heater cyclone, but this time there was only a very fine dust. This condition continued for an hour and a half. At this point the temperature of the carboniser bed dropped from 550 to 50°C in a period of 3 minutes, and the pressure drop across it rose to over four times its normal value. It was obvious that the carboniser was completely full of coal which must have blown through the screw feeder, since at no time was it turning.

Shut down.

The carboniser, transfer line and numbers 1, 2 and 3 condensers were all full of coal. To prevent this occurring again the purge gas line to the top of the coal feed hopper was shut off.

There was still sand in the burner chamber and it was found that the rods which force the screen support up against the ring welded to the inside of the shell were bent, due to their being heated at a faster rate than the shell. When the heater cooled down, the screen support slipped

allowing the sand to pass by. To prevent this two holes were drilled and tapped through the outer shell into the screen support so that it could be fixed in position with two screws.

The ring type pilot light was replaced by a single 1/4 in. burner to give a more stable and controlled flame.

